AD-A080 414 AIR FORCE INST OF TECH WRIGHT-PATTERSON AFB OH SCHOO--ETC F/G 9/3
SPATIAL DOMAIN AND SPATIAL FREQUENCY DOMAIN IMAGING.(U)
DEC 79 K W KIRLIN
UNCLASSIFIED AFIT/GEO/EE/79-3 NL

1 OF 2
AD
A080414

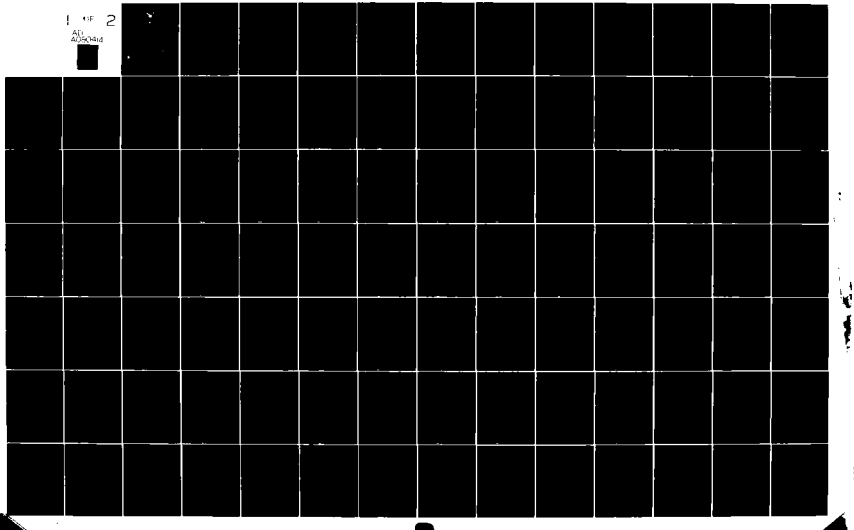

AFIT/GEO/EE/79-3

(6) SPATIAL DOMAIN AND SPATIAL FREQUENCY DOMAIN IMAGING.

(9) Master's THESIS

(10) Kevin W. Kirlin, Capt, USAF

(14) AFIT/GEO/EE/79-3

(11) Dec 79

(12) 147

Approved for public release; distribution unlimited

012 225

AFIT/GEO/EE/79-3

SPATIAL DOMAIN AND SPATIAL FREQUENCY DOMAIN IMAGING

THESIS

Presented to the Faculty of the School of Engineering
of the Air Force Institute of Technology
Air University
in Partial Fulfillment of the
Requirements of the Degree of
Master of Science

by
Kevin W. Kirlin, B.S.
Capt USAF
Graduate Electro-Optics
December 1979

Preface

Several people deserve thanks for helping me complete this thesis. I am very appreciative of the guidance and encouragement of my thesis advisor, Capt. Stanley Robinson. Without his intervention my unique brand of mathematics would have caused me to vanish into a blackhole. The comments of my readers, Lt. Col. Ronald Carpinella and Major Glenn Doughty, were invaluable in identifying areas requiring better organizational structure, further explanation or more mathematical rigor. Finally, I wish to thank my wife Merche not only for her untiring support but also for her excellent typing of this thesis.

Kevin W. Kirlin

Contents

List of Figures

Notation

A_{R_1}	Area of object field aperture
A_{R_2}	Area of image field aperture
a_i	Object field weighting coefficients
b_i	Image field weighting coefficients
$\mathcal{B}$	Fourier-Bessel transform
C_N^2	Refractive index structure parameter
CMF	Channel-Matched Filter (Receiver)
CTF	Coherent Transfer Function
CON	Complete orthonormal (set of eigenfunctions)
D_f	Degrees of freedom for a near-field, circularly-apertured, coherent object field propagated through the turbulent atmosphere
D_{fo}	Degrees of freedom for a near-field, circularly-apertured, coherent object field propagated through free-space
D_{fo}'	Degrees of freedom for a near-field, one-dimensional, incoherent object field propagated through free-space
$D_{fo}'/2$	Degrees of freedom for a near-field, one-dimensional, coherent object field propagated through free-space
d_i	Distance from receiving plane to image field plane
d_o	Distance from object field plane to receiving plane
d_1	Diameter or width of object field aperture
d_2	Diameter or width of receiving or image field aperture
$D(\bar{r}', \bar{r})$	Spherical wave structure function
$D_\phi(\bar{r}', \bar{r})$	Phase structure function
DOF	Degrees of freedom of an image field

$\hat{E}_{CMF}(\bar{r})$	Image field generated by Channel-Matched Filter Receiver
$E_I(\bar{r})$	An object (input) field
$\hat{E}_{MP}(\bar{r})$	Image field generated by Multiplicative-Phase Receiver
$E_N(\bar{r})$	An additive background noise field
E_o	Complex amplitude of a point source field
$E_o(\bar{r})$	An image (output) field
ϵ	An error constant
$\bar{f}$	Spatial frequency vector
$\lvert\bar{f}_c\rvert$	Spatial frequency cutoff of a free-space modulation transfer function
$\lvert\bar{f}_o\rvert$	Spatial frequency cutoff of a free-space coherent transfer function
$\lvert\bar{f}_1\rvert$	Spatial sampling frequency
$\lvert\bar{f}'\rvert$	Spatial frequency defined by $\lvert\bar{f}\rvert 2\lambda z/d_2$
$H_{CMF}(\bar{f})$	Coherent transfer function of Channel-Matched Filter Receiver
$H_{MP}(\bar{f})$	Coherent transfer function of Multiplicative-Phase Receiver
$h_{CMF}(\bar{r})$	Impulse response of Channel-Matched Filter Receiver
$h_{FS}(\bar{r}',\bar{r})$	Free-space impulse response
$h_{MP}(\bar{r})$	Impulse response of Multiplicative-Phase Receiver
$h_{TB}(\bar{r}',\bar{r})$	Turbulent impulse response
$h_{21}(\bar{r}',\bar{r})$	General impulse response
$I(\bar{r}_1)$	Real and even intensity distribution function of an incoherent object field
$I_m[\ ]$	Imaginary part of quantity in brackets
IMSE	Integrated mean square error

$J_i(x)$	Bessel function of the ith order
$K(\bar{r}',\bar{r})$	Imaging kernel
k	Wavenumber defined by $2\pi/\lambda$
L_o	Outer scale of the turbulent atmosphere
$\mathcal{l}$	Mean of log-amplitude fluctuations of the turbulent atmosphere
MP	Multiplicative-Phase (Receiver)
MTF	Modulation Transfer Function - the modulus of the optical transfer function
N	Upper limit of a summation
N_o	Amplitude of the autocorrelation of an additive background noise field
n_i	Noise coefficient
OTF	Optical Transfer Function
$P(\bar{r})$	Free-space pupil function
$\bar{P}(\bar{r})$	Turbulent pupil function
P_1	Object field plane
P_2	Receiving or image field plane
P_3	Image field plane
$\mathrm{Re}[\ ]$	Real part of quantity in brackets
R_1	Object field aperture
R_2	Receiving or image field aperture
R_3	Image field aperture
r_o	Coherence length of the turbulent atmosphere
r_1	Radius of object field aperture
r_2	Radius of receiving or image field aperture
$\bar{r}_1$	Position vector in object field plane
$\bar{r}_2$	Position vector in receiving or image field plane

$\bar{r}_3$	Position vector in image field plane
$S_c(\bar{f})$	Coherent power density spectrum
$S_I(\bar{f})$	Incoherent power density spectrum
SNR	Signal to noise ratio
$\tau_{A-COH}(\bar{f})$	Atmospheric coherent transfer function
$\tau_O(\bar{f})$	Free-space modulation transfer function
$\tau_{O-COH}(\bar{f})$	Free-space coherent transfer function
$\tau_{LE}(\bar{f})$	Fried's long-exposure, turbulent modulation transfer function
${}_{NF}\tau_{SE}(\bar{f})$	Fried's near-field, short-exposure, turbulent modulation transfer function
$\chi(\bar{r}',\bar{r})$	Log-Amplitude fluctuations of the turbulent atmosphere
z	Distance between object field and image field planes
σ^2	Total variance of log-amplitude and phase fluctuations of the turbulent atmosphere
σ_η^2	Variance of additive background noise
σ_χ^2	Variance of log-amplitude fluctuations of the turbulent atmosphere
σ_ϕ^2	Variance of phase fluctuations of the turbulent atmosphere
$\phi(\bar{r}',\bar{r})$	Phase fluctuations of the turbulent atmosphere
$\hat{\phi}(\bar{r}',\bar{r})$	Estimate of optimum multiplicative phase
$\epsilon\phi_\epsilon(\bar{r})$	Error of optimum multiplicative phase estimate
$\phi_i(\bar{r})$	Eigenfunction in object field plane
$\phi_o(\bar{r})$	Optimum multiplicative phase
$\Psi(\bar{r})$	Eigenfunction in image field plane
λ	Optical wavelength
λ_i	Power eigenvalue defined by $\lvert b_i\rvert^2/\lvert a_i\rvert^2$

$\delta(\ )$	Dirac delta function
Ω_S	Field of view subtended by an object field aperture when viewed from the center of an image field aperture
Ω_{DL}	Diffraction limited field of view of an image field aperture
$\langle\ \rangle$	Ensemble average

Abstract

An imaging system's object field to image field transformation operation is usually described in the (spatial) frequency domain using the system's transfer function. The limitation of this description is that the imaging system must be space-invariant. In contrast, an object field to image field transformation can be described in the spatial domain without requiring that the system be space-invariant.

For the frequency domain, a summary of free-space and turbulent transfer functions is presented. For the spatial domain, the Normal Mode Approach to imaging is described followed by a summary of spatial eigenvalue distributions and degrees of freedom expressions. The effect of additive background noise on the useable degrees of freedom of an image field is studied. The spatial domain and frequency domain are shown to be related when certain conditions are satisfied, one of which is space-invariance.

The operation of two ideal, adaptive imaging receivers (the Channel-Matched Filter and Multiplicative-Phase Receivers) is described and their imaging performance is compared using turbulent coherent transfer functions and minimum average integrated mean square error expressions.

I Introduction

Background

Imaging systems are typically composed of a channel through which an object field is propagated and a receiver at the channel output for imaging the object field. The manner in which these systems transform an object field into an image field is commonly described in the (spatial) frequency domain by using transfer functions. A transfer function indicates how the Fourier (sinusoidal) components of an object field are transformed into the corresponding components of an image field. If an object field is spatially coherent the function is called a Coherent Transfer Function (CTF). If an object field is spatially incoherent the function is called an Optical Transfer Function (OTF) and its modulus is called the Modulation Transfer Function (Ref 7:114).

In the frequency domain, the resolution capability of an imaging system is sometimes defined in terms of the highest nonzero spatial frequency (spatial frequency cutoff) of a CTF or MTF. The higher the spatial frequency cutoff the greater the resolution capability of an imaging system. For propagation of an object field through free-space the spatial frequency cutoff is due to the diffraction effects of the finite apertures of an imaging receiver. The free-space cutoff is the highest resolution attainable by an imaging system.

When the lack of space-invariance in an imaging system

prevents the use of transfer functions, it is useful to be able to describe imaging in another domain called the spatial domain. In the spatial domain, an object field to image field transformation is described in terms of object field and image field spatial modes and spatial eigenvalues. A spatial eigenvalue indicates the power loss associated with a single object field spatial mode to image field spatial mode transformation. When the spatial eigenvalues are ordered in magnitude (highest to lowest), they form a distribution that characterizes the modal transformation of an imaging system.

In the spatial domain, the resolution capability of an imaging system is usually defined as the number of nonzero eigenvalues in the spatial eigenvalue distribution. This number is called the degrees of freedom (DOF) of an image field. The greater the number of DOF of an image field, the greater is the resolution capability of an imaging system. The DOF of an image field depend on the geometry of an imaging system, the wavelength of the propagated object field and the propagation medium.

Another spatial domain resolution measure is the integrated mean square error (IMSE) of the image field. The error is the difference between the image field produced for free-space propagation and either the image field produced for propagation in other media or for additive background noise. The IMSE of the image field is expressible in terms of the

DOF of the image field.

Objectives

This thesis has three objectives. The first objective is to describe the Normal Mode Approach to spatial domain imaging and to present spatial eigenvalue distributions and DOF expressions associated with that approach. The second objective is to show how, and under what conditions, the spatial domain is related to the frequency domain. The third objective is to compare two ideal adaptive imaging receivers using their turbulent CTFs and the minimum average IMSEs of the image fields they generate. The receivers, to be described later, are the Channel-Matched Filter (CMF) Receiver and the Multiplicative-Phase (MP) Receiver.

Organization

Chapter II is a summary of the CTFs and MTFs for an object field propagated through either free-space or the turbulent atmosphere.

Chapter III is a description of the Normal Mode Approach to spatial domain imaging, a summary of spatial eigenvalue distributions and DOF expressions, and an examination of the effect additive background noise has on the useable DOF of an image field. In addition, Chapter III shows how the spatial domain and the frequency domain are related.

Chapter IV is a description of the CMF and MP Receivers

and a derivation of turbulent CTFs and image field, minimum average IMSE expressions for both receivers. This chapter is also a comparison of the resolution capabilities of the receivers.

Chapter V is a summary of conclusions and a discussion of areas requiring further study.

II Frequency Domain Imaging-Transfer Functions

The purpose of this chapter is to present, as background material, the coherent transfer functions (CTFs) and modulation transfer functions (MTFs) of an object field propagated through either free-space or the turbulent atmosphere. The first section of this chapter defines the imaging system geometry used in calculating the CTFs and MTFs. The next section is a summary of free-space CTFs and MTFs, and corresponding spatial frequency cutoffs, for the defined geometry. The final section is a summary of turbulent CTFs and MTFs.

General

Figure 1 shows an imaging system composed of an object field plane P_1, receiving plane P_2, and an image field plane P_3. P_2 has a circular aperture R_2 of diameter d_2. The region between P_1 and P_2 is called the propagation channel. The channel may be either free-space or the turbulent atmosphere. The region between P_2 and P_3 is the imaging receiver. This region could include optical elements but for simplicity it is assumed to be a free-space channel without such elements. The receiving plane P_2 is therefore both the input to the receiver and the output of the propagation channel. The imaging system of Figure 1 is assumed to be linear and space invariant. This assumption must be made if transfer functions are to be used to characterize the object field to image field transformation of the imaging system (Ref 7:19).

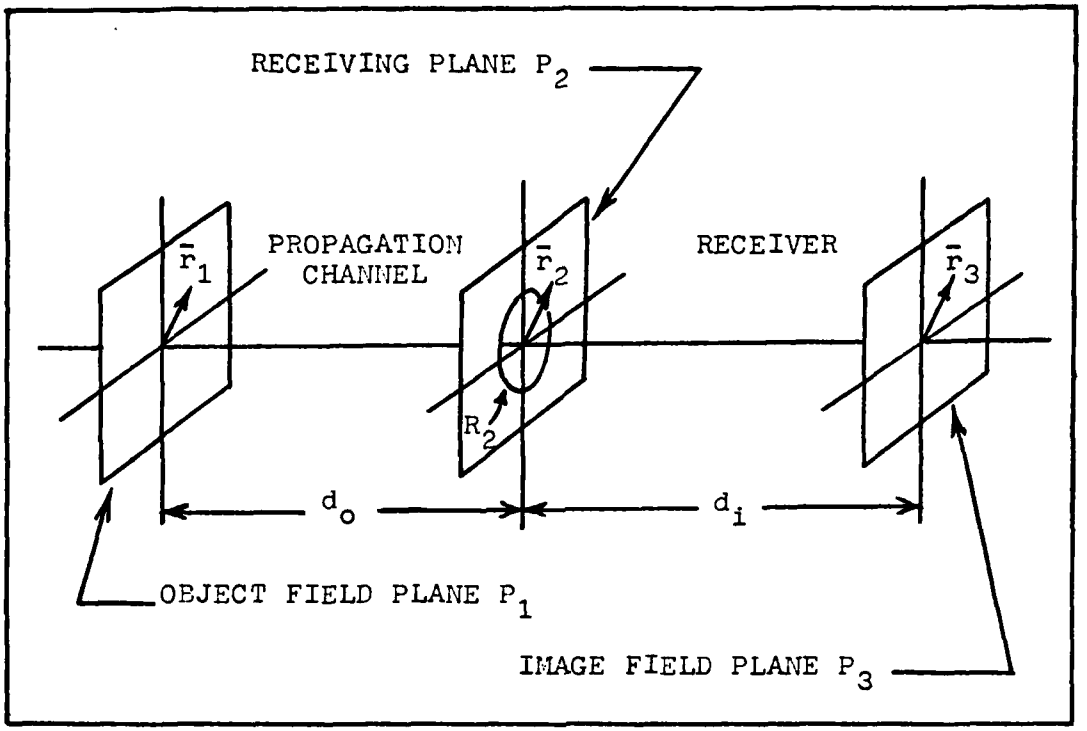

Figure 1 - Geometry for Calculation of Transfer Functions

Free-Space

Assume that the propagation channel of Figure 1 is free-space. Associated with the circular receiving aperture R_2 of Figure 1 is a free-space pupil function called $P(\bar{r}_2)$:

$$P(\bar{r}_2) = \text{circ}(2|\bar{r}_2|/d_2) \tag{1}$$

where

$$\text{circ}(x) = \begin{cases} 1 & ; \quad x \leq 1/2 \\ 0 & ; \quad \text{otherwise} \end{cases} \tag{2}$$

Goodman has shown (Ref 7:111) that for a coherent object field in P_1, the free-space CTF, called $\tau_{O\text{-}COH}(\bar{f})$, is

$$\tau_{O\text{-}COH}(\bar{f}) = P(\lambda d_i |\bar{f}|) \tag{3}$$

where λ is the optical wavelength of the object field, d_i is the length of the propagation channel, and $|\bar{f}|$ is a spatial frequency magnitude. Combining Eqs (1) and (3) yields

$$\tau_{O\text{-}COH}(\bar{f}) = \text{circ}(2\lambda d_i |\bar{f}|/d_2) \tag{4}$$

From Eq (4), the CTF spatial frequency cutoff, called $|\bar{f}_o|$, is

$$|\bar{f}_o| = d_2/2\lambda d_i \tag{5}$$

Goodman has shown (Ref 7:116) that for an incoherent object field in P_1, the free-space MTF, called $\tau_0(\bar{f})$, is the convolution of the pupil function of Eq (1) with itself. Completing this convolution yields

$$\tau_0(\bar{f}) = \begin{cases} 2\left[\cos^{-1}(\lambda d_i |\bar{f}|/d_2) - (\lambda d_i |\bar{f}|/d_2)\right. \\ \left. \times \sqrt{1 - (\lambda d_i |\bar{f}|/d_2)^2}\,\right]/\pi \quad ; \quad \lambda d_i |\bar{f}| \leq d_2 \\ 0 \quad ; \quad \text{otherwise} \end{cases} \tag{6}$$

From Eq (6), the MTF spatial frequency cutoff, called $|\bar{f}_c|$, is

$$|\bar{f}_c| = d_2/\lambda d_i \tag{7}$$

A comparison of Eqs (5) and (7) indicates that the spatial frequency cutoff for an incoherent object field is twice the cutoff for a coherent object field. This does not imply, however, that incoherent object fields yield "better" image fields than coherent object fields. As Goodman points out (Ref 7:125), the two cutoff frequencies describe resolution for different image quantities and are therefore not comparable. Equation (5) is the spatial frequency cutoff for a function which produces an image field amplitude distribution while Eq (7) is the cutoff for a function which produces an image field intensity distribution (power density).

Turbulent Atmosphere

Assume now that the propagation channel of Figure 1 is the turbulent atmosphere. An object field propagating through the turbulent atmosphere is effected by multiplicative log-amplitude, $\chi(\bar{r}_2,\bar{r}_1)$ and phase, $\phi(\bar{r}_2,\bar{r}_1)$, fluctuations. $\chi(\bar{r}_2,\bar{r}_1)$ and $\phi(\bar{r}_2,\bar{r}_1)$ are Gaussian random variables (Ref 17:209). Their first and second order statistics are given in Appendix A. Since $\chi(\bar{r}_2,\bar{r}_1)$ and $\phi(\bar{r}_2,\bar{r}_1)$ are in general functions of both the object field plane and the receiving plane, they violate the space invariance required

for obtaining transfer functions. There is a condition, however, under which $\chi(\bar{r}_2,\bar{r}_1)$ and $\phi(\bar{r}_2,\bar{r}_1)$ can be expressed as functions of only the receiving plane so as not to violate the space invariance of the imaging system. The condition is that the maximum spatial extent of an object field in P_1 of Figure 1 be less than an atmospheric coherence length r_o (Ref 15:462). For a spherical-wave object field, r_o is defined as (Ref 8:550)

$$r_o = d_o\left[0.423\ k^2 \int_0^{d_o} C_N^2(z) z^{\frac{5}{3}}\ dz\right]^{-\frac{3}{5}} \tag{8}$$

where $k = 2\pi/\lambda$ is the wave number of the object field, d_o is the length of the propagation channel, and $C_N^2(z)$ is the refractive-index structure parameter of the turbulent atmosphere (Ref 9:1526). For $\lambda = 0.55\mu$ and a vertical propagation path, r_o is approximately 11 cm (Ref 5:2622). When the object field meets the above condition it is said to lie within an isoplanatic patch. Since most object fields are spatially larger than an isoplanatic patch, isoplanatism is a severe (but necessary) restriction for obtaining a turbulent CTF.

When isoplanatism is a valid assumption, there is associated with the circular receiving aperture R_2 of Figure 1 a "turbulent" pupil function called $\bar{P}(\bar{r}_2)$:

$$\bar{P}(\bar{r}_2) = \bar{P}(\bar{r}_2)\exp\left[\chi(|\bar{r}_2|) + j\phi(|\bar{r}_2|)\right] \tag{9}$$

where $P(\bar{r}_2)$ is defined by Eq (1). Goodman has shown (Ref 7:121) that for a coherent object field in P_1 of Figure 1 the turbulent CTF, called $\tau_{COH}(\bar{f})$, is

$$\tau_{COH}(\bar{f}) = \bar{P}(\lambda d_i|\bar{f}|) \tag{10}$$

Combining Eqs (3), (9) and (10) yields

$$\tau_{COH}(\bar{f}) = \tau_{O-COH}(\bar{f})\exp\left[\chi(\lambda d_i|\bar{f}|) + j\phi(\lambda d_i|\bar{f}|)\right] \tag{11}$$

The ensemble average of Eq (11) with respect to the random variables $\chi(\lambda d_i|\bar{f}|)$ and $\phi(\lambda d_i|\bar{f}|)$ is

$$<\tau_{COH}(\bar{f})> = \tau_{O-COH}(\bar{f})<\exp\left[\chi(\lambda d_i|\bar{f}|) + j\phi(\lambda d_i|\bar{f}|)\right]> \tag{12}$$

It is shown in Appendix A that Eq (12) is equivalent to

$$<\tau_{COH}(\bar{f})> = \tau_{O-COH}(\bar{f})\exp\left[-\sigma^2/2\right] \tag{13}$$

where $\sigma^2 = \sigma_\chi^2 + \sigma_\phi^2$, and σ_χ^2 and σ_ϕ^2 are the variances of $\chi(\bar{r}_2)$ and $\phi(\bar{r}_2)$ respectively. Following Fried's example (Ref 4:1375), the exponential in Eq (13) can be thought of as an atmospheric CTF, called $\tau_{A-COH}(\bar{f})$. Equation (13) is then

$$\langle \tau_{COH}(\bar{f}) \rangle = \tau_{O-COH}(\bar{f})\, \tau_{A-COH}(\bar{f}) \tag{14}$$

For a spherical wave, Greenwood has indicated (Ref 8:550) that σ^2 of Eq (13) is

$$\sigma^2 = 4.93\,(L_o/r_o)^{\frac{5}{3}} \tag{15}$$

where r_o is the atmospheric coherence length defined by Eq (8) and L_o is the outer scale of the turbulent atmosphere. A typical value for L_o is 100 meters or one-fifth the height above the ground, whichever is less (Ref 9:1527). Substituting Eq (15) into Eq (13) gives

$$\langle \tau_{COH}(f) \rangle = \tau_{O-COH}(f) \exp\left[-2.47(L_o/r_o)^{\frac{5}{3}}\right] \tag{16}$$

Since the exponential in Eq (16) is not spatial frequency dependent, the spatial frequency cutoff of the turbulent CTF is the same as the spatial frequency cutoff of the free-space CTF. However, the amplitude of the turbulent CTF is, for all spatial frequencies, smaller than the amplitude of the free-space CTF since L_o is larger than r_o. The amplitude attenuation is usually due to turbulence-induced phase fluctuations rather than to log-amplitude fluctuations since σ_ϕ^2 is usually much larger than σ_χ^2 (Ref 8:550).

In reference 4, Fried has derived expressions for long and short-exposure turbulent MTFs. Long-exposure means that

the object field propagated through the turbulent atmosphere is viewed over a long enough time such that the turbulent MTF is equal to its ensemble average. Short-exposure means that the propagated object field is not viewed long enough to justify equating the turbulent MTF to its ensemble average. For short exposures, Fried has considered both near-field and far-field object fields. With reference to Figure 1, near-field means $d_2 >> \sqrt{d_o \lambda}$ while far-field means $d_2 << \sqrt{d_o \lambda}$. Only the near-field case is presented here.

Fried's ensemble-average, long-exposure, turbulent MTF, called $<\tau_{LE}(\bar{f})>$, is

$$<\tau_{LE}(\bar{f})> = \tau_0(\bar{f}) \exp\left[3.44(\lambda d_i |\bar{f}|/r_o)^{\frac{5}{3}}\right] \qquad (17)$$

where d_i is defined in Figure 1 and r_o is defined by Eq (8). The average of Eq (17) is an average over many different exposures. Although the exponential in Eq (17) is similar in form to the exponential in Eq (16), their effects are different. In Eq (16) the exponential represents a constant amplitude attenuation for all spatial frequencies while in Eq (17) the exponential is a spatial frequency dependent attenuation.

Fried's ensemble-average, near-field, short-exposure, turbulent MTF, called $<_{NF} \tau_{SE}(\bar{f})>$, is

$$<_{NF} \tau_{SE}(\bar{f})> = \tau_0(\bar{f}) \exp\left\{3.44(\lambda d_i |\bar{f}|/r_o)^{\frac{5}{3}}\right.$$

$$\times \left[1 - (\lambda d_i |\bar{f}|/d_2)^{\frac{1}{2}}\right]\Bigg\} \qquad (18)$$

where d_2 is the diameter of the circular receiving aperture of Figure 1. An examination of Eq (18) indicates that $<_{NF} \tau_{SE}(\bar{f})>$ approaches the free-space MTF, $\tau_o(\bar{f})$, as $|\bar{f}|$ approaches $d_2/\lambda d_i$. From Eq (7), $d_2/\lambda d_i$ is the spatial frequency cutoff of the free-space MTF.

All of the CTF and MTF expressions in this chapter are based on the assumption that the imaging system of Figure 1 is linear and space-invariant. When space-invariance is not a valid assumption, CTF and MTF expressions are meaningless. The loss of these expressions makes a frequency domain description of an object field to image field transformation very difficult. Fortunately this transformation can be described in a different domain without having to assume space-invariance. The other domain is called the spatial domain and it is the subject of the next chapter.

III Spatial Domain Imaging

This chapter has four purposes. The first purpose is to explain the Normal Mode Approach to spatial domain imaging. The second is to present spatial eigenvalue distributions for propagation of coherent or incoherent object fields through either free-space or the turbulent atmosphere and to give expressions for the degrees of freedom (DOF) of the resulting image fields. The third purpose is to determine the effect additive background noise has on the DOF of an image field. The final purpose is to show how, and under what conditions, the spatial domain is related to the frequency domain. The sections of this chapter are arranged in the same order as the purposes above.

Normal Mode Approach

Figure 2 shows the imaging system geometry to be used in explaining the Normal Mode Approach to spatial domain imaging. P_1 is an object field plane and P_2 is an image field plane. The region between P_1 and P_2 is called the propagation channel. Therefore, P_2 is not only an image field plane but also the output plane of the propagation channel. In later sections of this chapter the channel is either free-space or the turbulent atmosphere, but for now it is a general channel with a general impulse response called $h_{21}(\bar{r}_2,\bar{r}_1)$. The purpose of aperture R_1 of Figure 2 is to define the spatial extent of the object field as it enters the propagation channel.

Aperture R_2 serves the same purpose for the image field at the output of the propagation channel. In this section, the shapes of R_1 and R_2 are arbitrary but in later sections they are slit or circular apertures. Since in the Normal Mode Approach the spatial extents of object and image fields are defined in their respective planes, a receiving plane and a receiving aperture are not required in Figure 2 as they are in Figure 1. The imaging system of Figure 2 is linear but not necessarily space-invariant.

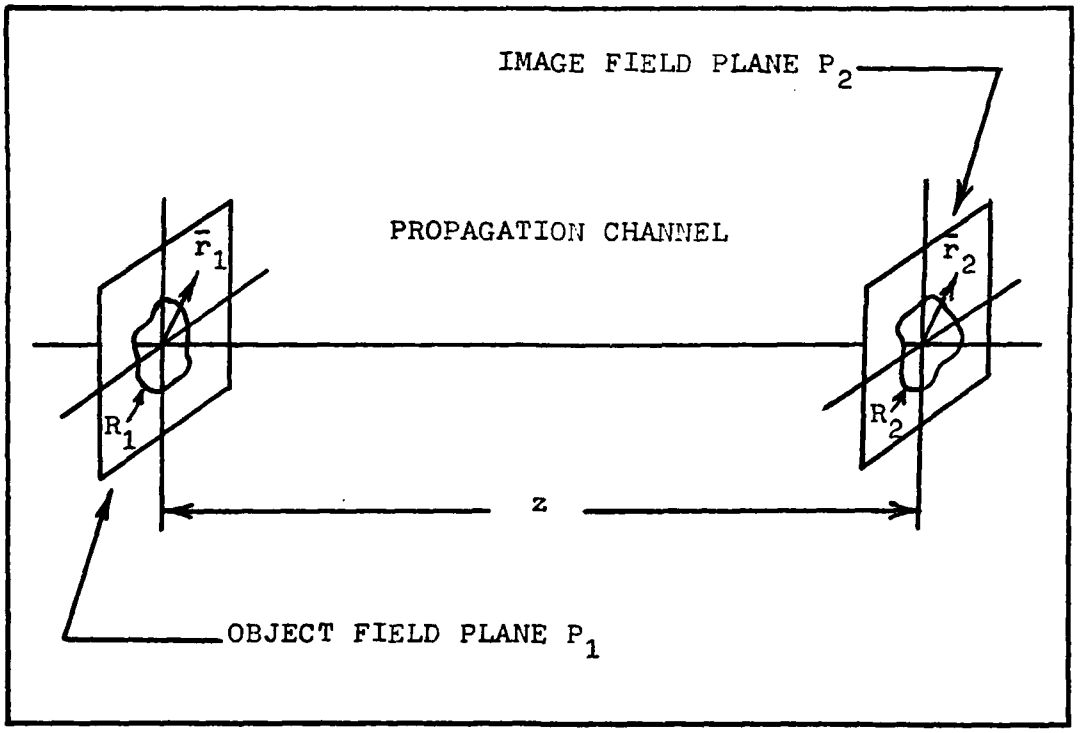

Figure 2 - Geometry for Normal Mode Imaging

In the Normal Mode Approach an object field $E_I(\bar{r}_1)$ in R_1 of Figure 2 is expressed as a weighted sum of a complete orthonormal (CON) set of spatial eigenfunctions (spatial modes) as

shown below:

$$E_I(\bar{r}_1) = \sum_{i=1}^{\infty} a_i \phi_i(\bar{r}_1) \tag{19}$$

where the $\phi_i(\bar{r}_1)$ are a CON set of spatial eigenfunctions defined in R_1 and the a_i object field weighting coefficients defined by

$$a_i = \int_{R_1} E_I(\bar{r}_1) \psi_i^*(\bar{r}_1) d\bar{r}_1 \tag{20}$$

Likewise, an image field $E_o(\bar{r}_2)$ in R_2 of Figure 2 is expressed as a weighted sum of a CON set of spatial eigenfunctions (spatial modes) as shown below:

$$E_o(\bar{r}_2) = \sum_{i=1}^{\infty} b_i \Psi_i(\bar{r}_2) \tag{21}$$

where the $\Psi_i(\bar{r}_2)$ are a CON set of spatial eigenfunctions defined in R_2 and the b_i are image field weighting coefficients defined by

$$b_i = \int_{R_2} E_o(\bar{r}_2) \Psi_i^*(\bar{r}_2) d\bar{r}_2 \tag{22}$$

In addition to Eq (21), the image field is expressed in terms of the object field and the general impulse response of the propagation channel by using the Huygens-Fresnel Principle (Ref 2:Chap 6):

$$E_o(\bar{r}_2) = \int_{R_1} E_I(\bar{r}_1) h_{21}(\bar{r}_2, \bar{r}_1) d\bar{r}_1 \qquad (23)$$

The Normal Mode Approach describes an object field to image field transformation by describing how much of the power of each of the spatial modes of the object field is transmitted through the propagation channel to the corresponding modes of the image field. On a per mode basis the fraction of power transmitted is given by the ratio of $|b_i|^2$ to $|a_i|^2$. This ratio is defined as

$$|b_i|^2 / |a_i|^2 = \lambda_i \qquad (24)$$

where λ_i is called the ith power spatial eigenvalue of the propagation channel. In the remainder of this thesis λ_i is referred to as simply the ith spatial eigenvalue. The square root of the ith spatial eigenvalue is related to the ith spatial modes of the object and image fields, and to the general impulse response of the propagation channel, by

$$\sqrt{\lambda_i}\ \Psi_i(\bar{r}_2) = \int_{R_1} \phi_i(\bar{r}_1) h_{21}(\bar{r}_2, \bar{r}_1) d\bar{r}_1 \qquad (25)$$

Equation (25) is derived in Appendix B. In Appendix B it is shown that one way Eq (25) is satisfied is for

$$\lambda_i\ \phi_i(\bar{r}') = \int_{R_1} K(\bar{r}_1', \bar{r}_1)\, \phi_i(\bar{r}_1) d\bar{r}_1 \quad ; \quad \bar{r}_1' \in R_1 \qquad (26)$$

where

$$K(\bar{r}_1',\bar{r}_1) = \int_{R_2} h_{21}(\bar{r}_2,\bar{r}_1)h_{21}^*(\bar{r}_2,\bar{r}_1')d\bar{r}_2 \quad ; \quad \bar{r}_1' \in R_1 \tag{27}$$

In Eqs (26) and (27), $K(\bar{r}_1',\bar{r}_1)$ is called an imaging kernel. Equation (26) is called a Fredholm Equation. For free-space propagation, Slepian and Pollack have shown (Ref 16:57) that the spatial eigenfunctions $\phi_i(\bar{r}_1)$ that satisfy Eq (26) are called prolate spheroidal wavefunctions. Using these wavefunctions, Eq (26) can be solved for free-space spatial eigenvalues. The eigenvalues can be ordered such that $\lambda_i \geq \lambda_{i+1}$. The ordered spatial eigenvalues form a distribution that characterizes the modal transformation of an imaging system. The number of nonzero spatial eigenvalues in the spatial eigenvalue distribution is called the degrees of freedom (DOF) of an image field. The greater the number of DOF of an image field, the greater is the resolution capability of an imaging system.

For propagation through the turbulent atmosphere, the imaging kernel and spatial eigenfunctions are random variables. Since the spatial eigenfunctions $\phi_i(\bar{r}_1)$ that satisfy Eq (26) are not known, Eq (26) cannot be solved for turbulence spatial eigenvalues. Therefore, turbulence spatial eigenvalues are also random variables. Shapiro has shown (Ref 13:2616), however, that turbulence spatial eigenvalues exhibit the same near-field and far-field distribution

behavior as free-space spatial eigenvalues. Spatial eigenvalue distributions for free-space and the turbulent atmosphere are presented in the next section.

Eigenvalue Distributions

Free-Space - The first free-sapce, spatial eigenvalue distribution presented is that for a circularly-apertured, coherent object field and a circularly-apertured image field. Circularly-apertured means that the object and image fields are spatially limited to circular regions. Specifically, this means that the object field aperture R_1 of Figure 2 and the image field aperture R_2 of Figure 2 are circular apertures of diameters d_1 and d_2 respectively.

The second free-space, spatial eigenvalue distribution presented should be that for a circularly-apertured, incoherent object field and a circularly-apertured image field. Unfortunately, this case is not only not found in the literature but it is also difficult to derive. Therefore, the second free-space spatial eigenvalue distribution presented is that for an one-dimensional, incoherent object field and a one-dimensional image field. One-dimensional means that apertures R_1 and R_2 of Figure 2 are slit apertures of widths d_1 and d_2 respectively.

The final free-space spatial eigenvalue distribution presented is that for a one-dimensional, coherent object field and a one-dimensional image field. This type of coherent

object field is considered in addition to the circularly-apertured, coherent object field because its spatial eigenvalue distribution is used in the last two sections of this chapter. In all the distributions presented, the spatial eigenvalues are ordered such that $\lambda_i \geq \lambda_{i+1}$.

For the case of a circularly-apertured, coherent object field, Shapiro has shown (Ref 13:2615) that the near-field, free-space, spatial eigenvalues exhibit the following rectangular behavior:

$$\lambda_i = \begin{cases} 1 & ; \quad i \leq D_{fo} \\ 0 & ; \quad i > D_{fo} \end{cases} \qquad i \geq 1 \quad , \quad i \in \text{integers} \tag{28}$$

where

$$D_{fo} = (\pi d_1 d_2 / 4 \lambda z)^2 \tag{29}$$

The near-field qualification of Eq (28) means that $D_{fo} \gg 1$. For a near-field, circularly-apertured, coherent object field (of diameter d_1) propagated a distance z through free-space, D_{fo} is called the number of DOF of the resulting circularly-apertured image field (of diameter d_2). If the object field is in the far-field ($D_{fo} \ll 1$), then there is only one spatial eigenvalue and its value is D_{fo}. In addition, the image field of a far-field object field has only one DOF. This would be the case for a point source.

Equation (29) is derived by combining Eqs (26) and (28), as is shown in Appendix C. Alternatively, Eq (29) can be

derived using the Sampling Theorem. The Sampling Theorem says (Ref 6:93) that the number of DOF of an image field is obtained by dividing the solid angle subtended by the object field aperture R_1 (when viewed from the image field aperture R_2) by the diffraction limited field of view of the image field aperture R_2. The Sampling Theorem derivation of Eq (29) is shown in Appendix D.

The spatial eigenvalue behavior given by Eq (28) is illustrated by the distribution of Figure 3.

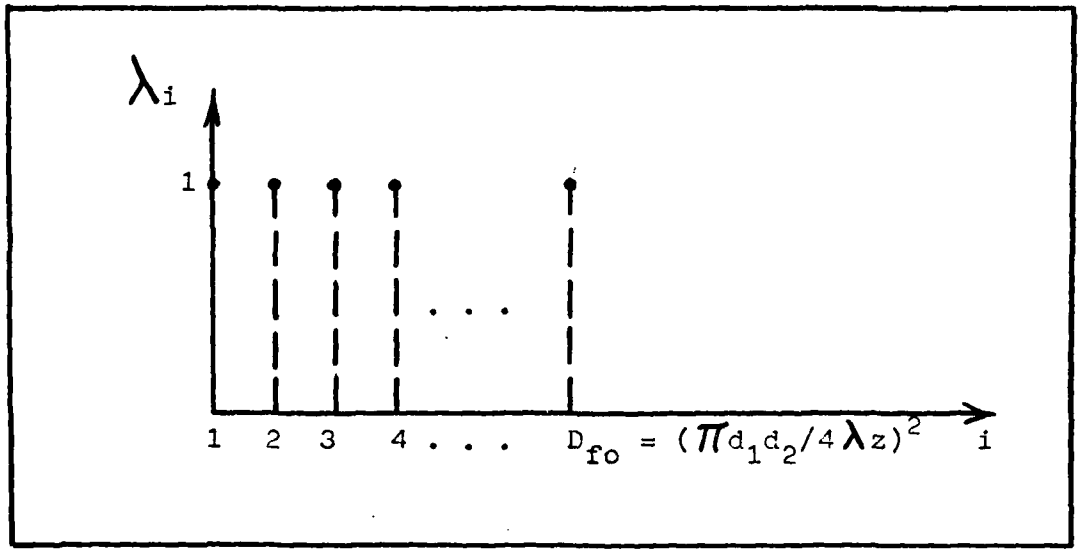

Figure 3 - Spatial Eigenvalue Distribution for Near-Field, Circularly-Apertured, Coherent Object Field Propagated through Free-Space

For the case of a one-dimensional, incoherent object field, Bendinelli, et. al., have shown (Ref 1:1500) that the near-field, free-space, spatial eigenvalues exhibit the

following triangular behavior:

$$\lambda_i = \begin{cases} 1 - (1/D_{fo}')i \quad ; \quad i \leq D_{fo}' \qquad i \geq 1 \ , \ i \in \text{integers} \\ 0 \qquad\qquad\qquad ; \quad i > D_{fo}' \end{cases} \tag{30}$$

where

$$D_{fo}' = d_1 d_2 / \lambda z \tag{31}$$

The near-field qualification of Eq (30) means that $D_{fo}' \gg 1$. For a near-field, one-dimensional, incoherent object field (of width d_1) propagated a distance z through free-space, D_{fo}' is called the number of DOF of the resulting one-dimensional image field (of width d_2). If the object field is in the far field ($D_{fo}' \ll 1$), then there is only one spatial eigenvalue and one DOF of the image field. However, Bendinelli, et. al., have not shown that the value of the one spatial eigenvalue is D_{fo}'.

The spatial eigenvalue behavior given by Eq (30) is illustrated by the distribution of Figure 4.

For the case of a one-dimensional, coherent object field, the near-field, free-space, spatial eigenvalues exhibit the following rectangular behavior (Ref 18:801):

$$\lambda_i = \begin{cases} 1 \ ; \ i \leq D_{fo}'/2 \qquad i \geq 1 \ , \ i \in \text{integers} \\ 0 \ ; \ i > D_{fo}'/2 \end{cases} \tag{32}$$

where

$$D_{fo}'/2 = d_1 d_2 / 2\lambda z \tag{33}$$

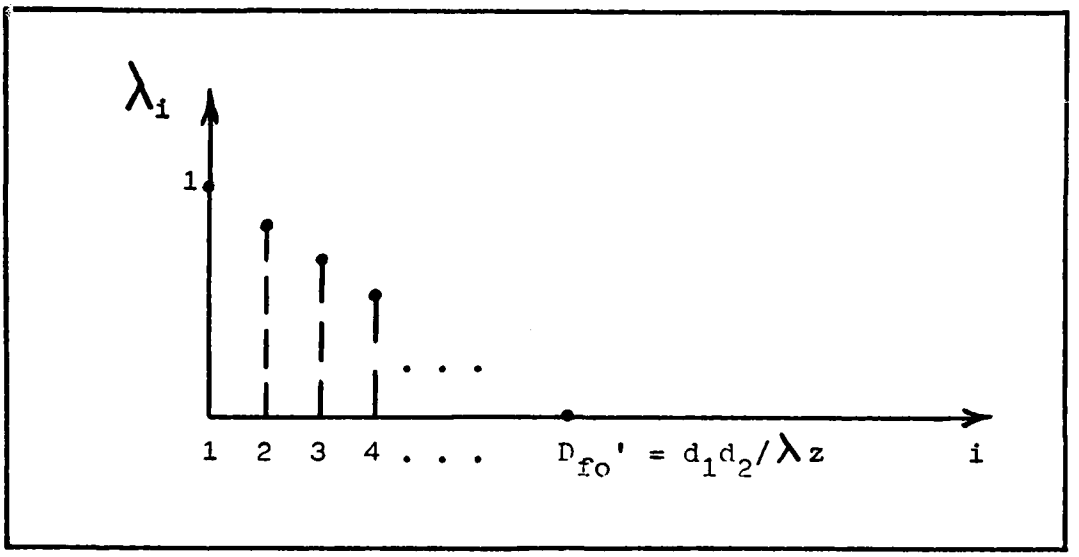

Figure 4 - Spatial Eigenvalue Distribution for Near-Field, One-Dimensional, Incoherent Object Field Propagated through Free-Space

The near-field qualification of Eq (32) means that $D_{fo}'/2 \gg 1$. For a near-field, one-dimensional, coherent object field (of width d_1) propagated a distance z through free-space, $D_{fo}'/2$ is called the number of DOF of the resulting one-dimensional image field (of width d_2). If the object field is in the far-field ($D_{fo}'/2 \ll 1$), then there is only one spatial eigenvalue and one DOF of the image field.

The spatial eigenvalue behavior given by Eq (32) is illustrated by the distribution of Figure 5.

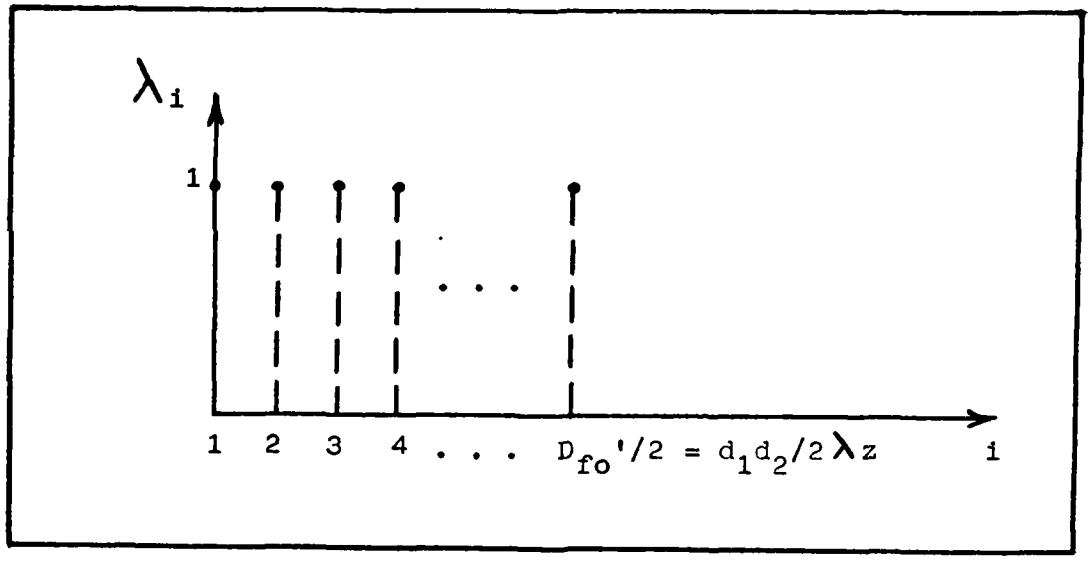

Figure 5 - Spatial Eigenvalue Distribution for Near-Field, One-Dimensional, Coherent Object Field Propagated through Free-Space

Turbulent Atmosphere - A turbulence spatial eigenvalue distribution is presented for a circularly-apertured, coherent object field and a circularly-apertured image field. Distributions are not presented for a circularly-apertured incoherent object field nor for a one-dimensional incoherent object field, as neither case is found in the literature nor can they be easily derived.

For the case of a circularly-apertured, coherent object field, Shapiro has shown (Ref 13:2616) that the near-field ($D_{fo} >> 1$), turbulence spatial eigenvalues are random variables that exhibit with high probability the following rectangular behavior:

$$\lambda_i = \begin{cases} 1 \;\; ; \;\; i \leq D_f & i \geq 1 \;\; , \;\; i \in \text{integers} \\ 0 \;\; ; \;\; i > D_f & \end{cases} \qquad (34)$$

where

$$D_f = (1/\lambda z)^2 \int_{R_1} \int_{R_2} \exp\left[2\chi(\bar{r}_2,\bar{r}_1)\right] d\bar{r}_2 \; d\bar{r}_1 \qquad (35)$$

For a near-field, circularly-apertured, coherent object field (of diameter d_1) propagated a distance z through the turbulent atmosphere, D_f is called the number of DOF of the resulting circularly-apertured image field (of diameter d_2). In Eq (35), $\chi(\bar{r}_2,\bar{r}_1)$ represents the random log-amplitude fluctuations of the turbulent atmosphere. Since $\chi(\bar{r}_2,\bar{r}_1)$ is a random variable, both D_f and the number of DOF are random variables. If the object field is in the far-field ($D_{fo} << 1$), then there is only one spatial eigenvalue and its value is D_f. Equation (35) is derived by combining Eqs (5C) and (32), as is shown in Appendix E. When $\chi(\bar{r}_2,\bar{r}_1) = 0$, as in free-space, Eq (35) reduces to Eq (29). The spatial eigenvalue behavior given by Eq (34) is the same as the behavior illustrated in Figure 3, but with D_{fo} replaced by D_f.

Energy conservation requires that the mean of $\chi(\bar{r}_2,\bar{r}_1)$ equal the negative of the variance of $\chi(\bar{r}_2,\bar{r}_1)$ (Ref 4:1374). In Appendix F it is shown that this requirement means that $\langle D_f \rangle = D_{fo}$. Since the number of DOF of an image field is a measure of the resolution capability of a spatial domain

imaging system, the statement $< D_f > = D_{fo}$ says that on the average the imaging system has the same resolution capability for the turbulent atmosphere as it does for free-space.

Additive Background Noise

This section analyzes the effect additive background noise has on the useable DOF of an image field when the object field is in the near-field, is one-dimensional and is propagated through free-space. In the analysis, apertures R_1 and R_2 of Figure 2 are slit apertures of widths d_1 and d_2 respectively. Both coherent and incoherent object fields are considered. The analysis is not extended, however, to circularly-apertured object fields nor to object fields propagated through the turbulent atmosphere.

The analysis follows the example of Bendinelli, et. al., (Ref 1:1499), and begins by calculating the average IMSE of the image field generated when background noise is present in the image field plane P_2 of Figure 2. The background noise is zero-mean, spatially white noise. The average IMSE of the image field is

$$< \text{IMSE(N)} > = \int_{R_2} < \left[E_o(\bar{r}_2) - E_o'(\bar{r}_2) \right]^2 > d\bar{r}_2 \qquad (36)$$

where

$$E_o(\bar{r}_2) = \sum_{i=1}^{\infty} b_i \Psi_i(\bar{r}_2) \qquad (21)$$

and where

$$E_o'(\bar{r}_2) = \sum_{i=1}^{N} (b_i + n_i)\, \Psi_i(\bar{r}_2) \qquad (37)$$

$E_o(\bar{r}_2)$ is the image field generated in the absence of background noise while $E_o'(\bar{r}_2)$ is an estimate of the image field generated when background noise is present. The number N in Eq (37) is chosen such that the average IMSE of the image field is minimized. This is the reason N appears as an argument in Eq (36). The n_i in Eq (37) are the random noise coefficients of the zero-mean, spatially white noise. The average of Eq (36) is with respect to these random noise coefficients. In Appendix G it is shown that Eq (36) is equivalent to

$$\langle \text{IMSE}\ (N) \rangle = \sum_{i=1}^{\infty} \lambda_i |a_i|^2 - \sum_{i=1}^{N} (\lambda_i |a_i|^2 - \sigma_\eta^2) \qquad (38)$$

where the a_i are object field weighting coefficients and σ_η^2 is the variance of the background noise.

The next step in the analysis is to minimize the average IMSE given by Eq (38). In general, the object field weighting coefficients are unordered. Therefore, in general all that can be said is that the second summation of Eq (38) must be positive for the average IMSE to be minimized. However, if the object field weighting coefficients are ordered such that $a_i \geq a_{i+1}$, then the average IMSE is minimized by choosing an N that maximizes the second summation of Eq (38).

The second summation cannot be maximized by simply letting N go to infinity because of the ordering of the spatial eigenvalues ($\lambda_i \geq \lambda_{i+1}$) and the ordering of the object field weighting coefficients ($a_i \geq a_{i+1}$). As N becomes too large, $\lambda_i |a_i|^2$ becomes less than σ_η^2 and the second summation begins to decrease rather than increase. Therefore, the N that maximizes the second summation of Eq (38) is the N that causes the term in the summation to equal zero or it is the largest N that insures the term remains a positive quantity. The latter qualification is necessary because the spatial eigenvalues and object field weighting coefficients assume discrete values that will not always permit an N to be chosen such that the term in the second summation of Eq (38) is exactly zero. Therefore, the N that minimizes the average IMSE given by Eq (38) is the largest N that satisfies the equation

$$|\lambda_{i=N}| \geq \sigma_\eta^2 / |a_{i=N}|^2 \tag{39}$$

Note that Eq (39) is equivalent to $|b_{i=N}|^2 \geq \sigma_\eta^2$ where the term $|b_{i=N}|^2$ is the power of Nth spatial mode of the image field and σ_η^2 is the power (variance) of the additive background noise. Since the N that satisfies Eq (39) tells how many image field spatial modes have powers greater than the noise power (i.e. these modes are discernible from the noise), N is the number of useable DOF of the image field.

Therefore, Eq (39) relates the useable DOF of an image field in additive background noise to the spatial eigenvalues of the propagation channel. Eq (39) is valid for both coherent and incoherent object fields.

For a near-field, one-dimensional, coherent object field propagated through free-space, the spatial eigenvalue behavior is given by Eq (32) and is illustrated in Figure 5. The number of DOF of the image field when there is no additive background noise is $D_{fo}'/2$, which is defined by Eq (33). Because of the rectangular behavior of the spatial eigenvalues, $D_{fo}'/2$ is also the N that satisfies Eq (39). Therefore, additive background noise has no effect on the number of DOF of the image field when the object field is coherent.

For a near-field, one-dimensional, incoherent object field propagated through free-space, the spatial eigenvalue behavior is given by Eq (30) and is illustrated in Figure 4. The number of DOF of the image field when there is no additive background noise is D_{fo}', which is defined by Eq (31). Because of the triangular behavior of the spatial eigenvalues, D_{fo}' is not the N that satisfies Eq (39). The N that satisfies Eq (39) for this case is

$$N = D_{fo}'(1 - \sigma_\eta^2/|a_{i=N}|^2) \; ; \; 0 \leq \sigma_\eta^2/|a_{i=N}|^2 \leq 1 \qquad (40)$$

Equation (40) is obtained by letting $i = N$ in Eq (30) and substituting the result into Eq (39). Since $|a_{i=N}|^2$ is

the power of the Nth spatial mode of the object field and σ_η^2 is the power (variance) of the additive background noise, the term $\sigma_\eta^2 / |a_{i=N}|^2$ in Eq (40) is an inverse power signal - to - noise ratio (SNR). When there is no additive background noise ($\sigma_\eta^2 = 0$), the inverse SNR in Eq (40) is zero and $N = D_{fo}'$ as expected. However, as the additive background noise increases, the number of useable DOF of the image field decreases until $N = 0$ for $\sigma_\eta^2 = |a_{i=N}|^2$. Therefore, additive background noise decreases the resolution capability of an imaging system when the object field to be imaged is incoherent.

Relationship Between Spatial Domain and Frequency Domain

In this section it is shown that when certain conditions are satisfied, it is asymptotically true that the spatial eigenvalues of a spatial domain imaging system are obtained by sampling the power density spectrum (frequency domain) of the impulse response of the imaging system. There are four conditions that must be satisfied for the above relationship between the two domains to be true. First, the spatial imaging kernel of the imaging system must be space-invariant so that it can be Fourier transformed to obtain the power density spectrum of the system's impulse response. Second, the object field propagated through the system must have a large spatial extent. Third, the maximum phase change across the object field must be less than some small radian measure such

as $\pi/8$. Finally, the object field must be in the near-field. Near-field means the number of DOF of the image field associated with the object field must be much greater than one.

The relationship between the spatial domain and the frequency domain is shown below for a near-field, one-dimensional object field propagated through free-space. Both coherent and incoherent object fields are considered. For a one-dimensional object field, object field aperture R_1 of Figure 2 is a slit aperture of width d_1. For the associated one-dimensional image field, image field aperture R_2 of Figure 2 is slit aperture of width d_2. The propagation channel of Figure 2 is free-space.

For a one-dimensional, coherent object field it is shown in Appendix H that the space-invariant, coherent imaging kernel is of the form

$$K(|\bar{r}_1-\bar{r}_1'|) = \sin(\pi d_2|\bar{r}_1-\bar{r}_1'|/\lambda z)/\pi|\bar{r}_1-\bar{r}_1'| \quad ; \quad \bar{r}_1' \in R_1 \tag{41}$$

The coherent power density spectrum $S_c(|\bar{f}|)$ of the impulse response associated with the coherent imaging kernel is the Fourier transform of Eq (41):

$$S_c(|\bar{f}|) = \text{rect}(|\bar{f}|\lambda z/d_2) \tag{42}$$

The power density spectrum given by Eq (42) is illustrated in Figure 6.

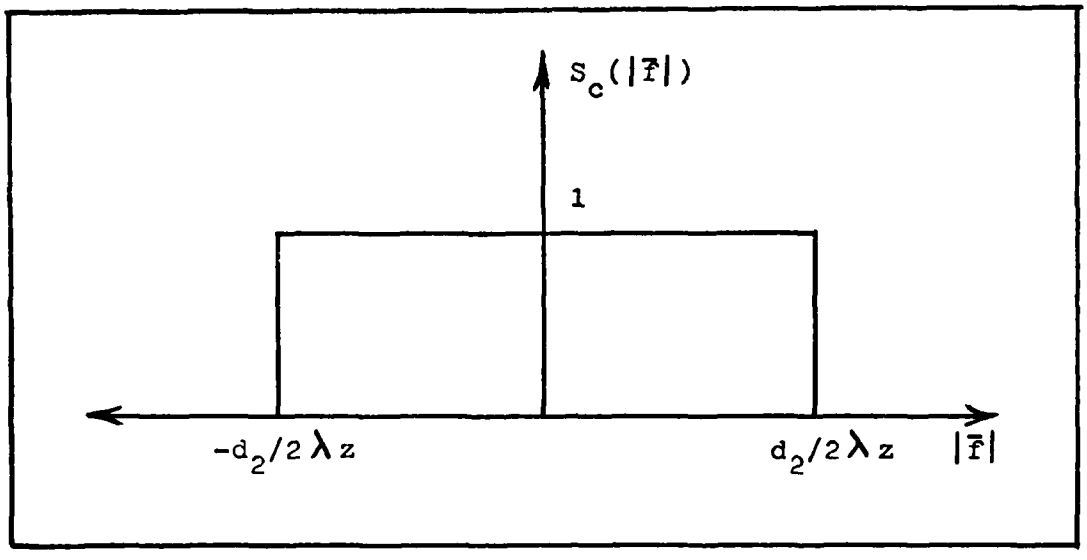

Figure 6 - Coherent Power Density Spectrum

The spatial eigenvalues associated with the coherent object field are obtained by sampling $S_c(|\bar{f}|)$. If temporal eigenvalues were wanted, the sampling frequency would be the reciprocal of the time period over which the object field was observed (Ref 19:206). Since spatial eigenvalues are actually wanted, the sampling frequency is the reciprocal of the width of the one-dimensional object field. Since the width of the object field is d_1 the spatial sampling frequency is $|\bar{f}_1| = 1/d_1$. Therefore, for large d_1 it is asymptotically true that the spatial eigenvalues associated with a near-field, one-dimensional, coherent object field are given by

$$\lambda_i = S_c(i|\vec{f}_1|) = S_c(i/d_1) \qquad i \geq 1,\ i \in \text{integers} \tag{43}$$

Applying Eq (43) yields the spatial eigenvalue distribution illustrated in Figure 7.

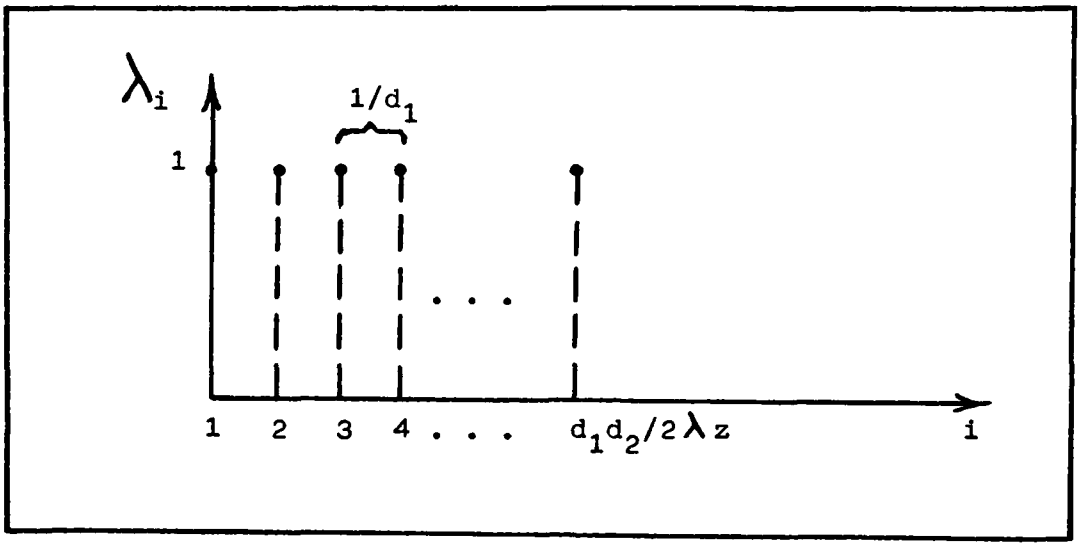

Figure 7 - Spatial Eigenvalue Distribution from Sampled Coherent Power Density Spectrum

The spatial eigenvalue behavior illustrated in Figure 7 is in agreement with the behavior given by Eqs (32) and (33). As the width of the one-dimensional object field increases, the spatial sampling frequency decreases and the discrete distribution of Figure 7 approaches a continuous distribution.

The above procedure is now repeated for a one-dimensional, incoherent object field. For this type of field, Bendinelli, et. al., have shown (Ref 1:1500) that the space-invariant, incoherent imaging kernel is of the form

$$K(|\bar{r}_1-\bar{r}_1'|) = \sin^2(\pi d_2|\bar{r}_1-\bar{r}_1'|/\lambda z)/(\pi d_2|\bar{r}_1-\bar{r}_1'|/\lambda z)^2$$

$$; \quad \bar{r}_1' \in R_1 \qquad (44)$$

The incoherent power density spectrum $S_I(|\bar{f}|)$ of the impulse response associated with the incoherent imaging kernel is the Fourier transform of Eq (44):

$$S_I(|\bar{f}|) = \Lambda(|\bar{f}|\lambda z/d_2) \qquad (45)$$

The power density spectrum given by Eq (45) is illustrated in Figure 8.

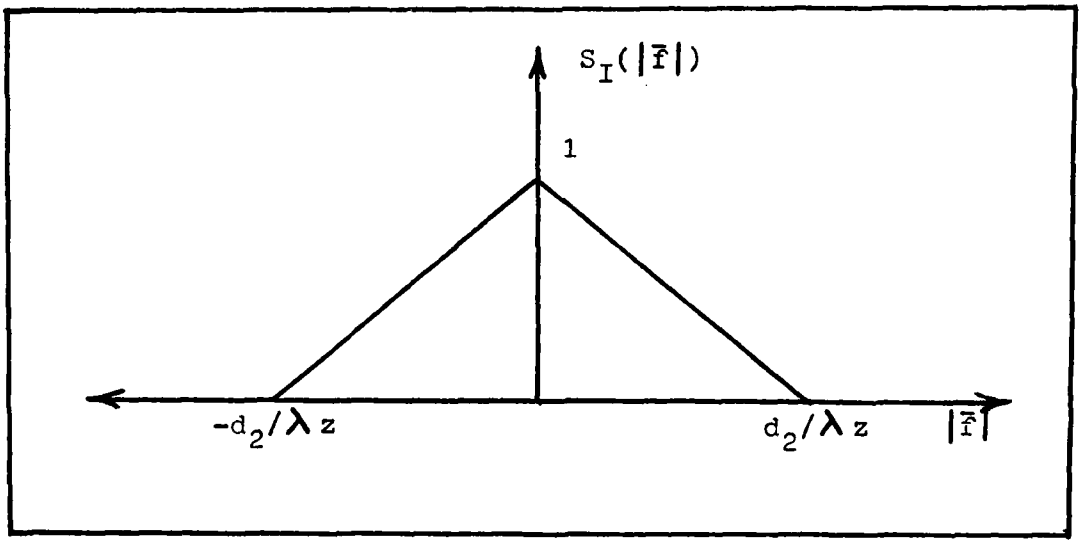

Figure 8 - Incoherent Power Density Spectrum

Again, the spatial sampling frequency is $|\bar{f}_1| = 1/d_1$. Therefore, for large d_1 it is asymptotically true that the

spatial eigenvalues associated with a near-field, one-dimensional, incoherent object field are given by

$$\lambda_i = S_I(i|\bar{f}_1|) = S_I(i/d_1) \qquad i \geq 1 \ , \ i \in \text{integers} \quad (46)$$

Applying Eq (46) yields the spatial eigenvalue distribution illustrated in Figure 9.

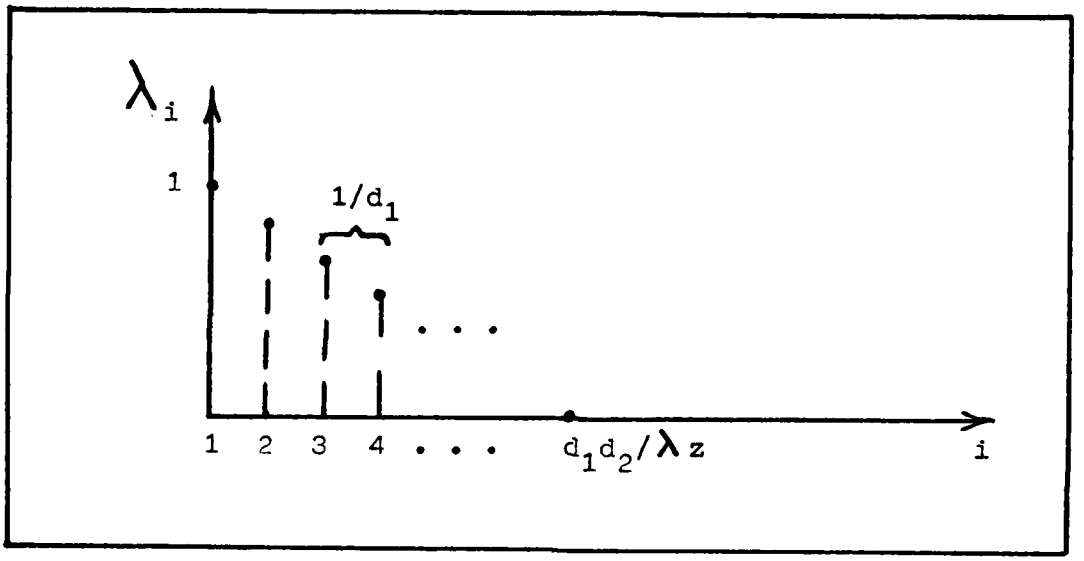

Figure 9 - Spatial Eigenvalue Distribution from Sampled Incoherent Power Density Spectrum

The spatial eigenvalue behavior illustrated in Figure 9 is in agreement with the behavior given by Eqs (30) and (31). As the width of the one-dimensional object field increases, the spatial sampling frequency decreases and the discrete distribution of Figure 9 approaches a continuous distribution.

The next chapter describes the operation of two adaptive imaging receivers and compares the resolution capabilities of the receivers in the spatial domain and the frequency domain.

IV Adaptive Imaging Receivers

This chapter has five purposes. The first purpose is to describe the operation of two ideal, adaptive imaging receivers. The two receivers are the Channel-Matched Filter (CMF) Receiver and the Multiplicative-Phase (MP) Receiver. The second purpose is to derive a turbulent coherent transfer function (CTF) for each receiver. The third purpose is to derive a minimum average integrated mean square error (IMSE) expression for the image field generated by each receiver. The error is the difference between the image field generated for free-space propagation versus the image field generated for propagation through the turbulent atmosphere. The fourth purpose is to use the derived turbulent CTFs and minimum average IMSE expressions to compare the frequency domain and spatial domain resolution capabilities of the CMF and MP Receivers. The final purpose of this chapter is to show the condition that must be satisfied for the results of this chapter to be applicable to object fields composed of many isoplanatic patches (extended object fields).

The first section of this chapter presents the imaging system geometry and field definitions used throughout the chapter. The second section describes the operation of the CMF and MP Receivers. The third section derives a turbulent CTF and minimum average IMSE expression for the CMF Receiver while the fourth section does the same for the MP Receiver. The fifth section compares the two receivers and the final

section is a discussion of extended object field imaging.

General

Figure 10 shows an adaptive imaging system composed of an object field plane P_1, receiving plane P_2 and an image field plane P_3. P_1 has a circular aperture R_1 of diameter d_1, P_2 has a circular aperture R_2 of diameter d_2, and P_3 has a circular aperture R_3 of diameter d_1 (same diameter as R_1). The region between P_1 and P_2 is called the propagation channel. The region between P_2 and P_3 is called the adaptive imaging receiver. The receiving plane P_2 is therefore both the input to the receiver and the output of the propagation channel. For mathematical convenience the length of the adaptive imaging receiver is the same length as the propagation channel. In a real imaging system lenses are used to considerably shorten the length of the adaptive imaging receiver.

The general impulse response of the propagation channel of Figure 10 is $h_{21}(\bar{r}_2,\bar{r}_1)$. When the propagation channel is free-space, the general impulse response is replaced by the free-space impulse response $h_{FS}(\bar{r}_2,\bar{r}_1)$. The free-space impulse response is defined as

$$h_{FS}(\bar{r}_2,\bar{r}_1) = \exp\left[jk(z + |\bar{r}_2-\bar{r}_1|^2/2z)\right]/j\lambda z \qquad (47)$$

Equation (47) is based on the paraxial and Fresnel approximations (Ref 7:58). The paraxial approximation is valid since the distance z between P_1 and P_2 of Figure 10 is much greater than the radii of R_1 and R_2. The Fresnel approximation is valid since the distance z between P_1 and P_2 satisfies the following condition:

$$z^3 \gg \left[k\,(x_2-x_1)^2 + (y_2-y_1)^2\right]^2\Big|_{MAX}/8 \qquad (48)$$

where (x_1,y_1) is a point in R_1 and (x_2,y_2) is a point in R_2.

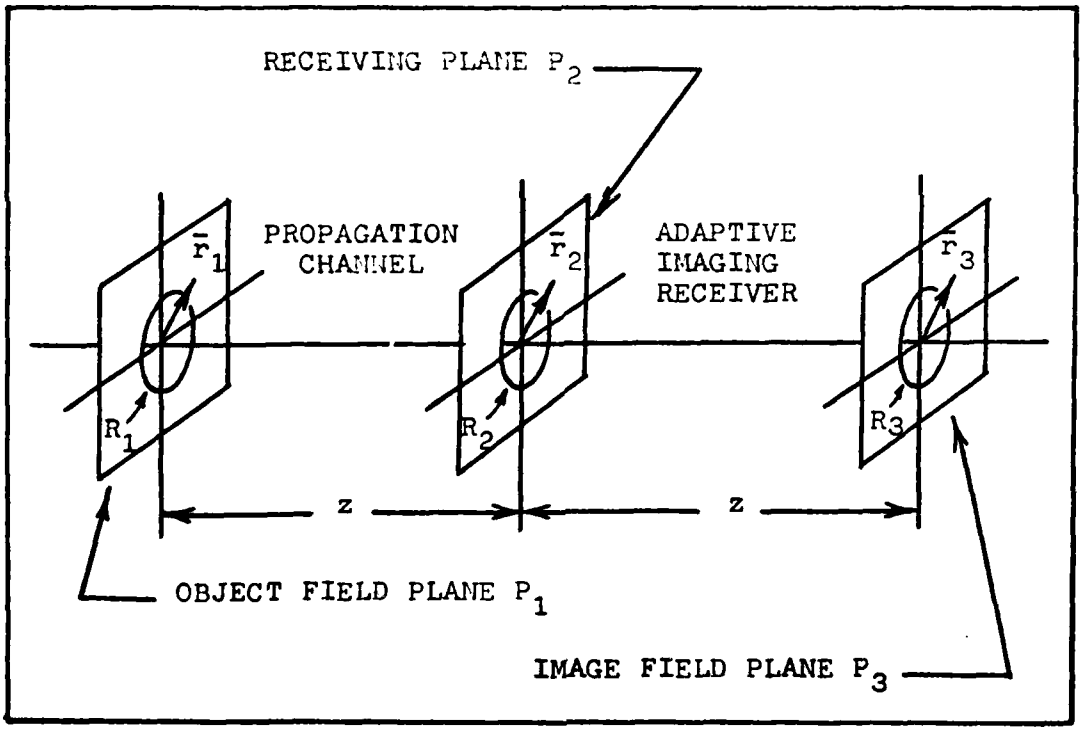

Figure 10 - Geometry for Adaptive Imaging

When the propagation channel of Figure 10 is the turbu-

lent atmosphere, the general impulse response is replaced by the turbulent impulse response $h_{TB}(\bar{r}_2,\bar{r}_1)$. The turbulent impulse response is defined as

$$h_{TB}(\bar{r}_2,\bar{r}_1) = \left\{\exp\left[jk(z + |\bar{r}_2-\bar{r}_1|^2/2z)\right]/j\lambda z\right\}$$

$$x \exp\left[\chi(\bar{r}_2,\bar{r}_1) + j\phi(\bar{r}_2,\bar{r}_1)\right] \qquad (49)$$

where $\chi(\bar{r}_2,\bar{r}_1)$ and $\phi(\bar{r}_2,\bar{r}_1)$ are turbulence-induced log-amplitude and phase fluctuations respectively. They are Gaussian random variables (Ref 17:209) with statistics as given in Appendix I.

$E_I(\bar{r}_1)$ is defined as an unknown but nonrandom object field in R_1 of Figure 10. $E_o(\bar{r}_2)$ is defined as the output field of the propagation channel of Figure 10. By the Huygens-Fresnel Principle (Ref 2:Chap 6), $E_o(\bar{r}_2)$ is

$$E_o(\bar{r}_2) = \int_{R_1} E_I(\bar{r}_1)h_{21}(\bar{r}_2,\bar{r}_1)d\bar{r}_1 \qquad (23)$$

$E_N(\bar{r}_2)$ is defined as a zero-mean, spatially white noise field in R_2 of Figure 10. The autocorrelation function of $E_N(\bar{r}_2)$ is

$$< E_N(\bar{r}_2)E_N^*(\bar{r}_2') > = N_o \delta(\bar{r}_2-\bar{r}_2') \qquad (50)$$

Since $E_N(\bar{r}_2)$ represents additive background noise, the

field $E(\bar{r}_2)$ at the input to the adaptive imaging receiver is

$$E(\bar{r}_2) = E_o(\bar{r}_2) + E_N(\bar{r}_2) \tag{51}$$

The field $E(\bar{r}_2)$ is used in the next section to describe the operation of the CMF and MP Receivers.

Operation of Channel-Matched Filter and Multiplicative-Phase Receivers

The CMF and MP Receivers are ideal, adaptive imaging receivers. They are called ideal because the general impulse response $h_{21}(\bar{r}_2,\bar{r}_1)$ of a propagation channel is known by the receivers. A real receiver does not have complete knowledge of this impulse response. They are called adaptive because they are able to vary their response to a propagated object field such that they partially compensate for the effects of the propagation channel. The effects of interest in this thesis are turbulence-induced log-amplitude and phase fluctuations.

The CMF Receiver operation is simply the propagation of the field $E(\bar{r}_2)$ from P_2 to P_3 of Figure 10 using a receiver impulse response that is the conjugate of the impulse response of the propagation channel. The resultirg image field $\hat{E}_{CMF}(\bar{r}_3)$ generated by the CMF Receiver is (Ref 14:2611)

$$\hat{E}_{CMF}(\bar{r}_3) = \int_{R_2} E(\bar{r}_2)h_{21}^*(\bar{r}_2,\bar{r}_3)d\bar{r}_2 \tag{52}$$

The MP Receiver operation is the multiplication of the field $E(\bar{r}_2)$ by an optimum phase and then the propagation of the field from P_2 to P_3 of Figure 10 using the free-space impulse response. An optimum multiplicative phase is a phase that minimizes the average IMSE of the image field generated by the MP Receiver. The image field $\hat{E}_{MP}(\bar{r}_3)$ generated by the MP Receiver is

$$\hat{E}_{MP}(\bar{r}_3) = \int_{R_2} E(\bar{r}_2)\exp\left[j\,\phi_o(\bar{r}_2)\right]h_{FS}(\bar{r}_2,\bar{r}_3)d\bar{r}_2 \qquad (53)$$

where $\phi_o(\bar{r}_2)$ is an optimum multiplicative phase defined in R_2 of Figure 10.

The next section uses Eq (52) as the basis for deriving the turbulent CTF of the CMF Receiver and the minimum average IMSE of the image field generated by the CMF Receiver.

Channel-Matched Filter Receiver

The turbulent CTF of the CMF Receiver is derived first followed by a derivation of the minimum average IMSE of the image field generated by the CMF Receiver. All averages are with respect to the random log-amplitude and phase fluctuations of the turbulent atmosphere.

Turbulent Coherent Transfer Function - When the propagation channel of Figure 10 is the turbulent atmosphere, the general impulse response $h_{21}^*(\bar{r}_2,\bar{r}_3)$ of Eq (52) is replaced by the turbulent impulse response $h_{TB}^*(\bar{r}_2,\bar{r}_3)$ defined by

Eq (49). For propagation through the turbulent atmosphere, Shapiro has shown (Ref 14:2612) that Eq (52) is rewritten as

$$\exp(jk|\bar{r}_3|^2/2z)\langle\hat{E}_{CMF}(\bar{r}_3)\rangle =$$

$$(d_2/2\lambda z)\int_{R_1}\exp(jk|\bar{r}_1|^2/2z)E_I(\bar{r}_1)\exp\left[-D(|\bar{r}_1-\bar{r}_3|)/2\right]$$

$$\times J_1(\pi|\bar{r}_1-\bar{r}_3|d_2/\lambda z)/(1/|\bar{r}_1-\bar{r}_3|)d\bar{r}_1 \qquad (54)$$

where $D(|\bar{r}_1-\bar{r}_3|)$ is the spherical wave structure function (Ref 4:1374). This function is defined as

$$D(|\bar{r}_1-\bar{r}_3|) = 1.09k^2C_N^2z(|\bar{r}_1-\bar{r}_3|)^{\frac{5}{3}} \qquad (55)$$

where $k = 2\pi/\lambda$ is the wave number, z is the propagation distance of the object field, and C_N^2 is the refractive index structure parameter of the turbulent atmosphere (Ref 9:1526). Equation (54) is derived in Appendix I.

Shapiro has also shown that the average image field $\langle\hat{E}_{CMF}(\bar{r}_3)\rangle$ is obtained by convolving the object field $E_I(\bar{r}_1)$ with the following CMF Receiver average impulse response $\langle h_{CMF}(\bar{r})\rangle$:

$$\langle h_{CMF}(\bar{r})\rangle = d_2\exp\left[-D(|\bar{r}|)/2\right]J_1(\pi|\bar{r}|d_2/\lambda z)/2\lambda z|\bar{r}| \qquad (56)$$

Note that Eq (56) does not include the quadratic phase factors of Eq (54). The factor on the right side of Eq (54) is not included because the propagation distance z satisfies the following condition:

$$z \gg k\left|\bar{r}_1\right|^2\Big|_{MAX}/2 \tag{57}$$

Therefore, the quadratic phase on the right side of Eq (54) is approximately unity over aperture R_1 of Figure 10 (Ref 7:61). The quadratic phase factor on the left side of Eq (54) is not included because it is an image field phase that is due to the geometry of the imaging system rather than to the propagation channel.

The average turbuelnt CTF $<H_{CMF}(\bar{f})>$ of the CMF Receiver is obtained by taking the Fourier transform of Eq (56). The average turbulent CTF is

$$<H_{CMF}(\bar{f})> = 2\pi\int_0^\infty \exp\left[-D(x\pi d_1/2\sqrt{D_{fo}})/2\right]J_1(2\pi x)$$

$$x\, J_o(2\pi\left|\bar{f}'\right| x)dx \tag{58}$$

where $\left|\bar{f}'\right| = \left|\bar{f}\right| 2\lambda z/d_2$ and D_{fo} is defined by Eq (29). Equation (58) is derived in Appendix I.

Shapiro has plotted $<H_{CMF}(\bar{f})>$ for propagation through the worst-case turbulent atmosphere (Ref 14:2612). The worst-case turbulent atmosphere means that apertures R_1 and

R_2 of Figure 10 are the same size and the variance of turbulence log-amplitude fluctuations is 0.5. Shapiro's plots indicate that the average turbulent CTF contains spatial frequencies higher than the free-space, diffraction-limited cutoff $|\bar{f}'|$. This increase in spatial frequency content is probably due to the refractive effect that the turbulent atmosphere has on the propagated object field. Refraction causes changes in the angle-of-arrival of the propagated object field at the CMF Receiver, which results in a spreading of the generated image field. This spreading shows up as an increase in the spatial frequency content of the average turbulent CTF. Because of this effect, the spatial frequency cutoff of the CTF is not a valid measure of the resolution capability of the CMF Receiver. In the following subsection it is shown that the average IMSE of the image field generated by the CMF Receiver is a valid resolution measure.

Integrated Mean Square Error of Image Field - The average IMSE of the image field $\hat{E}_{CMF}(\bar{r}_3)$ generated by the CMF Receiver is:

$$<\text{IMSE}> = \int_{R_3} < \left[E(\bar{r}_3) - \hat{E}_{CMF}(\bar{r}_3)\right]^2 > d\bar{r}_3 \qquad (59)$$

where $E(\bar{r}_3)$ is the image field for free-space propagation. $E(\bar{r}_3)$ is obtained from Eqs (23), (51) and (52) by replacing the general impulse responses with free-space impulse responses. When propagation is through the turbulent atmosphere

and the additive background noise is zero-mean, spatially white noise, it is shown in Appendix J that the average IMSE is

$$
\begin{aligned}
<\text{IMSE}> = \int_{R_3}\int_{R_2}\int_{R_2}\int_{R_1}\int_{R_1} & E_I(\bar{u})E_I^*(\bar{m})h_{FS}(\bar{v},\bar{u})h_{FS}^*(\bar{n},\bar{m}) \\
& \times h_{FS}^*(\bar{v},\bar{r}_3)h_{FS}(\bar{n},\bar{r}_3)<\Big\{1-\exp\big[\chi(\bar{n},\bar{m})\big] \\
& \times \exp\big[\chi(\bar{n},\bar{r}_3)\big]\exp\big[-j\,\phi(\bar{n},\bar{m}) + j\,\phi(\bar{n},\bar{r}_3)\big] \\
& + \exp\big[\chi(\bar{v},\bar{u}) + \chi(\bar{v},\bar{r}_3)\big]\exp\big[j\,\phi(\bar{v},\bar{u})\big] \\
& \times \exp\big[-j\,\phi(\bar{v},\bar{r}_3)\big] + \exp\big[\chi(\bar{v},\bar{u}) + \chi(\bar{n},\bar{m})\big] \\
& \times \exp\big[\chi(\bar{n},\bar{r}_3) + \chi(\bar{v},\bar{r}_3)\big]\exp\big[j\,\phi(\bar{v},\bar{u})\big] \\
& \times \exp\big[-j\,\phi(\bar{v},\bar{r}_3)\big]\exp\big[-j\,\phi(\bar{n},\bar{m}) + j\,\phi(\bar{n},\bar{r}_3)\big]\Big\}> \\
& \times d\bar{u}\,d\bar{m}\,d\bar{v}\,d\bar{n}\,d\bar{r}_3 + N_o D_{fo}
\end{aligned}
$$

$$
; \quad \bar{u}, \bar{m} \in R_1 \qquad \bar{v}, \bar{n} \in R_2 \qquad (60)
$$

where D_{fo} is defined by Eq (29). The integral term in Eq (60) is zero when the object field is isoplanatic. The object field is isoplanatic when its maximum spatial extent is less than the atmospheric coherence length r_o defined in Chapter II.

Isoplanatism permits the turbulence-induced log-amplitude and phase fluctuations of Eq (60) to be written as a function of only aperture R_2 of Figure 10 (Ref 15:463). For isoplanatic conditions, it is shown in Appendix J that Eq (60) reduces to

$$\langle \text{IMSE} \rangle = N_o D_{fo} \tag{61}$$

It is further shown in Appendix J that Eq (61) is valid for free-space propagation even though it is derived from Eq (60) which is based on propagation through the turbulent atmosphere. Therefore, when the object field is isoplanatic and the additive background noise is zero-mean, spatially white noise, the average IMSE of the image field of the CMF Receiver is the same for the turbulent atmosphere as it is for free-space.

Using a different approach than that used in Appendix J, Shapiro has shown (Ref 14:2611) that the IMSE of the image field, conditioned on knowledge of mode-amplitude estimator statistics, is

$$\text{IMSE} = N_o D_f \tag{62}$$

where D_f is defined by Eq (35). Since $\langle D_f \rangle = D_{fo}$ (Ref 13:Appendix), Shapiro's unconditional IMSE expression is the same as Eq (61).

Shapiro has also shown that Eq (61) is not only the

minimum average IMSE expression for the CMF Receiver but that it is also the smallest average IMSE achievable by any ideal, adaptive imaging receiver operating in zero-mean, spatially white background noise. The minimum average IMSE expression of Eq (61) is therefore a standard for comparing the minimum average IMSE expressions of other ideal, adaptive imaging receivers.

The next section derives the minimum average IMSE of the image field generated by the MP Receiver and the turbulent CTF of the MP Receiver.

Multiplicative-Phase Receiver

The minimum average IMSE of the image field generated by the MP Receiver is derived first followed by a derivation of the turbulent CTF. All averages are with respect to the random log-amplitude and phase fluctuations of the turbulent atmosphere.

Integrated Mean Square Error of the Image Field - The average IMSE of the image field $\hat{E}_{MP}(\bar{r}_3)$ generated by the MP Receiver is

$$\langle \text{IMSE} \rangle = \int_{R_2} \left\langle \left[E(\bar{r}_3) - \hat{E}_{MP}(\bar{r}_3) \right]^2 \right\rangle d\bar{r}_3 \qquad (63)$$

where $E(\bar{r}_3)$ is the image field for free-space propagation. $E(\bar{r}_3)$ is obtained from Eqs (23), (51) and (53). In Eq (23) the general impulse response is replaced by the free-space

impulse response and in Eq (53) $\phi_o(\bar{r}_2)$ is set equal to zero.

When propagation is through the turbulent atmosphere and the additive background noise is zero-mean, spatially white noise, it is shown in Appendix K that the average IMSE of the image field is minimized if the optimum multiplicative phase $\phi_o(\bar{r}_2)$ of Eq (53) is chosen such that the following sufficient condition is satisfied:

$$\mathrm{Im}\left\{\int_{R_3}\int_{R_2}\int_{R_1}\int_{R_1} E_I(\bar{u})E_I^*(\bar{m})h_{FS}(\bar{v},\bar{u})h_{FS}^*(\bar{n},\bar{m})h_{FS}^*(\bar{v},\bar{r}_3)\right.$$
$$\times\, h_{FS}(\bar{n},\bar{r}_3)<\exp\left[\chi(\bar{n},\bar{m})\right]\exp\left[-j\,\phi(\bar{n},\bar{m})-j\,\phi_o(\bar{n})\right]$$
$$\times\left[1-\exp\left[\chi(\bar{v},\bar{u})\right]\exp\left[j\,\phi(\bar{v},\bar{u})+j\,\phi_o(\bar{v})\right]\right]>$$
$$\left.\times\, d\bar{u}\,d\bar{m}\,d\bar{v}\,d\bar{r}_3\right\}=0\quad;\quad \bar{u},\bar{m}\in R_1\quad \bar{v},\bar{n}\in R_2 \qquad (64)$$

In Appendix L it is shown that, when the sufficient condition above is satisfied, the minimum average IMSE of the image field generated by the MP Receiver is

$$<\mathrm{IMSE}>=\int_{R_3}\int_{R_2}\int_{R_2}\int_{R_1}\int_{R_1} E_I(\bar{u})E_I^*(\bar{m})h_{FS}(\bar{v},\bar{u})h_{FS}^*(\bar{n},\bar{m})$$
$$\times\, h_{FS}^*(\bar{v},\bar{r}_3)h_{FS}(\bar{n},\bar{r}_3)\left[1-2<\exp\left[\chi(\bar{v},\bar{u})\right]\right.$$
$$\left.\times\,\exp\left[j\,\phi(\bar{v},\bar{u})+j\,\phi_o(\bar{v})\right]>+<\exp\left[\chi(\bar{v},\bar{u})\right]\right.$$

$$\times \exp\left[\chi(\bar{n},\bar{m})\right]\exp\left[j\phi(\bar{v},\bar{u}) + j\phi_o(\bar{v}) - j\phi(\bar{n},\bar{m})\right]$$

$$\times \exp\left[-j\phi_o(\bar{n})\right]>\Big] \, d\bar{u}\, d\bar{m}\, d\bar{v}\, d\bar{n}\, d\bar{r}_3 + N_o D_{fo}$$

$$; \quad \bar{u}, \bar{m} \in R_1 \quad \bar{v}, \bar{n} \in R_2 \qquad (65)$$

Turbulent Coherent Transfer Function - Before the turbulent CTF of the MP Receiver can be derived, a choice must be made for $\phi_o(\bar{r}_2)$ in Eq (53). The choice should satisfy the sufficient condition of Eq (64) and therefore minimize the average IMSE of the image field generated by the MP Receiver. The problem is that there is no $\phi_o(\bar{r}_2)$ that meets this requirement without restrictions first being placed on the propagation conditions or type of object field propagated. However, since many real adaptive receivers cancel turbulence-induced phase fluctuations, a compromise choice is $\phi_o(\bar{r}_2) = -\phi(\bar{r}_2)$. For this choice of $\phi_o(\bar{r}_2)$ and propagation through the turbulent atmosphere, it is shown in Appendix M that Eq (53) is rewritten as

$$\exp(jk|\bar{r}_3|^2/2z)<\hat{E}_{MP}(\bar{r}_3)> = (d_2/2\lambda z)\exp(-\nabla_x^2/2)$$

$$\times \int_{R_1} \exp(jk|\bar{r}_1|^2/2z)E_I(\bar{r}_1)\exp\left[-D_\phi(0,\bar{r}_1)/2\right]$$

$$\times J_1(\pi|\bar{r}_1-\bar{r}_3|d_2/\lambda z)(1/|\bar{r}_1-\bar{r}_3|)d\bar{r}_1 \qquad (66)$$

where $D_\phi(0,\bar{r}_1)$ is the phase structure function defined by Eq (18I) and σ_x^2 is the variance of turbulence-induced-log-amplitude fluctuations.

Since the phase structure function of Eq (66) is not space-invariant, it is not possible to obtain a space-invariant impulse response and then Fourier transform the response to obtain the turbulent CTF of the MP Receiver. However, if the object field is isoplanatic, then the phase structure function in Eq (66) is zero. In this case, the average image field $\langle \hat{E}_{MP}(\bar{r}_3) \rangle$ is obtained by convolving the object field $E_I(\bar{r}_1)$ with the following MP Receiver average impulse response $\langle h_{MP}(\bar{r}) \rangle$:

$$\langle h_{MP}(\bar{r}) \rangle = \exp(-\sigma_x^2/2) d_2 J_1(\pi|\bar{r}|d_2/\lambda z)/2\lambda z|\bar{r}| \quad (67)$$

Note that Eq (67) does not include the quadratic phase factors of Eq (66). They are not included for the reasons given in the previous section. The average turbulent CTF $\langle H_{MP}(\bar{f}) \rangle$ of the MP Receiver is obtained by taking the Fourier transform of Eq (67). The average turbulent CTF is

$$\langle H_{MP}(f) \rangle = \exp(-\sigma_x^2/2) 2\pi \int_0^\infty J_1(2\pi x) J_o(2\pi|\bar{f}'|x)dx \quad (68)$$

where $|\bar{f}'| = |\bar{f}|2\lambda z/d_2$.

The following section uses the turbulent CTFs and

minimum average IMSE expressions derived in this section and the previous section to compare the resolution capabilities of the CMF and MP Receivers.

Comparison of Channel-Matched Filter and Multiplicative-Phase Receivers

The resolution capabilities of the CMF and MP Receivers are first compared in the frequency domain using their turbulent CTFs. This is followed by a comparison in the spatial domain using the minimum average IMSE expressions.

Since the turbulent CTF of the MP Receiver is based on the assumption that the object field is isoplanatic, this same assumption must be applied to the turbulent CTF of the CMF Receiver before a valid comparison of the two receivers can be made. If the object field is isoplanatic, then the spherical wave structure function in Eq (58) is zero and the average turbulent CTF of the CMF Receiver is

$$\langle H_{CMF}(\bar{f}) \rangle = 2\pi \int_0^\infty J_1(2\pi x) J_o(2\pi |\bar{f}'| x) dx \qquad (69)$$

where $|\bar{f}'| = |\bar{f}| 2\lambda z/d_2$.

Comparing Eqs (68) and (69), it is seen that except for a constant amplitude attenuation the turbulent CTF of the MP Receiver is identical to that of the CMF Receiver. Since the attenuation in Eq (68) is independent of spatial frequency the two turbulent CTFs have the same spatial frequency

cutoff. Since this cutoff is not a valid measure of the resolution capability of the CMF Receiver it is also not a valid resolution measure for the MP Receiver. Except for the constant amplitude attenuation in Eq (68), the turbulent CTFs are similar in another way. They both approach $\mathrm{circ}(|\bar{f}|2\lambda z/d_2)$ as $d_2 \rightarrow \infty$, where d_2 is the diameter of the input aperture of either the CMF or the MP Receiver. Recall that $\mathrm{circ}(|\bar{f}|2\lambda z/d_2)$ is the diffraction-limited CTF of a free-space imaging system with a circular aperture of diameter d_2. Therefore, a CMF Receiver with a large input aperture achieves free-space, diffraction-limited resolution of isoplanatic object fields propagated through the turbulent atmosphere as does a large-aperture MP Receiver that only cancels turbulence-induced phase fluctuations.

For the joint conditions of propagation of an isoplanatic object field through the turbulent atmosphere and zero-mean, spatially white background noise, the minimum average IMSE expression of the CMF Receiver is given by Eq (61). For the same conditions, the comparable expression for the MP Receiver is obtained from Eq (65) by letting the turbulence-induced log-amplitude and phase fluctuations be a function of only aperture R_2 of Figure 10. This modification of Eq (65) accounts for an isoplanatic object field.

Comparing Eqs (61) and (65), it is seen that the minimum average IMSE of the image field generated by the MP Receiver differs from the minimum average IMSE of the image field

generated by the CMF Receiver. The amount of difference is the value of the integral term in Eq (65). Since the minimum average IMSE of the image field generated by the CMF Receiver is the smallest average IMSE achievable by any ideal, adaptive imaging receiver operating in zero-mean, spatially white background noise, the integral term in Eq (65) must be non-negative. Therefore, the minimum average IMSE of the image field generated by the MP Receiver is equal to or greater than that of the CMF Receiver. The CMF Receiver can generate an image field having D_{fo} degrees of freedom without the average IMSE of the image field exceeding the minimum average IMSE of Eq (61). The same is true for the MP Receiver only when the integral term in Eq (65) is zero.

There are at least two cases where a value can be chosen for $\phi_o(\bar{r}_2)$ that not only satisfies the sufficient condition given by Eq (64) but also eliminates the integral term in Eq (65). In these two cases the MP Receiver generates an image field having the same minimum average IMSE as an image field generated by the CMF Receiver. The first case is free-space propagation and the proper choice for $\phi_o(\bar{r}_2)$ is $\phi_o(\bar{r}_2) = 0$. The second case is that of an isoplanatic object field propagated through a turbulent atmosphere that only induces phase fluctuations in the field. In this case the proper choice for $\phi_o(\bar{r}_2)$ is $\phi_o(\bar{r}_2) = -\phi(\bar{r}_2)$; the cancellation of turbulence-induced phase fluctuations. This choice is valid for all classes of object fields (coherent,

incoherent, point source, etc.) as long as the field is isoplanatic.

There are at least two cases where the choice of $\phi_o(\bar{r}_2) = -\phi(\bar{r}_2)$ satisfies the sufficient condition given by Eq (64) but does not eliminate the integral term in Eq (65). In these cases the average IMSE of the image field generated by the MP Receiver is a minimum for that receiver but it is greater than the minimum average IMSE of the image field generated by the CMF Receiver. The first case is propagation of a point source field through the turbulent atmosphere while the second is propagation of an isoplanatic, incoherent object field with a real and even object intensity distribution function through the turbulent atmosphere. In both cases the turbulent atmosphere induces log-amplitude and phase fluctuations in the propagated field. It is shown in Appendix N that the sufficient condition given by Eq (64) is satisfied in both cases when $\phi_o(\bar{r}_2) = -\phi(\bar{r}_2)$. It is also shown in Appendix N that the minimum average IMSE of the image field associated with a point source field with a complex amplitude E_o is

$$<\text{IMSE}> = (d_2/2\lambda z)^2 E_o E_o^* \left[1 - 2\exp(-\sigma_x^2/2) + \exp(-\sigma_x^2)\right] \times \int_{R_3} \left[J_1(\pi d_2 |\bar{r}_3|/\lambda z)\right]^2 (1/|\bar{r}_3|)^2 \, d\bar{r}_3 + N_o D_{fo} \tag{70}$$

where σ_x^2 is the variance of turbulence-induced log-amplitude

fluctuations. From Appendix N, the minimum average IMSE of the image field associated with an isoplanatic, incoherent object field with a real and even object intensity distribution function $I(\bar{r}_1)$ is

$$\langle \text{IMSE} \rangle = (d_2/2\lambda z)^2 \left[1 - 2\exp(-\sigma_x^2/2) + \exp(-\sigma_x^2)\right]$$

$$\times \int_{R_3}\int_{R_1} I(\bar{r}_1)\left[J_1(\pi d_2|\bar{r}_3-\bar{r}_1|/\lambda z)\right]^2$$

$$\times (1/|\bar{r}_3-\bar{r}_1|)^2 \, d\bar{r}_1 \, d\bar{r}_3 + N_o D_{fo} \qquad (71)$$

The next section presents the condition that a imaging system must satisfy for the results of this section to be applicable to an object field that extends spatially beyond an isoplanatic patch.

Imaging Extended Object Fields

Much of the preceding work is based on the assumption that the object fields do not extend spatially beyond a single isoplantic patch. Since most object fields of interest are composed of many isoplanatic patches, this would seem to restrict the usefulness of the work. This is not a restriction, however, provided the propagation channel of the imaging system is underspread, Shapiro has shown (Ref 12:472) that an underspread channel is one that insures that the image fields associated with spatially disjoint isoplanatic patches

of an object field are essentially disjoint themselves. Since the image fields are essentially disjoint, imaging an extended object field is reduced to an imaging of each isoplanatic patch and a summation of all the resulting image fields.

The next chapter summarizes the conclusions reached in this thesis and suggests areas requiring further study.

V Conclusion

Conclusions

Space-invariance in an imaging system is a prerequisite for deriving frequency domain transfer functions. In contrast, the spatial domain counterpart of transfer functions, spatial eigenvalue distributions, are derived using the Normal Mode Approach without requiring an imaging system to be space-invariant. This is the main advantage of a spatial domain imaging description.

If a spatial domain imaging system is space-invariant, then for a spatially-large object field it is asymptotically true that the system's spatial eigenvalues and hence its spatial eigenvalue distribution are conveniently obtained by sampling the power density spectrum of the system's impulse response. Since the power density spectrum is a frequency domain concept, the two domains are related through the sampling process. Besides space-invariance and a spatially-large object field, two other conditions must be satisfied for the sampling to yield a correct spatial eigenvalue distribution. The object field being propagated through the system must be in the near field and the maximum phase change across the field must be small.

The shape of an imaging system's spatial eigenvalue distribution depends only on whether an object field propagated through the system is coherent or incoherent. If the object field is coherent the distribution has a rectangular shape.

If the object field is incoherent the distribution has a triangular shape. The highest nonzero eigenvalue order of a spatial eigenvalue distribution is a function of an imaging system's input and output apertures, the propagation medium of the system and the wavelength of an object field propagated through the system. In addition, if the object field is incoherent the highest nonzero eigenvalue order is also a function of any additive background noise in the imaging system. The highest nonzero eigenvalue order is not effected by additive background noise if the object field is coherent.

From the frequency domain, it is concluded that a CMF Receiver with a large input aperture achieves free-space, diffraction-limited resolution of isoplanatic object fields propagated through the turbulent atmosphere. The same conclusion is made for a MP Receiver operating so as to cancel turbulence-induced phase fluctuations.

From the spatial domain, it is concluded that for imaging isoplanatic object fields in zero-mean, spatially white background noise, the CMF Receiver can generate an image field having the maximum obtainable DOF and also the minimum obtainable average IMSE of any ideal adaptive imaging receiver. There are at least two cases when the preceding statement also applies to the MP Receiver. These cases are an object field propagated through free-space and an isoplanatic object field propagated through a turbulent atmosphere that only induces phase fluctuations in the field. In the latter case the MP

Receiver generates an image field having the minimum obtainable average IMSE by cancelling the turbulence-induced phase fluctuations in the propagated object field. For point source fields and isoplanatic, incoherent object fields with real and even object intensity distribution functions, phase cancellation minimizes the average IMSE of the image field generated by the MP Receiver but not to the minimum obtainable average value of the CMF Receiver.

Suggestions for Further Study

The relationship between the spatial domain and frequency domain was shown for a one-dimensional object field propagated through free-space. This relationship should be verified for two-dimensional object fields (square and circular apertures) and for propagation through the turbulent atmosphere.

The sufficient condition given by Eq (64), for minimizing the average IMSE of the field generated by the MP Receiver, is complicated. If possible, an attempt should be made to express the optimum multiplicative phase of the sufficient condition in terms of the object field.

Bibliography

1. Bendinelli, M., et. al., "Degrees of Freedom and Eigenfunctions for the Noisy Image," JOSA, 64 (11): 1498-1502 (November 1974)

2. Born, M. and E. Wolf, Principles of Optics (Fifth Edition). New York: Pergamon Press, 1975.

3. Fante, R., "The Effect of Source Temporal Coherence on Light Scintillations in Weak Turbulence," JOSA, 69 (1): 71-73 (January 1979)

4. Fried, D., "Optical Resolution Through a Randomly Inhomogeneous Medium for Very Long and Very Short Exposures," JOSA, 56 (10): 1372-1379 (October 1964)

5. Fried, D. and G. Mevers, "Evaluation of r_o for Propagation Down Through the Atmosphere," Applied Optics, 13 (11): 2620-2622 (November 1974)

6. Gagliardi, R. and S. Karp, Optical Communications. New York: John Wiley and Sons, 1976.

7. Goodman, J., Introduction to Fourier Optics. New York: McGraw-Hill, 1968.

8. Greenwood, D., "Mutual Coherence Function of a Wave Front Corrected by Zonal Adaptive Optics," JOSA, 69 (4): 549-554 (April 1979)

9. Lawrence, R. and J. Strohbehn, "A Survey of Clear-Air Propagation Effects Relevant to Optical Communications," Proceedings of the IEEE, 58 (10): 1523-1545 (October 1970)

10. Papoulis, A., Probability, Random Variables and Stochastic Processes. New York: McGraw-Hill, 1965.

11. Papoulis, A., Systems and Transforms with Applications in Optics. New York: McGraw-Hill, 1968.

12. Shapiro, J., "Diffraction-Limited Atmospheric Imaging of Extended Objects," JOSA, 66 (5): 469-477 (May 1976)

13. Shapiro, J., "Normal-Mode Approach to Wave Propagation in the Turbulent Atmosphere," Applied Optics, 13 (11): 2614-2619 (November 1974)

14. Shapiro, J., "Optimum Adaptive Imaging Through Atmospheric Turbulence," Applied Optics, 13 (11): 2609-2613 (November 1974)

15. Shapiro, J., "Propagation-Medium Limitations on Phase-Compensated Atmospheric Imaging," JOSA, 66 (5): 460-469 (May 1976)

16. Slepian, D. and H. Pollack, "Prolate Spheroidal Wave Functions, Fourier Analysis and Uncertainty-I," BSTJ, 40 (-): 43-63 (January 1961)

17. Tatarskii, V., Wave Propagation in a Turbulent Medium. New York: Dover, 1967.

18. Toraldo di Francia, G., "Degrees of Freedom of an Image," JOSA, 59 (7): 799-804 (July 1969)

19. Van Trees, H., Detection, Estimation and Modulation Theory-Part I. John Wiley and Sons, Inc., 1968.

Appendix A - Turbulent Coherent Transfer Function

This appendix derives Eq (13), which is the average transfer function for the imaging system of Figure 1 when the propagation channel is the turbulent atmosphere and the object field is coherent. The derivation begins with Eq (12):

$$\langle \tau_{COH}(\bar{f}) \rangle = \tau_{O-COH}(\bar{f}) \langle \exp\left[\chi(\lambda d_i|\bar{f}|) + j\,\phi(\lambda d_i|\bar{f}|)\right] \rangle \quad (12)$$

where $\tau_{O-COH}(\bar{f})$ is the free-space CTF defined by Eq (4), and $\chi(\lambda d_i|\bar{f}|)$ and $\phi(\lambda d_i|\bar{f}|)$ are respectively the log-amplitude and phase fluctuations of the turbulent atmosphere. Since $\chi(\lambda d_i|\bar{f}|)$ and $\phi(\lambda d_i|\bar{f}|)$ are independent random variables (Ref 4:1374), the average on the right side of Eq (12) is written as two averages (Ref 11:211):

$$\langle \tau_{COH}(\bar{f}) \rangle = \tau_{O-COH}(\bar{f}) \langle \exp\left[\chi(\lambda d_i|\bar{f}|)\right] \rangle \times \langle \exp\left[j\,\phi(\lambda d_i|\bar{f}|)\right] \rangle \quad (1A)$$

Prior to evaluating the averages on the right side of Eq (1A), the first and second order statistics of $\chi(\lambda d_i|\bar{f}|)$ and $\phi(\lambda d_i|\bar{f}|)$ are given:

$$\langle \chi(\lambda d_i|\bar{f}|) \rangle = \ell = -\sigma_x^2 \quad (2A)$$

$$\langle \phi(\lambda d_i|\bar{f}|) \rangle = 0 \tag{3A}$$

$$\langle \phi^2(\lambda d_i|\bar{f}|) \rangle = \sigma_\phi^2 \tag{4A}$$

Equation (2A) is a consequence of energy-conservation considerations (Ref 4:1374). It can be shown (Ref 4:1374) that the first average on the right side of Eq (1A) is equivalent to

$$\langle \exp[\chi(\lambda d_i|\bar{f}|)] \rangle = \exp[\langle \chi(\lambda d_i|\bar{f}|) \rangle] \times \exp\left\{\langle [\chi(\lambda d_i|\bar{f}|) - \langle \chi(\lambda d_i|\bar{f}|) \rangle]^2 \rangle / 2\right\} \tag{5A}$$

Substituting Eq (2A) into Eq (5A) yields

$$\langle \exp[\chi(\lambda d_i|\bar{f}|)] \rangle = \exp(-\sigma_\chi^2/2) \tag{6A}$$

It can be shown (Ref 4:1374) that the second average on the right side of Eq (1A) is equivalent to

$$\langle \exp[j\phi(\lambda d_i|\bar{f}|)] \rangle = \exp[\langle j\phi(\lambda d_i|\bar{f}|) \rangle] \times \exp\left\{-\langle [\phi(\lambda d_i|\bar{f}|) - \langle \phi(\lambda d_i|\bar{f}|) \rangle]^2 \rangle / 2\right\} \tag{7A}$$

Substituting Eqs (3A) and (4A) into Eq (7A) yields

$$\langle \exp\left[\chi(\lambda d_i|\bar{f}|)\right]\rangle = \exp(-\nabla_\phi^2/2) \qquad (8A)$$

Substituting Eqs (6A) and (8A) into Eq (1A) yields

$$\langle \tau_{COH}(\bar{f})\rangle = \tau_{O-COH}(\bar{f})\exp\left[-(\nabla_x^2+\nabla_\phi^2)/2\right] \qquad (9A)$$

Finally, letting $\nabla^2 = \nabla_x^2 + \nabla_\phi^2$ yields Eq (13):

$$\langle \tau_{COH}(\bar{f})\rangle = \tau_{O-COH}(\bar{f})\exp(\nabla^2/2) \qquad (13)$$

Appendix B - Fredholm Equation for Normal Mode Imaging

This appendix derives Eq (25) from Eqs (19), (21) and (23). Eq (25) is then used to obtain Eq (26), which is a Fredholm Equation for Normal Mode Imaging. Equations (19), (21) and (23) are repeated below:

$$E_I(\bar{r}_1) = \sum_{i=1}^{\infty} a_i \phi_i(\bar{r}_1) \tag{19}$$

$$E_o(\bar{r}_2) = \sum_{i=1}^{\infty} b_i \Psi_i(\bar{r}_2) \tag{21}$$

$$E_o(\bar{r}_2) = \int_{R_1} E_I(\bar{r}_1) h_{21}(\bar{r}_2, \bar{r}_1) d\bar{r}_1 \tag{23}$$

Substituting Eqs (19) and (21) into Eq (23) yields

$$\sum_{i=1}^{\infty} b_i \Psi_i(\bar{r}_2) = \int_{R_1} \sum_{i=1}^{\infty} a_i \phi_i(\bar{r}_1) h_{21}(\bar{r}_2, \bar{r}_1) d\bar{r}_1 \tag{1B}$$

Changing the order of integration-summation on the right side of Eq (1B) yields

$$\sum_{i=1}^{\infty} b_i \Psi_i(\bar{r}_2) = \sum_{i=1}^{\infty} a_i \int_{R_1} \phi_i(\bar{r}_1) h_{21}(\bar{r}_2, \bar{r}_1) d\bar{r}_1 \tag{2B}$$

If the $\phi_i(\bar{r}_1)$ and $\Psi_i(\bar{r}_2)$ are chosen such that Eq (2B) is satisfied term by term, then the following is true:

$$b_i \Psi_i(\bar{r}_2) = a_i \int_{R_1} \phi_i(\bar{r}_1) h_{21}(\bar{r}_2, \bar{r}_1) d\bar{r}_1 \tag{3B}$$

The ratio of b_i to a_i is defined as

$$b_i/a_i = \sqrt{\lambda_i} \tag{4B}$$

Substituting Eq (48) into Eq (2B) yields Eq (25):

$$\sqrt{\lambda_i}\ \Psi_i(\bar{r}_2) = \int_{R_1} \phi_i(\bar{r}_1) h_{21}(\bar{r}_2,\bar{r}_1) d\bar{r}_1 \tag{25}$$

Since the $\Psi_i(\bar{r}_2)$ in Eq (25) are a CON set of spatial eigenfunctions, the following is true:

$$\int_{R_2} \Psi_i(\bar{r}_2) \Psi_j^*(\bar{r}_2) d\bar{r}_2 = \delta_{ij} \tag{5B}$$

Expressing Eq (25) in terms of $\Psi_i(\bar{r}_2)$ and the conjugate of Eq (25) in terms of $\Psi_j^*(\bar{r}_2)$, and then substituting the resulting expressions into Eq (58) yields

$$\delta_{ij} = (1/\sqrt{\lambda_i\ \lambda_j}) \int_{R_2}\int_{R_1} \phi_i(\bar{r}_1) h_{21}(\bar{r}_2,\bar{r}_1) d\bar{r}_1$$

$$\times \int_{R_1} \phi_j^*(\bar{r}_1') h_{21}^*(\bar{r}_2,\bar{r}_1') d\bar{r}_1\ d\bar{r}_2 \quad ; \quad \bar{r}_1' \in R_1 \tag{6B}$$

Changing the order of integration in Eq (6B) yields

$$\delta_{ij} = (1/\sqrt{\lambda_i\ \lambda_j}) \int_{R_1}\int_{R_1}\int_{R_2} h_{21}(\bar{r}_2,\bar{r}_1) h_{21}^*(\bar{r}_2,\bar{r}_1') d\bar{r}_2$$

$$\times \phi_i(\bar{r}_1)d\bar{r}_1 \phi_j^*(\bar{r}_1')d\bar{r}_1' \quad ; \quad \bar{r}_1' \in R_1 \qquad (7B)$$

One way Eq (7B) is satisfied is for

$$\lambda_i \phi_i(\bar{r}_1') = \int_{R_1}\int_{R_2} h_{21}(\bar{r}_2,\bar{r}_1)h_{21}^*(\bar{r}_2,\bar{r}_1')d\bar{r}_2 \phi_i(\bar{r}_1)d\bar{r}_1$$

$$; \quad \bar{r}_1' \in R_1 \qquad (8B)$$

where the imaging kernel $K(r_1',r_1)$ is defined as

$$K(\bar{r}_1',\bar{r}_1) = \int_{R_2} h_{21}(\bar{r}_2,\bar{r}_1)h_{21}^*(\bar{r}_2,\bar{r}_1')d\bar{r}_2 \quad ; \quad \bar{r}_1' \in R_1 \qquad (27)$$

Substituting Eq (27) into Eq (8B) yields Eq (26):

$$\lambda_i \phi_i(\bar{r}_1') = \int_{R_1} K(\bar{r}_1',\bar{r}_1) \phi_i(\bar{r}_1)d\bar{r}_1 \quad ; \quad \bar{r}_1' \in R_1 \qquad (26)$$

Appendix C - Degrees of Freedom Expression for a Near-Field, Circularly-Apertured, Coherent Object Field Propagated through Free-Space

This appendix derives Eq (29), which is the DOF expression for a near-field, circularly-apertured, coherent object field propagated through free-space. The derivation begins with Eq (25):

$$\lambda_i \phi_i(\bar{r}_1') = \int_{R_1} K(\bar{r}_1', \bar{r}_1)\, \phi_i(\bar{r}_1) d\bar{r}_1 \quad ; \quad \bar{r}_1' \in R_1 \qquad (25)$$

Multiplying both sides of Eq (25) by $\phi_i^*(\bar{r}_1')$ and integrating over R_1 yields

$$\lambda_i \int_{R_1} \phi_i(\bar{r}_1')\, \phi_i^*(\bar{r}_1') d\bar{r}_1' = \int_{R_1}\int_{R_1} K(\bar{r}_1', \bar{r}_1)\, \phi_i(\bar{r}_1)\, \phi_i^*(\bar{r}_1') \times d\bar{r}_1\, d\bar{r}_1' \quad ; \quad \bar{r}_1 \in R_1 \qquad (1C)$$

Using the orthogonality of the $\phi_i^*(\bar{r}_1)$ to simplify the left side of Eq (1C) yields

$$\lambda_i = \int_{R_1}\int_{R_1} K(\bar{r}_1', \bar{r}_1)\, \phi_i(\bar{r}_1)\, \phi_i^*(\bar{r}_1') d\bar{r}_1\, d\bar{r}_1' \quad ; \quad \bar{r}_1 \in R_1 \qquad (2C)$$

Summing both sides of Eq (2C) over all values of i yields

$$\sum_{i=1}^{\infty} \lambda_i = \int_{R_1}\int_{R_1} K(\bar{r}_1', \bar{r}_1) \sum_{i=1}^{\infty} \phi_i(\bar{r}_1)\, \phi_i^*(\bar{r}_1') d\bar{r}_1\, d\bar{r}_1' \quad ; \quad \bar{r}_1 \in R_1 \qquad (3C)$$

Applying Mercer's Theorem to the right side of Eq (3C) yields

$$\sum_{i=1}^{\infty}\lambda_i = \int_{R_1}\int_{R_1} K(\bar{r}_1',\bar{r}_1)\,\delta(\bar{r}_1'-\bar{r}_1)d\bar{r}_1\,d\bar{r}_1' \quad ; \quad \bar{r}_1' \in R_1 \tag{4C}$$

Using the sifting property of the delta function, Eq (4C) is simplified to

$$\sum_{i=1}^{\infty}\lambda_i = \int_{R_1} K(\bar{r}_1,\bar{r}_1)d\bar{r}_1 \tag{5C}$$

For free-space propagation, the imaging kernel $K(\bar{r}_1,\bar{r}_1)$ in Eq (5C) is defined as

$$K(\bar{r}_1,\bar{r}_1) = \int_{R_2} h_{FS}(\bar{r}_2,\bar{r}_1)h_{FS}^{*}(\bar{r}_2,\bar{r}_1)d\bar{r}_2 \tag{6C}$$

where

$$h_{FS}(\bar{r}_2,\bar{r}_1) = \exp\left[jk(z + |\bar{r}_2-\bar{r}_1|^2/2z)\right]/j\lambda z \tag{47}$$

Substituting Eq (47) into Eq (6C) yields

$$K(\bar{r}_1,\bar{r}_1) = (1/\lambda z)^2\int_{R_2} d\bar{r}_2 = \pi(d_2/2\lambda z)^2 \tag{7C}$$

where R_2 is a circular aperture of diameter d_2. Substituting Eq (7C) into Eq (5C) yields

$$\sum_{i=1}^{\infty}\lambda_i = \pi(d_2/2\lambda z)^2\int_{R_1} d\bar{r}_1 = (\pi d_1 d_2/4\lambda z)^2 \qquad (8C)$$

where R_1 is a circular aperture of diameter d_1. For a near-field, circularly-apertured, coherent object field propagated through free-space the spatial eigenvalue behavior is given by Eq (28):

$$\lambda_i = \begin{cases} 1 \;\; ; \;\; i \leq D_{fo} \\ 0 \;\; ; \;\; i > D_{fo} \end{cases} \qquad i \geq 1 \;\; , \; i \in \text{integers} \qquad (28)$$

From Eq (28), the summation of λ_i over all values of i yields

$$\sum_{i=1}^{\infty}\lambda_i = D_{fo} \qquad (9C)$$

Equating Eqs (8C) and (9C) yields Eq (29):

$$D_{fo} = (\pi d_1 d_2/4\lambda z)^2 \qquad (29)$$

Appendix D - Sampling Theorem Derivation of a Degrees of Freedom Expression

This appendix derives Eq (29) using the Sampling Theorem. Equation (29) is the DOF expression for a near-field, circularly-apertured, coherent object field propagated through free-space. The Sampling Theorem says (Ref 6:93) that the number of DOF of an image field is obtained by dividing the solid angle subtended by an object field aperture R_1 (when viewed from the image field aperture R_2) by the diffraction limited field of view of the image field R_2. In this appendix apertures R_1 and R_2 are circular apertures of diameters d_1 and d_2 respectively. The apertures, solid angle Ω_S and field of view Ω_{DL} mentioned above are illustrated in Figure 11. P_1 of Figure 11 is an object field plane while P_2 is an image field plane. The planes are separated by free-space.

The solid angle Ω_S subtended by the object field aperture R_1 of Figure 11 is

$$\Omega_S = A_{R_1}/z^2 \tag{1D}$$

where

$$A_{R_1} = \pi d_1^2/4 \tag{2D}$$

The diffraction limited field of view Ω_{DL} of the image field aperture R_2 of Figure 11 is (Ref 6:93)

$$\Omega_{DL} = \lambda^2/A_{R_2} \tag{3D}$$

where

$$A_{R_2} = \pi d_2^{\,2}/4 \tag{4D}$$

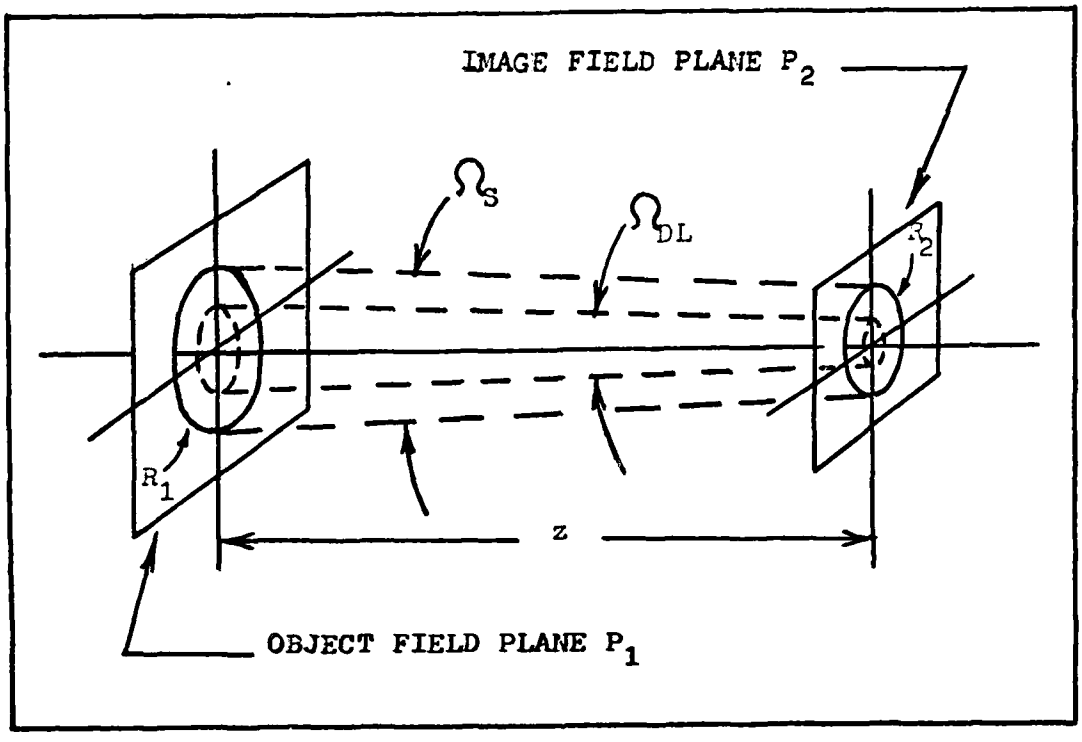

Figure 11 - Sampling Theorem Geometry

Dividing Eq (1D) by Eq (3D) yields Eq (29):

$$D_{fo} = (A_{R_1}/z^2)/(\lambda^2/A_{R_2}) = (\pi d_1 d_2/4\lambda z)^2 \tag{29}$$

where D_{fo} is the number of DOF of the image field associated with the object field described at the beginning of this appendix.

Appendix E - Degrees of Freedom Expression for a Near-Field, Circularly-Apertured, Coherent Object Field Propagated through The Turbulent Atmosphere

This appendix derives Eq (35), which is the DOF expression for a near-field, circularly-apertured, coherent object field propagated through the turbulent atmosphere. The derivation begins with Eq (5C) from Appendix C:

$$\sum_{i=1}^{\infty}\lambda_i = \int_{R_1} K(\bar{r}_1,\bar{r}_1)d\bar{r}_1 \tag{5C}$$

For propagation through the turbulent atmosphere, the imaging kernel $K(\bar{r}_1,\bar{r}_1)$ in Eq (5C) is defined as

$$K(\bar{r}_1,\bar{r}_1) = \int_{R_2} h_{TB}(\bar{r}_2,\bar{r}_1)h_{TB}^{*}(\bar{r}_2,\bar{r}_1)d\bar{r}_2 \tag{1E}$$

where

$$h_{TB}(\bar{r}_2,\bar{r}_1) = \left\{\exp\left[jk(z + |\bar{r}_2-\bar{r}_1|^2/2z)\right]/j\lambda z\right\}$$

$$x \exp\left[\chi(\bar{r}_2,\bar{r}_1) + j\phi(\bar{r}_2,\bar{r}_1)\right] \tag{49}$$

Substituting Eq (49) into Eq (1E) yields

$$K(\bar{r}_1,\bar{r}_1) = (1/\lambda z)^2 \int_{R_2} \exp\left[2\chi(\bar{r}_2,\bar{r}_1)\right]d\bar{r}_2 \tag{2E}$$

Substituting Eq (2E) into Eq (5C) yields

$$\sum_{i=1}^{\infty}\lambda_i = (1/\lambda z)^2 \int_{R_1}\int_{R_2} \exp\left[2\chi(\bar{r}_2,\bar{r}_1)\right] d\bar{r}_2\, d\bar{r}_1 \qquad (3E)$$

For a near-field, circularly-apertured, coherent object field propagated through the turbulent atmosphere, the spatial eigenvalue behavior is given by Eq (34):

$$\lambda_i = \begin{cases} 1 \;;\; i \leq D_f & i \geq 1 \;,\; i \in \text{integers} \\ 0 \;;\; i > D_f \end{cases} \qquad (34)$$

From Eq (34), the summation of λ_i over all values of i yields

$$\sum_{i=1}^{\infty}\lambda_i = D_f \qquad (4E)$$

Equating Eqs (3E) and (4E) yields Eq (35):

$$D_f = (1/\lambda z)^2 \int_{R_1}\int_{R_2} \exp\left[2\chi(\bar{r}_2,\bar{r}_1)\right] d\bar{r}_2\, d\bar{r}_1 \qquad (35)$$

Appendix F - The Consequence of Energy Conservation with Regard to the Degrees of Freedom of an Image Field

This appendix shows that since the mean of $\chi(\bar{r}_2,\bar{r}_1)$ must equal the negative of the variance of $\chi(\bar{r}_2,\bar{r}_1)$, the average of D_f must equal D_{fo}. $\chi(\bar{r}_2,\bar{r}_1)$ represents the log-amplitude fluctuations of the turbulent atmosphere. D_f is the number of DOF of the image field associated with a near-field, circularly-apertured, coherent object field propagated through the turbulent atmosphere while D_{fo} is the number of DOF of the image field associated with the same object field propagated through free-space. $< D_f >$ and D_{fo} are defined as follows:

$$D_f = (1/\lambda z)^2 \int_{R_1}\int_{R_2} < \exp\left[2\chi(\bar{r}_2,\bar{r}_1)\right] > d\bar{r}_2\, d\bar{r}_1 \qquad (1F)$$

$$D_{fo} = (1/\lambda z)^2 \int_{R_1}\int_{R_2} d\bar{r}_2\, d\bar{r}_1 \qquad (2F)$$

It can be shown (Ref 3:71) that the average in Eq (1F) is equivalent to

$$< \exp\left[2\chi(\bar{r}_2,\bar{r}_1)\right] > = \exp\left[2<\chi(\bar{r}_2,\bar{r}_1)>\right] \times \exp\left\{<\left[2\chi(\bar{r}_2,\bar{r}_1) - 2<\chi(\bar{r}_2,\bar{r}_1)>\right]^2>/2\right\} \qquad (3F)$$

Energy conservation requires the following to be true

(Ref 4:1374):

$$\langle \chi(\bar{r}_2,\bar{r}_1) \rangle = \ell = -\sigma_x^2 \tag{4F}$$

where ℓ is the mean of $\chi(\bar{r}_2,\bar{r}_1)$ and σ_x^2 is the variance of $\chi(\bar{r}_2,\bar{r}_1)$. Substituting Eq (4F) into Eq (3F) yields

$$\langle \exp\left[2\chi(\bar{r}_2,\bar{r}_1)\right] \rangle = 1 \tag{5F}$$

Substituting Eq (5F) into Eq (1F) reduces Eq (1F) to Eq (2F) and yields

$$\langle D_f \rangle = D_{fo} \tag{6F}$$

Appendix G - Average IMSE of a Normal Mode Image Field in Additive Background Noise

This appendix derives Eq (38), which is the average IMSE of a Normal Mode image field in additive background noise. The derivation follows the example of Bendinelli, et. al., (Ref 1:1499). The average IMSE of the Normal Mode image field is

$$<\text{IMSE}(N)> = \int_{R_2} <\left[E_o(\bar{r}_2) - E_o'(\bar{r}_2)\right]^2> d\bar{r}_2 \qquad (36)$$

where

$$E_o(\bar{r}_2) = \sum_{i=1}^{\infty} b_i \Psi_i(\bar{r}_2) \qquad (21)$$

and where

$$E_o'(\bar{r}_2) = \sum_{i=1}^{N} (b_i + n_i) \Psi_i(\bar{r}_2) \qquad (37)$$

$E_o(\bar{r}_2)$ is the image field generated in aperture R_2 of Figure 2 in the absence of background noise while $E_o'(\bar{r}_2)$ is an estimate of the image field generated when background noise is present. The number N in Eq (37) is chosen such that the average IMSE of the image field is minimized. This is the reason N appears as an argument in Eq (36). The n_i in Eq (37) are the random noise coefficients of the zero-mean, spatially white noise. The average of Eq (36) is with respect to these random noise coefficients. The $\Psi_i(\bar{r}_2)$ in Eqs (21)

and (37) are a CON set of spatial eigenfunctions defined in image field aperture R_2 of Figure 2. The b_i in Eqs (21) and (23) are image field weighting coefficients that are related to object field weighting coefficients by

$$b_i = \sqrt{\lambda_i}\, a_i \tag{1G}$$

Substituting Eq (1G) into Eqs (21) and (37), and then substituting Eqs (21) and (37) into Eq (36) yields

$$\langle \text{IMSE}(N) \rangle = \int_{R_2} \left\langle \left[\sum_{i=N+1}^{\infty} \sqrt{\lambda_i}\, a_i \Psi_i(\bar{r}_2) - \sum_{i=1}^{N} n_i \Psi_i(\bar{r}_2) \right]^2 \right\rangle d\bar{r}_2 \tag{2G}$$

Expanding Eq (2G) and reversing the integration-summation order yields

$$\begin{aligned} \langle \text{IMSE}(N) \rangle = & \sum_{i=N+1}^{\infty} \sum_{j=N+1}^{\infty} \sqrt{\lambda_i}\, \sqrt{\lambda_j} a_i a_j \int_{R_2} \Psi_i(\bar{r}_2)\, \Psi_j^*(\bar{r}_2) d\bar{r}_2 \\ & + \sum_{i=1}^{N} \sum_{j=1}^{N} \langle n_i n_j \rangle \int_{R_2} \Psi_i(\bar{r}_2)\, \Psi_j^*(\bar{r}_2) d\bar{r}_2 \\ & - 2 \sum_{i=N+1}^{\infty} \sum_{j=1}^{N} \sqrt{\lambda_i} a_i \langle n_j \rangle \int_{R_2} \Psi_i(\bar{r}_2)\, \Psi_j^*(\bar{r}_2) d\bar{r}_2 \end{aligned} \tag{3G}$$

By the orthogonality of the $\Psi_i(\bar{r}_2)$

$$\int_{R_2} \Psi_i(\bar{r}_2)\, \Psi_j^*(\bar{r}_2) d\bar{r}_2 = \delta_{ij} \tag{4G}$$

Substituting Eq (4G) into Eq (3G), and noting that the last term in Eq (3G) is zero because the summations are over disjoint intervals, yields

$$\langle \text{IMSE}(N) \rangle = \sum_{i=N+1}^{\infty} \lambda_i |a_i|^2 + \sum_{i=1}^{N} \langle |n_i|^2 \rangle \qquad (5G)$$

Since the additive background noise is zero-mean, the average on the right side of Eq (5G) is

$$\langle |n_i|^2 \rangle = \sigma_\eta^2 \qquad (6G)$$

where σ_η^2 is the variance of the noise. Substituting Eq (6G) into Eq (5G) yields (after a rearrangement of terms) Eq (38):

$$\langle \text{IMSE}(N) \rangle = \sum_{i=N+1}^{\infty} \lambda_i |a_i|^2 - \sum_{i=1}^{N} (\lambda_i |a_i|^2 - \sigma_\eta^2) \qquad (38)$$

Appendix H - Space-Invariant Imaging Kernel for a Near-Field One-Dimensional Coherent Object Field Propagated through Free-Space

This appendix derives Eq (41), which is the space-invariant imaging kernel for a near-field ($D_{fo}'/2 \gg 1$), one-dimensional, coherent object field propagated through free-space. With respect to Figure 2, the general expression for the imaging kernel $K(\bar{r}_1', \bar{r}_1)$ is given by Eq (27):

$$K(\bar{r}_1', \bar{r}_1) = \int_{R_2} h_{21}(\bar{r}_2, \bar{r}_1) h_{21}^*(\bar{r}_2, \bar{r}_1') d\bar{r}_2 \quad ; \quad \bar{r}_1' \in R_1 \tag{27}$$

where R_1 is the object field aperture, R_2 is the image field aperture and $h_{21}(\bar{r}_2, \bar{r}_1)$ is the general impulse response of the propagation channel. For a one-dimensional object field, R_1 is a slit aperture of width d_1. For the associated one-dimensional image field, R_2 is a slit aperture of width d_2. For free-space propagation, the general impulse response $h_{21}(\bar{r}_2, \bar{r}_1)$ is replaced by the free-space impulse response $h_{FS}(\bar{r}_2, \bar{r}_1)$. For a space-invariant imaging kernel, $K(\bar{r}_1', \bar{r}_1)$ is replaced by $K(|\bar{r}_1 - \bar{r}_1'|)$. Therefore, for a near-field ($D_{fo}'/2 \gg 1$), one-dimensional, coherent object field propagated through free-space, the space-invariant imaging kernel from Eq (27) is

$$K(|\bar{r}_1 - \bar{r}_1'|) = \int_{-d_2/2}^{+d_2/2} h_{FS}(\bar{r}_2, \bar{r}_1) h_{FS}^*(\bar{r}_2, \bar{r}_1') d\bar{r}_2 \quad ; \quad \bar{r}_1' \in R_1 \tag{1H}$$

where

$$h_{FS}(\bar{r}_2,\bar{r}_1) = \exp\left[jk(z + |\bar{r}_2-\bar{r}_1|^2/2z)\right]/j\lambda z \qquad (47)$$

Substituting Eq (47) into Eq (1H) yields

$$K(|\bar{r}_1-\bar{r}_1'|) = (1/\lambda z)^2\exp\left[jk(|\bar{r}_1|^2 - |\bar{r}_1'|^2)/2z\right] \times \int_{-d_2/2}^{+d_2/2} \exp\left[-jk\bar{r}_2.(\bar{r}_1-\bar{r}_1')/2z\right]d\bar{r}_2 \quad ; \quad \bar{r}_1' \in R_1 \qquad (2H)$$

Evaluating the integral in Eq (2H) and using the identity $\sin(w) = \left[\exp(w) - \exp(-w)\right]/2j$ yields

$$K(|\bar{r}_1-\bar{r}_1'|) = (1/\lambda z)\exp\left[jk(|\bar{r}_1|^2 - |\bar{r}_1'|^2)/2z\right] \times \sin(\pi d_2|\bar{r}_1-\bar{r}_1'|/\lambda z)/\pi|\bar{r}_1-\bar{r}_1'| \quad ; \quad \bar{r}_1' \in R_1 \qquad (3H)$$

If the maximum phase change across the object field is less than some small radian measure such as $\pi/8$, then the quadratic phase term in Eq (3H) may be eliminated. The condition for elimination is

$$K(|\bar{r}_1|^2 - |\bar{r}_1'|^2)|_{MAX}/2z << \pi/8 \qquad (4H)$$

AD-A080 414 AIR FORCE INST OF TECH WRIGHT-PATTERSON AFB OH SCHOO--ETC F/G 9/3
SPATIAL DOMAIN AND SPATIAL FREQUENCY DOMAIN IMAGING.(U)
DEC 79 K W KIRLIN
UNCLASSIFIED AFIT/GEO/EE/79-3 NL

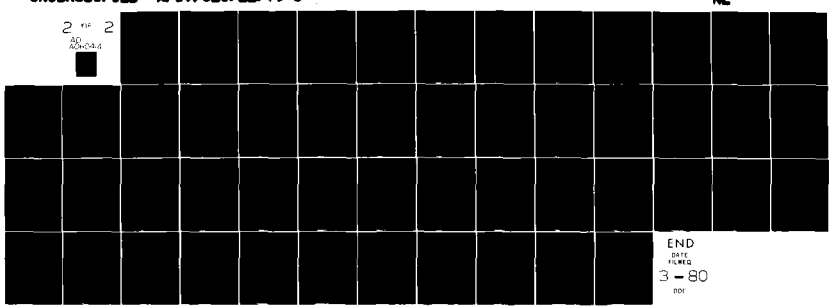

Since the width of the object field aperture is d_1, the quantity $(|\bar{r}_1|^2 - |\bar{r}_1'|^2)|_{MAX}$ in Eq (4H) is equivalent to

$$(|\bar{r}_1|^2 - |\bar{r}_1'|^2)|_{MAX} = (d_1/2)^2 \tag{5H}$$

Substituting Eq (5H) into Eq (4H) yields

$$z \gg 2d_1^2/\lambda \tag{6H}$$

When Eq (6H) is satisfied, Eq (3H) reduces to Eq (41):

$$K(|\bar{r}_1-\bar{r}_1'|) = \sin(\pi d_2|\bar{r}_1-\bar{r}_1'|/\lambda z)/\pi|\bar{r}_1-\bar{r}_1'| \quad ; \quad \bar{r}_1' \in R_1 \tag{41}$$

where the $(1/\lambda z)$ constant in Eq (3H) is dropped because it is unimportant to the general form of the coherent imaging kernel.

In addition to Eq (6H), there is another condition that must be satisfied for Eq (41) to be true. The additional condition is that the one-dimensional coherent object field be in the near-field. This means that

$$D_{fo}'/2 \gg 1 \tag{7H}$$

where

$$D_{fo}'/2 = d_1 d_2/2\lambda z \tag{33}$$

Substituting Eq (33) into Eq (7H) yields

$$d_2 \gg 2\lambda z/d_1 \tag{8H}$$

Therefore, for Eq (41) to be true, the propagation distance z must be large enough to satisfy Eq (6H) and the width of the image field aperture must be large enough to satisfy Eq (8H).

Appendix I - Image Field and Average Coherent Transfer Function of the Channel-Matched Filter Receiver

This appendix derives Eqs (54) and (58). Equation (54) is the expression for the image field generated by the CMF Receiver while Eq (58) is the expression for the average CTF of the CMF Receiver. The derivation of both equations begins with Eq (52):

$$\hat{E}_{CMF}(\bar{r}_3) = \int_{R_2} E(\bar{r}_2) h_{21}^*(\bar{r}_2,\bar{r}_3) d\bar{r}_2 \tag{52}$$

If propagation is through the turbulent atmosphere then the general impulse response, $h_{21}(\bar{r}_2,\bar{r}_3)$, of Eq (52) is replaced by the impulse response, $h_{TB}(\bar{r}_2,\bar{r}_3)$. Equation (52) is then rewritten as

$$\hat{E}_{CMF}(\bar{r}_3) = \int_{R_2} E(\bar{r}_2) h_{TB}^*(\bar{r}_2,\bar{r}_3) d\bar{r}_2 \tag{1I}$$

where

$$h_{TB}(\bar{r}_2,\bar{r}_3) = \left\{ \exp\left[jk(z + |\bar{r}_2-\bar{r}_3|^2/2z) \right] / j\lambda z \right\}$$

$$\times \exp\left[\chi(\bar{r}_2,\bar{r}_3) + j\phi(\bar{r}_2,\bar{r}_3) \right] \tag{49}$$

The field $E(\bar{r}_2)$ of Eq (52) is the input to the CMF Receiver. By Eq (51) it is

$$E(\bar{r}_2) = E_o(\bar{r}_2) + E_N(\bar{r}_2) \tag{51}$$

where $E_o(\bar{r}_2)$ is the output field of the propagation channel and $E_N(\bar{r}_2)$ is a zero-mean, spatially white noise field representing additive background noise. For propagation through the turbulent atmosphere the field $E_o(\bar{r}_2)$ is expressed as

$$E_o(\bar{r}_2) = \int_{R_1} E_I(\bar{r}_1) h_{TB}(\bar{r}_2, \bar{r}_1) d\bar{r}_1 \tag{2I}$$

where $E_I(\bar{r}_1)$ is an unknown but nonrandom object field in aperture R_1 of Figure 10. Substituting Eqs (51) and (2I) into Eq (1I) yields

$$\hat{E}_{CMF}(\bar{r}_3) = \int_{R_2}\int_{R_1} E_I(\bar{r}_1) h_{TB}(\bar{r}_2, \bar{r}_1) h_{TB}^*(\bar{r}_2, \bar{r}_3)\, d\bar{r}_1\, d\bar{r}_2 + \int_{R_2} E_N(\bar{r}_2) h_{TB}^*(\bar{r}_2, \bar{r}_3) d\bar{r}_2 \tag{3I}$$

Since $\chi(\bar{r}', \bar{r})$ and $\phi(\bar{r}', \bar{r})$ are random variables, the turbulent impulse response given by Eq (49) is a random function. Therefore, the image field given by Eq (3I) is also random. On the average however the field is

$$\langle \hat{E}_{CMF}(\bar{r}_3) \rangle = \int_{R_2}\int_{R_1} E_I(\bar{r}_1) \langle h_{TB}(\bar{r}_2, \bar{r}_1) h_{TB}^*(\bar{r}_2, \bar{r}_3) \rangle \times d\bar{r}_1\, d\bar{r}_2 \tag{4I}$$

where the second term in Eq (3I) is dropped because the noise field is zero-mean. Substituting Eq (49) into Eq (4I) yields

$$\exp(jk|\bar{r}_3|^2/2z)\langle\hat{E}_{CMF}(\bar{r}_3)\rangle = (1/\lambda z)^2 \int_{R_1} \exp(jk|\bar{r}_1|^2/2z)$$

$$\times E_I(\bar{r}_1) \int_{R_2} \exp\left[-jk(\bar{r}_1-\bar{r}_3).\bar{r}_2/z\right] \langle \exp\left[\chi(\bar{r}_2,\bar{r}_1)\right]$$

$$\times \exp\left[\chi(\bar{r}_2,\bar{r}_3)\right]\rangle\langle\exp\left[j\phi(\bar{r}_2,\bar{r}_1) - j\phi(\bar{r}_2,\bar{r}_3)\right]\rangle$$

$$\times d\bar{r}_2\, d\bar{r}_1 \qquad (5I)$$

where the average of the right side of Eq (5I) is written as two separate averages of $\chi(\bar{r}',\bar{r})$ and $\phi(\bar{r}',\bar{r})$ since these are independent random variables (Ref 4:1374). Furthermore, $\chi(\bar{r}',\bar{r})$ and $\phi(\bar{r}',\bar{r})$ are Gaussian random variables (Ref 4:1374) with the following statistics:

$$\langle\chi(\bar{r}',\bar{r})\rangle = \mathcal{L} = -\nabla_\chi^2 \qquad (6I)$$

$$\langle\phi(\bar{r}',\bar{r})\rangle = 0 \qquad (7I)$$

$$\langle\phi^2(\bar{r}',\bar{r})\rangle = \nabla_\phi^2 \qquad (8I)$$

It can be shown (Ref 4:1374) that the first average on the right side of Eq (5I) can be expressed as

$$\langle \exp\left[\chi(\bar{r}_2,\bar{r}_1) + \chi(\bar{r}_2,\bar{r}_3)\right]\rangle = \exp\left[\langle \chi(\bar{r}_2,\bar{r}_1)\rangle\right]$$

$$\times \exp\left[\langle \chi(\bar{r}_2,\bar{r}_3)\rangle\right] \exp\left\{\langle\left[\chi(\bar{r}_2,\bar{r}_1)\right.\right.$$

$$\left.\left. - \langle \chi(\bar{r}_2,\bar{r}_1)\rangle\right]^2\rangle/2\right\} \exp\left\{\langle\left[\chi(\bar{r}_2,\bar{r}_3)\right.\right.$$

$$\left.\left. - \langle \chi(\bar{r}_2,\bar{r}_3)\rangle\right]^2\rangle/2\right\} \qquad (9I)$$

Substituting Eq (6I) into Eq (9I) yields

$$\langle \exp\left[\chi(r_2,r_1) + \chi(r_2,r_3)\right]\rangle =$$

$$\exp(-2\sigma_\chi^2) \exp\left\{\left[\langle \chi^2(\bar{r}_2,\bar{r}_1)\rangle - \ell^2\right]/2\right\}$$

$$\times \exp\left\{\left[\langle \chi^2(\bar{r}_2,\bar{r}_3)\rangle - \ell^2\right]/2\right\} \qquad (10I)$$

Since $\sigma_\chi^2 = \langle \chi^2(\bar{r}',\bar{r})\rangle - \ell^2$, Eq (10I) is simplified to

$$\langle \exp\left[\chi(\bar{r}_2,\bar{r}_1) + \chi(\bar{r}_2,\bar{r}_3)\right]\rangle =$$

$$\exp\left\{-\left[\langle \chi^2(\bar{r}_2,\bar{r}_1)\rangle + \langle \chi^2(\bar{r}_2,\bar{r}_3)\rangle - 2\ell^2\right]/2\right\} \qquad (11I)$$

Equation (11I) is reduced further to

$$\langle \exp\left[\chi(\bar{r}_2,\bar{r}_1) + \chi(\bar{r}_2,\bar{r}_3)\right]\rangle =$$

$$\exp\left\{-\langle\left[\chi(\bar{r}_2,\bar{r}_1) - \chi(\bar{r}_2,\bar{r}_3)\right]^2\rangle/2\right\} \qquad (12I)$$

Now, the log-amplitude structure function is defined as (Ref 4:1374)

$$D_\chi(\bar{\rho}',\bar{\rho}) = \langle\left[\chi(\bar{r}'+\bar{\rho}' , \bar{r}+\bar{\rho}) - \chi(\bar{r}',\bar{r})\right]^2\rangle \qquad (13I)$$

Using Eq (13I) in Eq (12I) where $\bar{\rho}' = 0$ and $\bar{\rho} = \bar{r}_1-\bar{r}_3$ gives

$$\langle \exp\left[\chi(\bar{r}_2,\bar{r}_1) + \chi(\bar{r}_2,\bar{r}_3)\right]\rangle = \exp\left[-D_\chi(|\bar{r}_1-\bar{r}_3|)/2\right] \qquad (14I)$$

The second average on the right side of Eq (5I) can be expressed as

$$\langle \exp\left[j\,\phi(\bar{r}_2,\bar{r}_1) - j\,\phi(\bar{r}_2,\bar{r}_3)\right]\rangle =$$

$$\exp\left[j\,\langle\phi(\bar{r}_2,\bar{r}_1)\rangle - j\langle\phi(\bar{r}_2,\bar{r}_3)\rangle\right]$$

$$\times \exp\left\{-\langle\left[\phi(\bar{r}_2,\bar{r}_1) - \langle\phi(\bar{r}_2,\bar{r}_1)\rangle\right]^2\rangle/2\right\}$$

$$\times \exp\left\{-\langle\left[\phi(\bar{r}_2,\bar{r}_3) - \langle\phi(\bar{r}_2,\bar{r}_3)\rangle\right]^2\rangle/2\right\} \qquad (15I)$$

Substituting Eq (7I) into Eq (15I) gives

$$\left\langle \exp\left[j\phi(\bar{r}_2,\bar{r}_1) - j\phi(\bar{r}_2,\bar{r}_3)\right]\right\rangle =$$

$$\exp\left\{-\left[\left\langle\phi^2(\bar{r}_2,\bar{r}_1)\right\rangle + \left\langle\phi^2(\bar{r}_2,\bar{r}_3)\right\rangle\right]/2\right\} \quad (16I)$$

Since $\phi(\bar{r}',\bar{r})$ is zero-mean, Eq (16I) is simplified to

$$\left\langle \exp\left[j\phi(\bar{r}_2,\bar{r}_1) - j\phi(\bar{r}_2,\bar{r}_3)\right]\right\rangle =$$

$$\exp\left\{-\left\langle\left[\phi(\bar{r}_2,\bar{r}_1) - \phi(\bar{r}_2,\bar{r}_3)\right]^2\right\rangle/2\right\} \quad (17I)$$

Now, the phase structure function is defined as (Ref 4:1374)

$$D_\phi(\bar{p}',\bar{p}) = \left\langle\left[\phi(\bar{r}'+\bar{p}' \ , \ \bar{r}+\bar{p}) - \phi(\bar{r}',\bar{r})\right]^2\right\rangle \quad (18I)$$

Using Eq (18I) in Eq (17I) where $\bar{p}' = 0$ and $\bar{p} = \bar{r}_1-\bar{r}_3$ yields

$$\left\langle \exp\left[j\phi(\bar{r}_2,\bar{r}_1) - j\phi(\bar{r}_2,\bar{r}_3)\right]\right\rangle = \exp\left[-D_\phi(\left|\bar{r}_1-\bar{r}_3\right|)/2\right] \quad (19I)$$

Substituting Eqs (14I) and (19I) into Eq (5I) gives

$$\exp(jk|\bar{r}_3|^2/2z)\langle\hat{E}_{CMF}(\bar{r}_3)\rangle =$$

$$(1/\lambda z)^2 \int_{R_1} \exp(jk|\bar{r}_1|^2/2z) E_I(\bar{r}_1) \exp\left[-D(|\bar{r}_1-\bar{r}_3|)/2\right]$$

$$\times \int_{R_2} \exp\left[-j2\pi(\bar{r}_1-\bar{r}_3).\bar{r}_2/\lambda z\right] d\bar{r}_2\, d\bar{r}_1 \qquad (20I)$$

where $D(|\bar{r}_1-\bar{r}_3|) = D_x(|\bar{r}_1-\bar{r}_3|) + D_\phi(|\bar{r}_1-\bar{r}_3|)$ is the spherical wave structure function and where the wave number k in the inner integral is replaced by $2\pi/\lambda$. Note that the inner integral of Eq (20I) is the two-dimensional spatial Fourier transform of aperture R_2, where $(\bar{r}_1-\bar{r}_3)/\lambda z = \bar{f}$ is a two-dimensional spatial frequency vector. Since R_2 is a circular aperture of radius $d_2/2$, the inner integral is actually a Fourier-Bessel transform of $\text{circ}(2|\bar{r}_2|/d_2)$ where

$$\text{circ}(2|\bar{r}_2|/d_2) = \begin{cases} 1 \;;\; |\bar{r}_2| \le d_2/2 \\ 0 \;;\; \text{otherwise} \end{cases} \qquad (21I)$$

From a table of Fourier-Bessel transforms, the transform of Eq (21I) is

$$\mathcal{B}\left[\text{circ}(2|\bar{r}_2|/d_2)\right] = d_2\lambda z J_1(\pi|\bar{r}_1-\bar{r}_3|d_2/\lambda z)/2|\bar{r}_1-\bar{r}_3| \qquad (22I)$$

Replacing the inner integral of Eq (20I) with Eq (22I) yields Eq (54):

$$\exp(jk|\bar{r}_3|^2/2z)\langle\hat{E}_{CMF}(\bar{r}_3)\rangle =$$

$$(d_2/2\lambda z)\int_{R_1}\exp(jk|\bar{r}_1|^2/2z)E_I(\bar{r}_1)\exp\left[-D(|\bar{r}_1-\bar{r}_3|)/2\right]$$

$$x\ J_1(\pi|\bar{r}_1-\bar{r}_3|d_2/\lambda z)/(1/|\bar{r}_1-\bar{r}_3|)d\bar{r}_1 \qquad (54)$$

If the quadratic phase factors in Eq (55) are ignored, then the CMF Receiver average image field, $\langle\hat{E}_{CMF}(\bar{r}_3)\rangle$, is obtained by convolving the object field, $E_I(\bar{r}_1)$, with the following CMF Receiver average impulse response $\langle h_{CMF}(\bar{r})\rangle$:

$$\langle h_{CMF}(\bar{r})\rangle = d_2\exp\left[-D(|\bar{r}|)/2\right]J_1(\pi|\bar{r}|d_2/\lambda z)/2\lambda z\ \bar{r} \qquad (56)$$

The average CTF, $\langle H_{CMF}(\bar{f})\rangle$, of the CMF Receiver is obtained by taking the Fourier transform of Eq (56):

$$\langle H_{CMF}(\bar{f})\rangle = (d_2/2\lambda z)\int_{-\infty}^{+\infty}\exp\left[-D(|\bar{r}|)/2\right]J_1(\pi|\bar{r}|d_2/\lambda z)$$

$$x\ \exp(-j2\pi|\bar{f}||\bar{r}|)(1/|\bar{r}|)d\bar{r} \qquad (23I)$$

Let $x = |\bar{r}|d_2/2\lambda z$ and $|\bar{f}'| = |\bar{f}|2\lambda z/d_2$ so that Eq (23I) becomes

$$\langle H_{CMF}(\bar{f})\rangle = (d_2/2\lambda z)\int_{-\infty}^{+\infty}\exp\left[-D(x2\lambda z/d_2)/2\right]J_1(2\pi x)$$

$$x\ \exp(-j2\pi|\bar{f}'|x)(1/x)dx \qquad (24I)$$

Expressing the argument of the spherical wave structure function in terms of D_{fo}, the free-space DOF for a circularly-apertured object, yields

$$<H_{CMF}(\bar{f})> = (d_2/2\lambda z)\int_{-\infty}^{+\infty}\exp\left[-D(x\pi d_1/2\sqrt{D_{fo}})/2\right]J_1(2\pi x)$$

$$\cdot \quad x\ \exp(-j2\pi|\bar{f}'|x)(1/x)dx \qquad (25I)$$

where

$$D_{fo} = (\pi d_1 d_2/4\lambda z)^2 \qquad (29)$$

Using a table of Fourier-Bessel transforms (Ref 11:145), Eq (25I) is simplified to Eq (58):

$$<H_{CMF}(\bar{f})> = 2\pi\int_{0}^{+\infty}\exp\left[-D(x\pi d_1/2\sqrt{D_{fo}})/2\right]J_1(2\pi x)$$

$$x\ J_o(2\pi|\bar{f}'|x)dx \qquad (58)$$

Appendix J - Average IMSE of the Image Field of the Channel-Matched Filter Receiver

This appendix derives the expression for the average IMSE of the image field generated by the CMF Receiver, when propagation is through the turbulent atmosphere and the additive background noise is zero-mean, spatially white noise. Another average IMSE expression is derived for the same conditions in conjunction with isoplanatism. For the background noise described above, it is shown that the average IMSE for the joint conditions of isoplanatism and propagation through the turbulent atmosphere is the same as the average IMSE for free-space propagation. The average IMSE of the image field generated by the CMF Receiver is

$$\langle \text{IMSE} \rangle = \int_{R_3} \left\langle \left[E(\bar{r}_3) - \hat{E}_{CMF}(\bar{r}_3) \right]^2 \right\rangle d\bar{r}_3 \tag{59}$$

where $E(\bar{r}_3)$ is the field for free-space propagation and is expressed as

$$E(\bar{r}_3) = \int_{R_2} \int_{R_1} E_I(\bar{r}_1) h_{FS}(\bar{r}_2, \bar{r}_1) h_{FS}^*(\bar{r}_2, \bar{r}_3) d\bar{r}_1 \, d\bar{r}_2 + \int_{R_2} E_N(\bar{r}_2) h_{FS}^*(\bar{r}_2, \bar{r}_3) d\bar{r}_2 \tag{1J}$$

Using Eqs (23), (51) and (52), the image field $\hat{E}_{CMF}(\bar{r}_3)$ generated by the CMF Receiver is expressed as

$$\hat{E}_{CMF}(\bar{r}_3) = \int_{R_2}\int_{R_1} E_I(\bar{r}_1)h_{21}(\bar{r}_2,\bar{r}_1)h_{21}^*(\bar{r}_2,\bar{r}_3)d\bar{r}_1\, d\bar{r}_2$$

$$+ \int_{R_2} E_N(\bar{r}_2)h_{21}^*(\bar{r}_2,\bar{r}_3)d\bar{r}_2 \qquad (2J)$$

In Eqs (1J) and (2J), $E_I(\bar{r}_1)$ is an unknown but non-random object field in aperture R_1 of Figure 10, $E_N(\bar{r}_2)$ is a zero-mean, spatially white noise field representing additive background noise, $h_{21}(\bar{r}',\bar{r})$ is the general impulse response, and $h_{FS}(\bar{r}',\bar{r})$ is the free-space impulse response defined by Eq (47). Substituting Eqs (1J) and (2J) into Eq (59) and expanding yields

$$\langle \text{IMSE} \rangle = \int_{R_3}\int_{R_2}\int_{R_2}\int_{R_1}\int_{R_1} E_I(\bar{u})E_I^*(\bar{m})h_{FS}(\bar{v},\bar{u})h_{FS}^*(\bar{n},\bar{m})$$

$$\times\, h_{FS}^*(\bar{v},\bar{r}_3)h_{FS}(\bar{n},\bar{r}_3)d\bar{u}\, d\bar{m}\, d\bar{v}\, d\bar{n}\, d\bar{r}_3$$

$$- 2\text{Re}\left[\int_{R_3}\int_{R_2}\int_{R_2}\int_{R_1}\int_{R_1} E_I(\bar{u})E_I^*(\bar{m})h_{FS}(\bar{v},\bar{u})h_{FS}^*(\bar{v},\bar{r}_3)\right.$$

$$\left.\times \langle h_{21}^*(\bar{n},\bar{m})h_{21}(\bar{n},\bar{r}_3)\rangle d\bar{u}\, d\bar{m}\, d\bar{v}\, d\bar{n}\, d\bar{r}_3\right]$$

$$- 2\text{Re}\left[\int_{R_3}\int_{R_2}\int_{R_2}\int_{R_1} E_I(\bar{u})\langle E_N^*(\bar{n})\rangle h_{FS}(\bar{v},\bar{u})\right.$$

$$\left.\times\, h_{FS}^*(\bar{v},\bar{r}_3)\langle h_{21}(\bar{n},\bar{r}_3)\rangle d\bar{u}\, d\bar{v}\, d\bar{n}\, d\bar{r}_3\right]$$

$$+ \int_{R_3}\int_{R_2}\int_{R_2}\int_{R_1}\int_{R_1} E_I(\bar{u})E_I^*(\bar{m})\langle h_{21}(\bar{v},\bar{u})h_{21}^*(\bar{n},\bar{m})\rangle$$

$$\times h_{21}^{*}(\bar{v},\bar{r}_3)h_{21}(\bar{n},\bar{r}_3)\rangle d\bar{u}\, d\bar{m}\, d\bar{v}\, d\bar{n}\, d\bar{r}_3$$

$$- 2\mathrm{Re}\left[\int_{R_3}\int_{R_2}\int_{R_2}\int_{R_1} E_I(\bar{u})\langle E_N^{*}(\bar{n})\rangle\langle h_{21}(\bar{v},\bar{u})\right.$$

$$\left.\times h_{21}^{*}(\bar{v},\bar{r}_3)h_{21}(\bar{n},\bar{r}_3)\rangle d\bar{u}\, d\bar{m}\, d\bar{v}\, d\bar{n}\, d\bar{r}_3\right]$$

$$+ \int_{R_3}\int_{R_2}\int_{R_2}\langle E_N(\bar{v})E_N^{*}(\bar{n})\rangle\langle h_{21}^{*}(\bar{v},\bar{r}_3)$$

$$\times h_{21}(\bar{n},\bar{r}_3)\rangle d\bar{v}\, d\bar{n}\, d\bar{r}_3 \quad ; \quad \bar{u},\ \bar{m} \in R_1 \quad \bar{v},\ \bar{n} \in R_2 \tag{3J}$$

The third and fifth terms of Eq (3J) are zero because the noise field is zero-mean. Since the additive background noise is spatially white noise

$$\langle E_N(\bar{v})E_N^{*}(\bar{n})\rangle = N_o\,\delta(\bar{v}-\bar{n}) \tag{50}$$

For propagation through the turbulent atmosphere, the general impulse response, $h_{21}(\bar{r}',\bar{r})$, of Eq (3J) is replaced by the turbulent impulse response, $h_{TB}(\bar{r}',\bar{r})$. The turbulent impulse response is written as

$$h_{TB}(\bar{r}',\bar{r}) = h_{FS}(\bar{r}',\bar{r})\exp\left[\chi(\bar{r}',\bar{r}) + j\,\phi(\bar{r}',\bar{r})\right] \tag{4J}$$

Substituting Eqs (50) and (4J) into Eq (3J) yields

$$
\begin{aligned}
\langle \mathrm{IMSE} \rangle = \int_{R_3}\int_{R_2}\int_{R_2}\int_{R_1}\int_{R_1} & E_I^*(\bar{m}) h_{FS}(\bar{v},\bar{u}) h_{FS}^*(\bar{n},\bar{m}) \\
& \times h_{FS}^*(\bar{v},\bar{r}_3) h_{FS}(\bar{n},\bar{r}_3) \Big\langle \Big\{ 1 - \exp\left[\chi(\bar{n},\bar{m})\right] \\
& \times \exp\left[\chi(\bar{n},\bar{r}_3)\right] \exp\left[-j\phi(\bar{n},\bar{m}) + j\phi(\bar{n},\bar{r}_3)\right] \\
& + \exp\left[\chi(\bar{v},\bar{u}) + \chi(\bar{v},\bar{r}_3)\right] \exp\left[j\phi(\bar{v},\bar{u})\right] \\
& \times \exp\left[-j\phi(\bar{v},\bar{r}_3)\right] + \exp\left[\chi(\bar{v},\bar{u}) + \chi(\bar{n},\bar{m})\right] \\
& \times \exp\left[\chi(\bar{n},\bar{r}_3) + \chi(\bar{v},\bar{r}_3)\right] \exp\left[j\phi(\bar{v},\bar{u})\right] \\
& \times \exp\left[-j\phi(\bar{v},\bar{r}_3)\right] \exp\left[-j\phi(\bar{n},\bar{m}) - j\phi(\bar{n},\bar{r}_3)\right] \Big\} \Big\rangle \\
& \times d\bar{u}\, d\bar{m}\, d\bar{v}\, d\bar{n}\, d\bar{r}_3 + \left[N_o/(\lambda z)^2\right] \\
& \times \int_{R_3}\int_{R_2} \Big\langle \exp\left[2\chi(\bar{n})\right] \Big\rangle d\bar{r}_2\, d\bar{r}_3
\end{aligned}
$$

$$
; \quad \bar{u}, \bar{m} \in R_1 \quad \bar{v}, \bar{n} \in R_2 \qquad \text{(5J)}
$$

where the second term of Eq (3J) is expanded using the identity, $\mathrm{Re}(w) = (w+w^*)/2$, and a change of variables ($\bar{u} \leftrightarrow \bar{m}$ and $\bar{v} \leftrightarrow \bar{n}$) is performed on the w^* term of the expansion. Equation (5J), specifically the second term, can be simplified even more. Using Eqs (6I) and (9I), it can be shown that

$$\langle \exp\left[2\chi(\bar{n})\right] \rangle = 1 \qquad (6J)$$

Substituting Eq (6J) into Eq (5J) yields

$$\begin{aligned}
\langle \text{IMSE} \rangle = \int_{R_3}\int_{R_2}\int_{R_2}\int_{R_1}\int_{R_1} & E_I(\bar{u})E_I^*(\bar{m})h_{FS}(\bar{v},\bar{u})h_{FS}^*(\bar{n},\bar{m}) \\
& \times h_{FS}^*(\bar{v},\bar{r}_3)h_{FS}(\bar{n},\bar{r}_3)\Big\langle\Big\{1 - \exp\left[\chi(\bar{n},\bar{m})\right] \\
& \times \exp\left[\chi(\bar{n},\bar{r}_3)\right]\exp\left[-j\phi(\bar{n},\bar{m}) + j\phi(\bar{n},\bar{r}_3)\right] \\
& + \exp\left[\chi(\bar{v},\bar{u}) + \chi(\bar{v},\bar{r}_3)\right]\exp\left[j\phi(\bar{v},\bar{u})\right] \\
& \times \exp\left[-j\phi(\bar{v},\bar{r}_3)\right] + \exp\left[\chi(\bar{v},\bar{u}) + \chi(\bar{n},\bar{m})\right] \\
& \times \exp\left[\chi(\bar{n},\bar{r}_3) + \chi(\bar{v},\bar{r}_3)\right]\exp\left[j\phi(\bar{v},\bar{u})\right] \\
& \times \exp\left[-j\phi(\bar{v},\bar{r}_3)\right]\exp\left[-j\phi(\bar{n},\bar{m}) + j\phi(\bar{n},\bar{r}_3)\right]\Big\}\Big\rangle \\
& \times d\bar{u}\, d\bar{m}\, d\bar{v}\, d\bar{n}\, d\bar{r}_3 + \left[N_o/(\lambda z)^2\right] \\
& \times \int_{R_3}\int_{R_2} d\bar{r}_2\, d\bar{r}_3 \quad ; \quad \bar{u},\, \bar{m} \in R_1 \quad \bar{v},\, \bar{n} \in R_2
\end{aligned} \qquad (7J)$$

Still more simplification is possible. Since R_2 is a circular aperture of radius $d_2/2$ and R_3 is a circular aperture of radius $d_1/2$ (same radius as R_1), Eq (7J) reduces to

$$
\begin{aligned}
<\text{IMSE}> = \int_{R_3}\int_{R_2}\int_{R_2}\int_{R_1}\int_{R_1} & E_I(\bar{u})E_I^{*}(\bar{m})h_{FS}(\bar{v},\bar{u})h_{FS}^{*}(\bar{n},\bar{m}) \\
& \times h_{FS}^{*}(\bar{v},\bar{r}_3)h_{FS}(\bar{n},\bar{r}_3) < \Big\{ 1 - \exp\left[\chi(\bar{n},\bar{m})\right] \\
& \times \exp\left[\chi(n,r_3)\right]\exp\left[-j\,\phi(\bar{n},\bar{m}) + j\,\phi(\bar{n},\bar{r}_3)\right] \\
& + \exp\left[\chi(\bar{v},\bar{u}) + \chi(\bar{v},\bar{r}_3)\right]\exp\left[j\,\phi(\bar{v},\bar{u})\right] \\
& \times \exp\left[-j\,\phi(\bar{v},\bar{r}_3)\right] + \exp\left[\chi(\bar{v},\bar{u}) + \chi(\bar{n},\bar{m})\right] \\
& \times \exp\left[\chi(\bar{n},\bar{r}_3) + \chi(\bar{v},\bar{r}_3)\right]\exp\left[j\,\phi(\bar{v},\bar{u})\right] \\
& \times \exp\left[-j\,\phi(\bar{v},\bar{r}_3)\right]\exp\left[-j\,\phi(\bar{n},\bar{m}) + j\,\phi(\bar{n},\bar{r}_3)\right]\Big\} > \\
& \times du\,dm\,dv\,dn\,dr_3 + N_o D_{fo}
\end{aligned}
$$

$$
; \quad \bar{u}, \bar{m} \in R_1 \quad \bar{v}, \bar{n} \in R_2 \qquad (60)
$$

where

$$
D_{fo} = \left[\pi d_1 d_2 / 4\lambda z\right]^2 \qquad (29)
$$

Equation (60) is the average IMSE of the image field generated by the CMF Receiver when propagation is through the turbulent atmosphere and the additive background noise is zero-mean, spatially white noise. If the object field is also isoplantic, then the first term of Eq (60) becomes

zero. For isoplanatic object fields, $\chi(\bar{r}',\bar{r}) \longrightarrow \chi(\bar{r}')$ and $\phi(\bar{r}',\bar{r}) \longrightarrow \phi(\bar{r}')$, and Eq (60) becomes

$$\begin{aligned} <\text{IMSE}> = \int_{R_3}\int_{R_2}\int_{R_2}\int_{R_1}\int_{R_1} & E_I(\bar{u})E_I^*(\bar{m})h_{FS}(\bar{v},\bar{u})h_{FS}^*(\bar{n},\bar{m}) \\ & \times h_{FS}^*(\bar{v},\bar{r}_3)h_{FS}(\bar{n},\bar{r}_3)\Big\{1 - <\exp\left[2\chi(\bar{n})\right]> \\ & - <\exp\left[2\chi(\bar{v})\right]> + <\exp\left[2\chi(\bar{n}) + 2\chi(\bar{v})\right]>\Big\} \\ & \times d\bar{u}\, d\bar{m}\, d\bar{v}\, d\bar{n}\, d\bar{r}_3 + N_o D_{fo} \end{aligned}$$

$$; \quad \bar{u}, \bar{m} \in R_1 \quad \bar{v}, \bar{n} \in R_2 \qquad (8J)$$

Using Eqs (6I) and (9I), it can be shown that

$$<\exp\left[2\chi(\bar{n}) + 2\chi(\bar{v})\right]> = 1 \qquad (9J)$$

When Eqs (6J) and (9J) are substituted into Eq (8J), the first term becomes zero as alleged and Eq (8J) reduces to Eq (61):

$$<\text{IMSE}> = N_o D_{fo} \qquad (61)$$

Equation (61) is based on the conditions of isoplanatism, propagation through the turbulent atmosphere, and zero-mean,

spatially white noise. The same result applies however for the conditions of free-space propagation and zero-mean, spatially white noise. This is shown by letting $\chi(\bar{r}',\bar{r})$ and $\phi(\bar{r}',\bar{r})$ in Eq (5J) equal zero. The first term of Eq (5J) becomes zero and Eq (5J) reduces to

$$\langle \text{IMSE} \rangle = N_o/(\lambda z)^2 \int_{R_3}\int_{R_2} d\bar{r}_2 \, d\bar{r}_3 \tag{10J}$$

Since R_2 is a circular aperture of radius $d_2/2$ and R_3 is a circular aperture of radius $d_1/2$ (same radius as R_1), Eq (10J) is equivalent to

$$\langle \text{IMSE} \rangle = N_o D_{fo} \tag{61}$$

where

$$D_{fo} = \left[\pi d_1 d_2/4\lambda z\right]^2 \tag{29}$$

Appendix K - Sufficient Condition for Minimizing the Average IMSE of the Image Field of the Multiplicative Phase Receiver

This appendix derives Eq (64). Eq (64) is the sufficient condition that the optimum multiplicative phase of the MP Receiver must satisfy for the average IMSE of the receiver image field to be minimized. The average IMSE of the image field generated by the MP Receiver is

$$<\text{IMSE}> = \int_{R_3} < \left[E(\bar{r}_3) - \hat{E}_{MP}(\bar{r}_3)\right]^2 > d\bar{r}_3 \qquad (63)$$

where $E(\bar{r}_3)$ is the field for free-space propagation and is expressed as

$$E(\bar{r}_3) = \int_{R_2}\int_{R_1} E_I(\bar{r}_1) h_{FS}(\bar{r}_2,\bar{r}_1) h_{FS}^*(\bar{r}_2,\bar{r}_3)\, d\bar{r}_1\, d\bar{r}_2 + \int_{R_2} E_N(\bar{r}_2) h_{FS}^*(\bar{r}_2,\bar{r}_3) d\bar{r}_2 \qquad (1K)$$

Using Eqs (23), (51) and (53), the image field $\hat{E}_{MP}(\bar{r}_3)$ generated by the MP Receiver is expressed as

$$\hat{E}_{MP}(\bar{r}_3) = \int_{R_2}\int_{R_1} E_I(\bar{r}_1) \exp\left[j\hat{\phi}(\bar{r}_2)\right] h_{21}(\bar{r}_2,\bar{r}_1) \times h_{FS}^*(\bar{r}_2,\bar{r}_3) d\bar{r}_1\, d\bar{r}_2 + \int_{R_2} E_N(\bar{r}_2) \times \exp\left[j\hat{\phi}(\bar{r}_2)\right] h_{FS}^*(\bar{r}_2,\bar{r}_3) d\bar{r}_2 \qquad (2K)$$

where the optimum multiplicative phase $\phi_o(\bar{r}_2)$ has been replaced by an optimum phase estimate $\hat{\phi}(\bar{r}_2)$. In Eqs (1K) and (2K), $E_I(\bar{r}_1)$ is an unknown but nonrandom object field in aperture R_1 of Figure 10, $E_N(\bar{r}_2)$ is a zero-mean, spatially white noise field representing additive background noise, $h_{21}(\bar{r}',\bar{r})$ is the general impulse response, and $h_{FS}(\bar{r}',\bar{r})$ is the free-space impulse response defined by Eq (47). Substituting Eqs (1K) and (2K) into Eq (63) and expanding yields

$$
\begin{aligned}
<\text{IMSE}> = & \int_{R_3}\int_{R_2}\int_{R_2}\int_{R_1}\int_{R_1} E_I(\bar{u})E_I^*(\bar{m})h_{FS}(\bar{v},\bar{u})h_{FS}^*(\bar{n},\bar{m}) \\
& \times h_{FS}^*(\bar{v},\bar{r}_3)h_{FS}(\bar{n},\bar{r}_3)d\bar{u}\,d\bar{m}\,d\bar{v}\,d\bar{n}\,d\bar{r}_3 \\
& - 2\text{Re}\Bigg[\int_{R_3}\int_{R_2}\int_{R_2}\int_{R_1}\int_{R_1} E_I(\bar{u})E_I^*(\bar{m})h_{FS}(\bar{v},\bar{u})h_{FS}^*(\bar{v},\bar{r}_3) \\
& \times h_{FS}(\bar{n},\bar{r}_3)<\exp\left[-j\hat{\phi}(\bar{n})\right]h_{21}^*(\bar{n},\bar{m})> \\
& \times d\bar{u}\,d\bar{m}\,d\bar{v}\,d\bar{n}\,d\bar{r}_3\Bigg] \\
& - 2\text{Re}\Bigg[\int_{R_3}\int_{R_2}\int_{R_2}\int_{R_1} E_I(\bar{u})<E_N^*(\bar{n})><\exp\left[-j\hat{\phi}(\bar{n})\right]> \\
& \times h_{FS}(\bar{v},\bar{u})h_{FS}^*(\bar{v},\bar{r}_3)h_{FS}(\bar{n},\bar{r}_3)d\bar{u}\,d\bar{v}\,d\bar{n}\,d\bar{r}_3\Bigg] \\
& + \int_{R_3}\int_{R_2}\int_{R_2}\int_{R_1}\int_{R_1} E_I(\bar{u})E_I^*(\bar{m})h_{FS}^*(\bar{v},\bar{r}_3)h_{FS}(\bar{n},\bar{r}_3) \\
& \times <\exp\left[j\hat{\phi}(\bar{v}) - j\hat{\phi}(\bar{n})\right]h_{21}(\bar{v},\bar{u})h_{21}^*(\bar{n},\bar{m})>
\end{aligned}
$$

$$x\, d\bar{u}\, d\bar{m}\, d\bar{v}\, d\bar{n}\, d\bar{r}_3$$

$$- 2\mathrm{Re}\left[\int_{R_3}\int_{R_2}\int_{R_2}\int_{R_1} E_I(\bar{u})\langle E_N^*(\bar{n})\rangle h_{FS}^*(\bar{v},\bar{r}_3)\right.$$

$$x\, h_{FS}(\bar{n},\bar{r}_3)\langle \exp\left[j\hat{\phi}(\bar{v}) - j\hat{\phi}(\bar{n})\right] h_{21}(\bar{v},\bar{u})\rangle$$

$$\left. x\, d\bar{u}\, d\bar{v}\, d\bar{n}\, d\bar{r}_3\right]$$

$$+ \int_{R_3}\int_{R_2}\int_{R_2} \langle E_N(\bar{v})E_N^*(\bar{n})\rangle h_{FS}^*(\bar{v},\bar{r}_3)h_{FS}(\bar{n},\bar{r}_3)$$

$$x \langle \exp\left[j\hat{\phi}(\bar{v}) - j\hat{\phi}(\bar{n})\right]\rangle d\bar{v}\, d\bar{n}\, d\bar{r}_3$$

$$;\quad \bar{u},\, \bar{m} \in R_1 \quad \bar{v},\, \bar{n} \in R_2 \qquad (3K)$$

The third and fifth terms of Eq (3K) are zero because the noise field is zero-mean. Now let the optimum phase estimate, $\hat{\phi}(\bar{r}_2)$ be written as

$$\hat{\phi}(\bar{r}_2) = \phi_o(\bar{r}_2) + \epsilon\phi_\epsilon(\bar{r}_2) \qquad (4K)$$

where $\phi_o(\bar{r}_2)$ is the optimum multiplicative phase and $\epsilon\phi_\epsilon(\bar{r}_2)$ is the phase error of the optimum phase estimate. Substituting Eq (4K) into Eq (3K) yields

$$\langle \mathrm{IMSE} \rangle = \int_{R_3}\int_{R_2}\int_{R_2}\int_{R_1}\int_{R_1} E_I(\bar{u})E_I^*(\bar{m})h_{FS}(\bar{v},\bar{u})h_{FS}^*(\bar{n},\bar{m})$$

$$\times h_{FS}^{*}(\bar{v},\bar{r}_3)h_{FS}(\bar{n},\bar{r}_3)d\bar{u}\ d\bar{m}\ d\bar{v}\ d\bar{n}\ d\bar{r}_3$$

$$- \int_{R_3}\int_{R_2}\int_{R_2}\int_{R_1}\int_{R_1} E_I(\bar{u})E_I^{*}(\bar{m})h_{FS}(\bar{v},\bar{u})h_{FS}^{*}(\bar{v},\bar{r}_3)$$

$$\times h_{FS}(\bar{n},\bar{r}_3)\exp\left[-j\epsilon\phi_{\epsilon}(\bar{n})\right]<\exp\left[-j\phi_o(\bar{n})\right]$$

$$\times h_{21}^{*}(\bar{n},\bar{m})>\ d\bar{u}\ d\bar{m}\ d\bar{v}\ d\bar{n}\ d\bar{r}_3$$

$$- \int_{R_3}\int_{R_2}\int_{R_2}\int_{R_1}\int_{R_1} E_I^{*}(\bar{u})E_I(\bar{m})h_{FS}^{*}(\bar{v},\bar{u})h_{FS}(\bar{v},\bar{r}_3)$$

$$\times h_{FS}^{*}(\bar{n},\bar{r}_3)\exp\left[j\epsilon\phi_{\epsilon}(\bar{n})\right]<\exp\left[j\phi_o(\bar{n})\right]h_{21}(\bar{n},\bar{m})>$$

$$\times d\bar{u}\ d\bar{m}\ d\bar{v}\ d\bar{n}\ d\bar{r}_3$$

$$+ \int_{R_3}\int_{R_2}\int_{R_2}\int_{R_1}\int_{R_1} E_I(\bar{u})E_I^{*}(\bar{m})h_{FS}^{*}(\bar{v},\bar{r}_3)h_{FS}(\bar{n},\bar{r}_3)$$

$$\times \exp\left[j\epsilon\phi_{\epsilon}(\bar{v}) - j\epsilon\phi_{\epsilon}(\bar{n})\right]<\exp\left[j\phi_o(\bar{v}) - j\phi_o(\bar{n})\right]$$

$$\times h_{21}(\bar{v},\bar{u})h_{21}^{*}(\bar{n},\bar{m})>\ d\bar{u}\ d\bar{v}\ d\bar{m}\ d\bar{n}\ d\bar{r}_3$$

$$+ \int_{R_3}\int_{R_2}\int_{R_2}<E_N(\bar{v})E_N^{*}(\bar{n})>h_{FS}^{*}(\bar{v},\bar{r}_3)h_{FS}(\bar{n},\bar{r}_3)$$

$$\times \exp\left[j\epsilon\phi_{\epsilon}(\bar{v}) - j\epsilon\phi_{\epsilon}(\bar{n})\right]<\exp\left[j\phi_o(\bar{v}) - j\phi_o(\bar{n})\right]>$$

$$\times d\bar{v}\ d\bar{n}\ d\bar{r}_2 \quad ; \quad \bar{u},\ \bar{m}\in R_1 \quad \bar{v},\ \bar{n}\in R_2 \qquad (5K)$$

where the second term of Eq (3K) is expanded using the identity $\mathrm{Re}(w) = (w+w^*)/2$. To obtain a condition for $\phi_o(\bar{r}_2)$ such that the average IMSE is minimized, take the derivative of Eq (5K) with respect to ϵ, let $\epsilon = 0$, and set the result equal to zero:

$$\partial \langle \mathrm{IMSE} \rangle / \partial \epsilon \Big|_{\epsilon=0} = \int_{R_2} j\phi_\epsilon(\bar{n}) \Bigg[\int_{R_3}\int_{R_2}\int_{R_1}\int_{R_1} E_I(\bar{u}) E_I^*(\bar{m})$$

$$\times h_{FS}(\bar{v},\bar{u}) h_{FS}^*(\bar{v},\bar{r}_3) h_{FS}(\bar{n},\bar{r}_3)$$

$$\times \langle \exp[-j\phi_o(\bar{n})] h_{21}^*(\bar{n},\bar{m}) \rangle d\bar{u}\, d\bar{m}\, d\bar{v}\, d\bar{r}_3 \Bigg] d\bar{n}$$

$$+ \int_{R_2} j\phi_\epsilon(\bar{n}) \Bigg[- \int_{R_3}\int_{R_2}\int_{R_1}\int_{R_1} E_I^*(\bar{u}) E_I(\bar{m}) h_{FS}^*(\bar{v},\bar{u})$$

$$\times h_{FS}(\bar{v},\bar{r}_3) h_{FS}^*(\bar{n},\bar{r}_3) \langle \exp[j\phi_o(\bar{n})] h_{21}(\bar{n},\bar{m}) \rangle$$

$$\times d\bar{u}\, d\bar{m}\, d\bar{v}\, d\bar{r}_3 \Bigg] d\bar{n}$$

$$+ \int_{R_2} j\phi_\epsilon(\bar{n}) \Bigg[\int_{R_3}\int_{R_2}\int_{R_1}\int_{R_1} E_I(\bar{u}) E_I^*(\bar{m}) h_{FS}(\bar{v},\bar{r}_3)$$

$$\times h_{FS}^*(\bar{n},\bar{r}_3) \langle \exp[-j\phi_o(\bar{v}) - j\phi_o(\bar{n})] h_{21}(\bar{n},\bar{u})$$

$$\times h_{21}^*(\bar{v},\bar{m}) \rangle d\bar{u}\, d\bar{m}\, d\bar{v}\, d\bar{r}_3 \Bigg] d\bar{n}$$

$$+ \int_{R_2} j\phi_\epsilon(\bar{n}) \Bigg[- \int_{R_3}\int_{R_2}\int_{R_1}\int_{R_1} E_I(\bar{u}) E_I^*(\bar{m}) h_{FS}^*(\bar{v},\bar{r}_3)$$

$$
\times h_{FS}(\bar{n},\bar{r}_3)\langle \exp\left[j\phi_o(\bar{v}) - j\phi_o(\bar{n})\right] h_{21}(\bar{v},\bar{u})
$$

$$
\times h_{21}^*(\bar{n},\bar{m})\rangle d\bar{u}\, d\bar{m}\, d\bar{v}\, d\bar{r}_3 \Big] d\bar{n}
$$

$$
+ \int_{R_2} j\phi_\epsilon(\bar{n}) \Big[\int_{R_3}\int_{R_2} \langle E_N^*(\bar{v}) E_N(\bar{n})\rangle h_{FS}(\bar{v},\bar{r}_3)
$$

$$
\times h_{FS}^*(\bar{n},\bar{r}_3)\langle \exp\left[-j\phi_o(\bar{v}) + j\phi_o(\bar{n})\right]\rangle d\bar{v}\, d\bar{r}_3 \Big] d\bar{n}
$$

$$
+ \int_{R_2} j\phi_\epsilon(\bar{n}) \Big[- \int_{R_3}\int_{R_2} \langle E_N(\bar{v}) E_N^*(\bar{n})\rangle h_{FS}^*(\bar{v},\bar{r}_3)
$$

$$
\times h_{FS}(\bar{n},\bar{r}_3)\langle \exp\left[j\phi_o(\bar{v}) - j\phi_o(\bar{n})\right]\rangle d\bar{v}\, d\bar{r}_3 \Big] d\bar{n} = 0
$$

$$
; \quad \bar{u},\ \bar{m} \in R_1 \quad \bar{v},\ \bar{n} \in R_2 \qquad (6K)
$$

where the fourth term of Eq (5K) is expanded to give the third and fourth terms of Eq (6K), and the fifth term of Eq (5K) is expanded to give the fifth and sixth terms of Eq (6K). Equation (6K) is true if the sum of the terms in brackets is equal to zero. Setting the sum equal to zero and performing a change of variables ($\bar{u} \leftrightarrow \bar{m}$) in the third term of the sum yields

$$
\int_{R_3}\int_{R_2}\int_{R_1}\int_{R_1} E_I(\bar{u}) E_I^*(\bar{m}) h_{FS}(\bar{v},\bar{u}) h_{FS}^*(\bar{v},\bar{r}_3) h_{FS}(\bar{n},\bar{r}_3)
$$

$$
\times \langle \exp\left[-j\phi_o(\bar{n})\right] h_{21}^*(\bar{n},\bar{m})\rangle d\bar{u}\, d\bar{m}\, d\bar{v}\, d\bar{r}_3
$$

$$
- \int_{R_3}\int_{R_2}\int_{R_1}\int_{R_1} E_I^*(\bar{u})E_I(\bar{m})h_{FS}^*(\bar{v},\bar{u})h_{FS}(\bar{v},\bar{r}_3)h_{FS}^*(\bar{n},\bar{r}_3)
$$

$$
x \left\langle \exp\left[j\phi_o(\bar{n})\right] h_{21}(\bar{n},\bar{m}) \right\rangle d\bar{u}\, d\bar{m}\, d\bar{v}\, d\bar{r}_3
$$

$$
+ \int_{R_3}\int_{R_2}\int_{R_1}\int_{R_1} E_I^*(\bar{u})E_I(\bar{m})h_{FS}(\bar{v},\bar{r}_3)h_{FS}^*(\bar{n},\bar{r}_3)
$$

$$
x \left\langle \exp\left[-j\phi_o(\bar{v}) + j\phi_o(\bar{n})\right] h_{21}^*(\bar{v},\bar{u})h_{21}(\bar{n},\bar{m}) \right\rangle
$$

$$
x\, d\bar{u}\, d\bar{m}\, d\bar{v}\, d\bar{r}_3
$$

$$
- \int_{R_3}\int_{R_2}\int_{R_1}\int_{R_1} E_I(\bar{u})E_I^*(\bar{m})h_{FS}^*(\bar{v},\bar{r}_3)h_{FS}(\bar{n},\bar{r}_3)
$$

$$
x \left\langle \exp\left[j\phi_o(\bar{v}) - j\phi_o(\bar{n})\right] h_{21}(\bar{v},\bar{u})h_{21}^*(\bar{n},\bar{m}) \right\rangle
$$

$$
x\, d\bar{u}\, d\bar{m}\, d\bar{v}\, d\bar{r}_3
$$

$$
+ \int_{R_3}\int_{R_2} \left\langle E_N^*(\bar{v})E_N(\bar{n}) \right\rangle h_{FS}(\bar{v},\bar{r}_3)h_{FS}^*(\bar{n},\bar{r}_3)
$$

$$
x \left\langle \exp\left[-j\phi_o(\bar{v}) + j\phi_o(\bar{n})\right] \right\rangle d\bar{v}\, d\bar{r}_3
$$

$$
- \int_{R_3}\int_{R_2} \left\langle E_N(\bar{v})E_N^*(\bar{n}) \right\rangle h_{FS}^*(\bar{v},\bar{r}_3)h_{FS}(\bar{n},\bar{r}_3)
$$

$$
x \left\langle \exp\left[j\phi_o(\bar{v}) - j\phi_o(\bar{n})\right] \right\rangle d\bar{v}\, d\bar{r}_2 = 0
$$

$$
; \quad \bar{u}, \bar{m} \in R_1 \quad \bar{v}, \bar{n} \in R_2 \qquad (7K)
$$

Note that the first and second terms, third and fourth terms, and fifth and sixth terms of Eq (7K) are conjugate pairs. Therefore, by using the identity $(w-w^*) = 2i\mathrm{Im}(w)$, Eq (7K) is simplified to

$$\mathrm{Im}\left\{\int_{R_3}\int_{R_2}\int_{R_1}\int_{R_1} E_I(\bar{u})E_I^*(\bar{m})h_{FS}^*(\bar{v},\bar{r}_3)h_{FS}(\bar{n},\bar{r}_3)\left\langle \exp\left[-j\phi_o(\bar{n})\right]\right.\right.$$
$$\left.\times\, h_{21}^*(\bar{n},\bar{m})\left[h_{FS}(\bar{v},\bar{u}) - \exp\left[j\phi_o(\bar{v})\right]h_{21}(\bar{v},\bar{u})\right]\right\rangle$$
$$\left.\times\, d\bar{u}\, d\bar{m}\, d\bar{v}\, d\bar{r}_3\right\}$$
$$- \mathrm{Im}\left\{\int_{R_3}\int_{R_2}\left\langle E_N(\bar{v})E_N^*(\bar{n})\right\rangle h_{FS}^*(\bar{v},\bar{r}_3)h_{FS}(\bar{n},\bar{r}_3)\right.$$
$$\left.\times\left\langle \exp\left[j\phi_o(\bar{v}) - j\phi_o(\bar{n})\right]\right\rangle d\bar{v}\, d\bar{r}_3\right\} = 0$$
$$; \quad \bar{u},\ \bar{m} \in R_1 \quad \bar{v},\ \bar{n} \in R_2 \qquad (8K)$$

Since the additive background noise is spatially white noise

$$\left\langle E_N(\bar{v})E_N^*(\bar{n})\right\rangle = N_o\,\delta(\bar{v}-\bar{n}) \qquad (50)$$

Substituting Eq (50) into Eq (8K) gives

$$\mathrm{Im}\left\{\int_{R_3}\int_{R_2}\int_{R_1}\int_{R_1} E_I(\bar{u})E_I^*(\bar{m})h_{FS}^*(\bar{v},\bar{r}_3)h_{FS}(\bar{n},\bar{r}_3)\right.$$

$$x \left\langle \exp\left[-j\,\phi_o(\bar{n})\right] h_{21}{}^{*}(\bar{n},\bar{m}) \left[h_{FS}(\bar{v},\bar{u}) - \exp\left[j\,\phi_o(\bar{v})\right] \right.\right.$$

$$\left.\left. x\; h_{21}(\bar{v},\bar{u}) \right] \right\rangle d\bar{u}\; d\bar{m}\; d\bar{v}\; d\bar{r}_3 \Bigg\}$$

$$- \mathrm{Im}\left\{ \left[N_o/(\lambda z)^2 \right] \int_{R_2} d\bar{r}_2 \right\} = 0 \quad ; \quad \bar{u},\ \bar{m} \in R_1 \quad \bar{v},\ \bar{n} \in R_2 \tag{9K}$$

The second term on the left side of Eq (9K) is zero because the quantity in $\{\quad\}$ is real. Therefore, Eq (9K) is simplified to

$$\mathrm{Im}\left\{ \int_{R_3}\int_{R_2}\int_{R_1}\int_{R_1} E_I(\bar{u}) E_I{}^{*}(\bar{m}) h_{FS}{}^{*}(\bar{v},\bar{r}_3) h_{FS}(\bar{n},\bar{r}_3) \right.$$

$$x \left\langle \exp\left[-j\,\phi_o(\bar{n})\right] h_{21}{}^{*}(\bar{n},\bar{m}) \left[h_{FS}(\bar{v},\bar{u}) - \exp\left[j\,\phi_o(\bar{v})\right] \right.\right.$$

$$\left.\left.\left. x\; h_{21}(\bar{v},\bar{u}) \right] \right\rangle d\bar{u}\; d\bar{m}\; d\bar{v}\; d\bar{r}_3 \right\} = 0 \quad ; \quad \bar{u},\ \bar{m} \in R_1 \quad \bar{v},\ \bar{n} \in R_2 \tag{10K}$$

For propagation through the turbulent atmosphere, the general impulse response, $h_{21}(\bar{r}',\bar{r})$, of Eq (10K) is replaced by the turbulent impulse response, $h_{TB}(\bar{r}',\bar{r})$. The turbulent impulse response is written as

$$h_{TB}(\bar{r}',\bar{r}) = h_{FS}(\bar{r}',\bar{r}) \exp\left[\chi(\bar{r}',\bar{r}) + j\,\phi(\bar{r}',\bar{r})\right] \tag{11K}$$

Substituting Eq (11K) into Eq (10K) yields Eq (64):

$$\text{Im} \int_{R_3}\int_{R_2}\int_{R_1}\int_{R_1} E_I(\bar{u})E_I^*(\bar{m})h_{FS}(\bar{v},\bar{u})h_{FS}^*(\bar{n},\bar{m})h_{FS}^*(\bar{v},\bar{r}_3)$$

$$\times\, h_{FS}(\bar{n},\bar{r}_3)\Big\langle \exp\left[\chi(\bar{n},\bar{m})\right]\exp\left[-j\phi(\bar{n},\bar{m}) - j\phi_o(\bar{n})\right]$$

$$\times\left[1 - \exp\left[\chi(\bar{v},\bar{u})\right]\exp\left[j\phi(\bar{v},\bar{u}) + j\phi_o(\bar{v})\right]\right]\Big\rangle$$

$$\left.\times\, d\bar{u}\, d\bar{m}\, d\bar{v}\, d\bar{r}_3\right\} = 0 \quad ; \quad \bar{u},\ \bar{m} \in R_1 \quad \bar{v},\ \bar{n} \in R_2 \qquad (64)$$

Appendix L - Minimum Average IMSE of the Image Field of the Multiplicative Phase Receiver

This appendix derives Eq (65), which is the expression for the minimum average IMSE of the image field generated by the MP Receiver. The average IMSE of the image field generated by the MP Receiver is

$$
\begin{aligned}
\langle \text{IMSE} \rangle = \int_{R_2} \Bigg[\int_{R_3}\int_{R_2}\int_{R_1}\int_{R_1} & E_I(\bar{u}) E_I^*(\bar{m}) h_{FS}(\bar{v},\bar{u}) h_{FS}^*(\bar{n},\bar{m}) \\
& \times h_{FS}^*(\bar{v},\bar{r}_3) h_{FS}(\bar{n},\bar{r}_3) d\bar{u}\, d\bar{m}\, d\bar{v}\, d\bar{r}_3 \Bigg] d\bar{n} \\
- \int_{R_2} \Bigg[\int_{R_3}\int_{R_2}\int_{R_1}\int_{R_1} & E_I(\bar{u}) E_I^*(\bar{m}) h_{FS}(\bar{v},\bar{u}) h_{FS}^*(\bar{v},\bar{r}_3) \\
& \times h_{FS}(\bar{n},\bar{r}_3) \langle \exp\left[-j\phi_o(\bar{n})\right] h_{21}^*(\bar{n},\bar{m}) \rangle \\
& \times d\bar{u}\, d\bar{m}\, d\bar{v}\, d\bar{r}_3 \Bigg] d\bar{n} \\
- \int_{R_2} \Bigg[\int_{R_3}\int_{R_2}\int_{R_1}\int_{R_1} & E_I^*(\bar{u}) E_I(\bar{m}) h_{FS}^*(\bar{v},\bar{u}) h_{FS}(\bar{v},\bar{r}_3) \\
& \times h_{FS}^*(\bar{n},\bar{r}_3) \langle \exp\left[j\phi_o(\bar{n})\right] h_{21}(\bar{n},\bar{m}) \rangle \\
& \times d\bar{u}\, d\bar{m}\, d\bar{v}\, d\bar{r}_3 \Bigg] d\bar{n} \\
+ \int_{R_2} \Bigg[\int_{R_3}\int_{R_2}\int_{R_1}\int_{R_1} & E_I(\bar{u}) E_I^*(\bar{m}) h_{FS}^*(\bar{v},\bar{r}_3) h_{FS}(\bar{n},\bar{r}_3)
\end{aligned}
$$

$$x \left\langle \exp\left[j\phi_o(\bar{v}) - j\phi_o(\bar{n}) \right] h_{21}(\bar{v},\bar{u}) h_{21}^*(\bar{n},\bar{m}) \right\rangle$$

$$x \, d\bar{u} \, d\bar{m} \, d\bar{v} \, d\bar{r}_3 \Big] d\bar{n} + N_o D_{fo}$$

$$; \quad \bar{u}, \bar{m} \in R_1 \quad \bar{v}, \bar{n} \in R_2 \tag{1L}$$

Equation (1L) is obtained from Eq (3K) in the following way. The third and fifth terms of Eq (3K) are zero because the noise field is zero-mean. The second term of Eq (3K) is expanded using the identity $Re(w) = (w+w^*)/2$. The last term of Eq (3K) becomes $N_o D_{fo}$ because the noise field is spatially white noise. This is shown in Appendix J. The optimum multiplicative phase estimate $\hat{\phi}(\bar{r}_2)$ is replaced by the optimum multiplicative phase $\phi_o(\bar{r}_2)$. Finally, the integral order is rearranged to facilitate a forthcoming substitution.

The optimum multiplicative phase which minimizes the average IMSE given by Eq (1L) must satisfy the sufficient condition derived in Appendix K:

$$\mathrm{Im} \left\{ \int_{R_3} \int_{R_2} \int_{R_1} \int_{R_1} E_I(\bar{u}) E_I^*(\bar{m}) h_{FS}^*(\bar{v},\bar{r}_3) h_{FS}(\bar{n},\bar{r}_3) \right.$$

$$x \left\langle \exp\left[-j\phi_o(\bar{n})\right] h_{21}^*(\bar{n},\bar{m}) \left[h_{FS}(\bar{v},\bar{u}) - \exp\left[j\phi_o(\bar{v}) \right] \right.\right.$$

$$\left.\left. x \, h_{21}(\bar{v},\bar{u}) \right] \right\rangle d\bar{u} \, d\bar{m} \, d\bar{v} \, d\bar{r}_3 \Bigg\} = 0 \quad ; \quad \bar{u}, \bar{m} \in R_1 \quad \bar{v}, \bar{n} \in R_2 \tag{10K}$$

In its present form, Eq (10K) cannot be easily substituted into Eq (1L). However, using the identity $Im(w) = -i(w-w^*)/2$, Eq (10K) is put in the more useful form

$$\int_{R_3}\int_{R_2}\int_{R_1}\int_{R_1} E_I(\bar{u})E_I^*(\bar{m})h_{FS}^*(\bar{v},\bar{r}_3)h_{FS}(\bar{n},\bar{r}_3)$$

$$x \left\langle \exp\left[j\phi_o(\bar{v}) - j\phi_o(\bar{n})\right] h_{21}(\bar{v},\bar{u})h_{21}^*(\bar{n},\bar{m})\right\rangle d\bar{u}\, d\bar{m}\, d\bar{v}\, d\bar{r}_3$$

$$= \int_{R_3}\int_{R_2}\int_{R_1}\int_{R_1} E_I(\bar{u})E_I^*(\bar{m})h_{FS}(\bar{v},\bar{u})h_{FS}^*(\bar{v},\bar{r}_3)h_{FS}(\bar{n},\bar{r}_3)$$

$$x \left\langle \exp\left[-j\phi_o(\bar{n})\right] h_{21}^*(\bar{n},\bar{m})\right\rangle d\bar{u}\, d\bar{m}\, d\bar{v}\, d\bar{r}_3$$

$$- \int_{R_3}\int_{R_2}\int_{R_1}\int_{R_1} E_I^*(\bar{u})E_I(\bar{m})h_{FS}^*(\bar{v},\bar{u})h_{FS}(\bar{v},\bar{r}_3)h_{FS}^*(\bar{n},\bar{r}_3)$$

$$x \left\langle \exp\left[j\phi_o(\bar{n})\right] h_{21}(\bar{n},\bar{m})\right\rangle d\bar{u}\, d\bar{m}\, d\bar{v}\, d\bar{r}_3$$

$$+ \int_{R_3}\int_{R_2}\int_{R_1}\int_{R_1} E_I^*(\bar{u})E_I(\bar{m})h_{FS}(\bar{v},\bar{r}_3)h_{FS}^*(\bar{n},\bar{r}_3)$$

$$x \left\langle \exp\left[-j\phi_o(\bar{v}) + j\phi_o(\bar{n})\right] h_{21}^*(\bar{v},\bar{u})h_{21}(\bar{n},\bar{m})\right\rangle$$

$$x\, d\bar{u}\, d\bar{m}\, d\bar{v}\, d\bar{r}_3 \quad ; \quad \bar{u},\ \bar{m} \in R_1 \quad \bar{v},\ \bar{n} \in R_2 \qquad (2L)$$

Substituting Eq (2L) into the fourth term of Eq (1L) yields

$$\langle \text{IMSE} \rangle = \int_{R_3}\int_{R_2}\int_{R_2}\int_{R_1}\int_{R_1} E_I(\bar{u})E_I^*(\bar{m})h_{FS}^*(\bar{v},\bar{r}_3)h_{FS}(\bar{n},\bar{r}_3)$$

$$\times \Big[h_{FS}(\bar{v},\bar{u})h_{FS}^*(\bar{n},\bar{m}) - 2\, h_{FS}^*(\bar{n},\bar{m})\langle \exp\big[j\phi_o(\bar{v})\big]$$

$$\times\, h_{21}(\bar{v},\bar{u})\rangle + \langle \exp\big[j\phi_o(\bar{v}) - j\phi_o(\bar{n})\big]h_{21}(\bar{v},\bar{u})$$

$$\times\, h_{21}^*(\bar{n},\bar{m})\rangle\Big]\, d\bar{u}\, d\bar{m}\, d\bar{v}\, d\bar{n}\, d\bar{r}_3 \;+\; N_o D_{fo}$$

$$;\quad \bar{u},\, \bar{m} \in R_1 \quad \bar{v},\, \bar{n} \in R_2 \qquad (3L)$$

where a change of variables ($\bar{u} \leftrightarrow \bar{m}$ and $\bar{v} \leftrightarrow \bar{n}$) was performed on the third term of Eq (1L) and the third term on the right side of Eq (2L). For propagation through the turbulent atmosphere, the general impulse response, $h_{21}(\bar{r}',\bar{r})$, of Eq (3L) is replaced by the turbulent impulse response, $h_{TB}(\bar{r}',\bar{r})$. The turbulent impulse response is written as

$$h_{TB}(\bar{r}',\bar{r}) = h_{FS}(\bar{r}',\bar{r})\exp\big[\chi(\bar{r}',\bar{r}) + j\phi(\bar{r}',\bar{r})\big] \qquad (4L)$$

Substituting Eq (4L) into Eq (3L) yields Eq (65):

$$\langle \text{IMSE} \rangle = \int_{R_3}\int_{R_2}\int_{R_2}\int_{R_1}\int_{R_1} E_I(\bar{u})E_I^*(\bar{m})h_{FS}(\bar{v},\bar{u})h_{FS}^*(\bar{n},\bar{m})$$

$$\times\, h_{FS}^*(\bar{v},\bar{r}_3)h_{FS}(\bar{n},\bar{r}_3)\Big[1 - 2\langle \exp\big[\chi(\bar{v},\bar{u})\big]$$

$$\times \exp\left[j\phi(\bar{v},\bar{u}) + j\phi_o(\bar{v})\right]> \; + \; <\exp\left[\chi(\bar{v},\bar{u})\right]$$

$$\times \exp\left[\chi(\bar{n},\bar{m})\right] \exp\left[j\phi(\bar{v},\bar{u}) + j\phi_o(\bar{v}) - j\phi(\bar{n},\bar{m})\right]$$

$$\times \exp\left[-j\phi_o(\bar{n})\right]>\Big] \, d\bar{u}\, d\bar{m}\, d\bar{v}\, d\bar{n}\, d\bar{r}_3 \; + \; N_o D_{fo}$$

$$; \quad \bar{u}, \bar{m} \in R_1 \quad \bar{v}, \bar{n} \in R_2 \qquad (65)$$

Appendix M - Average Coherent Transfer Function of the Multiplicative Phase Receiver

This appendix derives Eq (66), which is the expression for the average CTF of the MP Receiver when it is operating so as to cancel turbulence-induced phase fluctuations. The image field generated by the MP Receiver is

$$\hat{E}_{MP}(\bar{r}_3) = \int_{R_2} E(\bar{r}_2)\exp\left[j\phi_o(\bar{r}_2)\right] h_{FS}^*(\bar{r}_2,\bar{r}_3)d\bar{r}_2 \qquad (53)$$

where $h_{FS}(\bar{r}_2,\bar{r}_3)$ is the free-space impulse response defined by Eq (47):

$$h_{FS}(\bar{r}_2,\bar{r}_3) = \exp\left[jk(z + \left|\bar{r}_2-\bar{r}_3\right|^2/2z\right]/j\lambda z \qquad (47)$$

The field $E(\bar{r}_2)$ of Eq (53) is the input to the MP Receiver. By Eq (51) it is

$$E(\bar{r}_2) = E_o(\bar{r}_2) + E_N(\bar{r}_2) \qquad (51)$$

where $E_o(\bar{r}_2)$ is the output field of the propagation channel and $E_N(\bar{r}_2)$ is a zero-mean, spatially white noise field. For propagation through the turbulent atmosphere, the field $E_o(\bar{r}_2)$ is expressed as

$$E_o(\bar{r}_2) = \int_{R_1} E_I(\bar{r}_1)h_{TB}(\bar{r}_2,\bar{r}_1)d\bar{r}_1 \qquad (1M)$$

where $E_I(\bar{r}_1)$ is an unknown but nonrandom object field in aperture R_1 of Figure 10 and where $h_{TB}(\bar{r}_2,\bar{r}_1)$ is the turbulent impulse response defined by Eq (49):

$$h_{TB}(\bar{r}_2,\bar{r}_1) = \exp\left[jk(z + \left|\bar{r}_2-\bar{r}_1\right|^2/2z)\right]/j\lambda z$$

$$\cdot \quad x \exp\left[\chi(\bar{r}_2,\bar{r}_1) + j\phi(\bar{r}_2,\bar{r}_1)\right] \tag{49}$$

Substituting Eqs (51) and (1M) into Eq (53) yields

$$\hat{E}_{MP}(\bar{r}_3) = \int_{R_2}\int_{R_1} E_I(\bar{r}_1)\exp\left[j\phi_o(\bar{r}_2)\right]h_{TB}(\bar{r}_2,\bar{r}_1)$$

$$x\ h_{FS}^*(\bar{r}_2,\bar{r}_3)d\bar{r}_1\ d\bar{r}_2 \ + \int_{R_2} E_N(\bar{r}_2)$$

$$x \exp\left[j\phi_o(\bar{r}_2)\right]h_{FS}^*(\bar{r}_2,\bar{r}_3)d\bar{r}_2 \tag{2M}$$

Since $\chi(\bar{r}',\bar{r})$ and $\phi(\bar{r}',\bar{r})$ are random variables, the turbulent impulse response given by Eq (49) is a random function. Therefore, the image field given by Eq (2M) is also random. On the average however the field is:

$$\langle\hat{E}_{MP}(\bar{r}_3)\rangle = \int_{R_2}\int_{R_1} E_I(\bar{r}_1)\langle\exp\left[j\phi_o(\bar{r}_2)\right]h_{TB}(\bar{r}_2,\bar{r}_1)\rangle$$

$$x\ h_{FS}^*(\bar{r}_2,\bar{r}_3)d\bar{r}_1\ d\bar{r}_2 \tag{3M}$$

where the second term in Eq (3M) is dropped because the noise

field is zero-mean. Substituting Eqs (47) and (49) into Eq (3M) yields

$$\exp(jk|\bar{r}_3|^2/2z)\langle\hat{E}_{MP}(\bar{r}_3)\rangle = (1/\lambda z)^2 \int_{R_1} \exp(jk|\bar{r}_1|^2/2z)$$
$$\times E_I(\bar{r}_1)\int_{R_2}\exp\left[-jk(\bar{r}_1-\bar{r}_3).\bar{r}_2/z\right]\langle\exp\left[\chi(\bar{r}_2,\bar{r}_1)\right]\rangle$$
$$\times\langle\exp\left[j\phi(\bar{r}_2,\bar{r}_1) - j\phi_o(\bar{r}_2)\right]\rangle d\bar{r}_2\, d\bar{r}_1 \qquad (4M)$$

where the average of the right side of Eq (4M) has been written as two separate averages of $\chi(\bar{r}',\bar{r})$ and $\phi(\bar{r}',\bar{r})$ since these are independent random variables (Ref 4:1374). Furthermore, $\chi(\bar{r}',\bar{r})$ and $\phi(\bar{r}',\bar{r})$ are Gaussian random variables (Ref 4:1374) with the statistics given by Eqs (6I), (7I) and (8I). Using Eqs (6I) and (9I) it can be shown that

$$\langle\exp\left[\chi(\bar{r}_2,\bar{r}_1)\right]\rangle = \exp(-\nabla_\chi^2/2) \qquad (5M)$$

When the MP Receiver is operating so as to cancel turbulence-induced phase fluctuations, then $\phi_o(\bar{r}_2) = -\phi(\bar{r}_2)$, or equivalently, $\phi_o(\bar{r}_2) = -\phi(\bar{r}_2,0)$. Substituting this choice of $\phi_o(\bar{r}_2)$ and Eq (5M) into Eq (4M) yields

$$\exp(jk|\bar{r}_3|^2/2z)\langle\hat{E}_{MP}(\bar{r}_3)\rangle = (1/\lambda z)^2\exp(-\nabla_\chi^2/2)$$

$$x \int_{R_1} \exp(jk|\bar{r}_1|^2/2z) E_I(\bar{r}_1) \int_{R_2} \exp\left[-jk(\bar{r}_1-\bar{r}_3).\bar{r}_2/z\right]$$

$$x \left\langle \exp\left[j\phi(\bar{r}_2,\bar{r}_1) - j\phi(\bar{r}_2,0)\right]\right\rangle d\bar{r}_2\, d\bar{r}_1 \qquad (6M)$$

Following the procedure used in Appendix I, the spatial average on the right side of Eq (6M) is written as

$$\left\langle \exp\left[j\phi(\bar{r}_2,\bar{r}_1) - j\phi(\bar{r}_2,0)\right]\right\rangle = \exp\left[-D_\phi(0,\bar{r}_1)/2\right] \quad (7M)$$

where $D_\phi(0,\bar{r}_1)$ is the phase structure function defined by Eq (18I). Substituting Eq (7M) into Eq (6M) yields

$$\exp(jk|\bar{r}_3|^2/2z)\left\langle \hat{E}_{MP}(\bar{r}_3)\right\rangle = (1/\lambda z)^2 \exp\left[-\nabla_x^2/2\right]$$

$$x \int_{R_1} \exp(jk|\bar{r}_1|^2/2z) E_I(\bar{r}_1) \exp\left[-D_\phi(0,\bar{r}_1)/2\right]$$

$$x \int_{R_2} \exp\left[-j2\pi(\bar{r}_1-\bar{r}_3).\bar{r}_2/\lambda z\right] d\bar{r}_2\, d\bar{r}_1 \qquad (8M)$$

where the wave number k in the inner integral is replaced by $2\pi/\lambda$. It is shown in Appendix I that the inner integral of Eq (8M) can be written as

$$\int_{R_2} \exp\left[-j2\pi(\bar{r}_1-\bar{r}_3).\bar{r}_2/\lambda z\right] d\bar{r}_2 = d_2 \lambda z J_1(\pi|\bar{r}_1-\bar{r}_3|d_2/\lambda z)$$

$$x\ (2/|\bar{r}_1-\bar{r}_3|) \qquad (9M)$$

Substituting Eq (9M) into Eq (8M) yields Eq (66):

$$\exp(jk|\bar{r}_3|^2/2z)\langle\hat{E}_{MP}(\bar{r}_3)\rangle = (d_2/2\lambda z)\exp(-\nabla_x^2/2)$$

$$\times \int_{R_1} \exp(jk|\bar{r}_1|^2/2z)E_I(\bar{r}_1)\exp\left[-D_\phi(0,\bar{r}_1)/2\right]$$

$$\times J_1(\pi|\bar{r}_1-\bar{r}_3|d_2/\lambda z)(1/|\bar{r}_1-\bar{r}_3|)d\bar{r}_1 \qquad (66)$$

Appendix N - Minimum Average IMSEs of Multiplicative Phase Receiver Image Fields for Point Sources and Incoherent Object Fields

This appendix shows that for a point source field the sufficient condition for minimizing the average IMSE of the image field generated by the MP Receiver is satisfied when the optimum multiplicative phase is chosen so as to cancel the turbulence-induced phase fluctuations. This statement is qualified by saying that propagation is through the turbulent atmosphere and the additive background noise is zero-mean, spatially white noise. For the above choice of the optimum phase, the minimum average IMSE of the image field of a point source field is derived. The result is Eq (70). The process of showing that the sufficient condition is satisfied and then calculating the minimum average IMSE of the image field, is repeated for an isoplanatic, incoherent object field with a real and even object intensity distribution function. The minimum average IMSE expression for this case is Eq (71).

When propagation is through the turbulent atmosphere and the additive background noise is zero-mean, spatially white noise, the sufficient condition that the optimum multiplicative phase must satisfy is

$$\mathrm{Im}\left\{\int_{R_3}\int_{R_2}\int_{R_1}\int_{R_1} E_I(\bar{u})E_I^*(\bar{m})h_{FS}(\bar{v},\bar{u})h_{FS}^*(\bar{n},\bar{m})h_{FS}^*(\bar{v},\bar{r}_3)\right.$$

$$x\, h_{FS}(\bar{n},\bar{r}_3) < \exp\left[\chi(\bar{n},\bar{m})\right] \exp\left[-j\phi(\bar{n},\bar{m}) - j\phi_o(\bar{n})\right]$$

$$x \left[1 - \exp\left[\chi(\bar{v},\bar{u})\right] \exp\left[j\phi(\bar{v},\bar{u}) + j\phi_o(\bar{v})\right]\right] >$$

$$x\, d\bar{u}\, d\bar{m}\, d\bar{v}\, d\bar{r}_3 \Bigg\} = 0 \qquad ; \quad \bar{u}, \bar{m} \in R_1 \quad \bar{v}, \bar{n} \in R_2 \qquad (64)$$

Equation (64) is derived in Appendix K. For a point source field with a complex amplitude E_o, the term $E_I(\bar{u})E_I^*(\bar{m})$ in Eq (64) is written as

$$E_I(\bar{u})E_I^*(\bar{m}) = E_o E_o^* \delta(\bar{u})\delta^*(\bar{m}) \qquad (1N)$$

Substituting Eq (1N) into Eq (64) and letting $\phi_o(\bar{r}_2) = -\phi(\bar{r}_2)$ gives

$$\mathrm{Im}\left\{(1/\lambda z)^2 E_o E_o^* \int_{R_3}\int_{R_2} h_{FS}^*(\bar{v},\bar{r}_3) h_{FS}(\bar{n},\bar{r}_3)\left[<\exp\left[\chi(\bar{n})\right]>\right.\right.$$

$$\left.\left. - <\exp\left[\chi(\bar{n}) + \chi(\bar{v})\right]>\right] d\bar{v}\, d\bar{r}_3 \right\} = 0 \quad ; \quad \bar{v}, \bar{n} \in R_2 \qquad (2N)$$

Using Eqs (6I) and (9I) it can be shown that

$$<\exp\left[\chi(\bar{n})\right]> = \exp\left[-\sigma_\chi^2/2\right] \qquad (3N)$$

$$<\exp\left[\chi(\bar{n}) + \chi(\bar{v})\right]> = \exp\left[-\sigma_\chi^2\right] \qquad (4N)$$

Substituting Eqs (3N) and (4N) into Eq (2N) and using Eq (47) to expand the free-space impulse responses yields

$$\mathrm{Im}\left\{(1/\lambda z)^4 E_o E_o^* \left[\exp(-\nabla_x^2/2) - \exp(-\nabla_x^2)\right] \iint_{R_2 R_3} \right.$$
$$\left. \times \exp\left[-j2\pi(\bar{n}-\bar{v}).\bar{r}_3/\lambda z\right] d\bar{r}_3\, d\bar{v} \right\} = 0 \quad ; \quad \bar{v},\ \bar{n} \in R_2 \tag{5N}$$

where the order of integration is switched and the wave number k in the impulse response is replaced by $2\pi/\lambda$. Note that the inner integral of Eq (5N) is a two-dimensional spatial Fourier transform of aperture R_3 where $(\bar{n}-\bar{v})/\lambda z = \bar{f}$ is a two-dimensional spatial frequency vector. Since R_3 is a circular aperture of radius $d_1/2$ (same as the radius of R_1), the inner integral is actually a Fourier-Bessel transform of $\mathrm{circ}(2|r_3|/d_1)$ where

$$\mathrm{circ}(2|\bar{r}_3|/d_1) = \begin{cases} 1 & ; \quad |\bar{r}_3| \le d_1/2 \\ 0 & ; \text{ otherwise} \end{cases} \tag{6N}$$

From a table of Fourier-Bessel transforms, the transform of Eq (6N) is

$$\mathcal{B}\left[\mathrm{circ}(2|\bar{r}_3|/d_1)\right] = d_1 \lambda z J_1(\pi|\bar{n}-\bar{v}|d_1/\lambda z)/2|\bar{n}-\bar{v}| \tag{7N}$$

Replacing the inner integral of Eq (5N) with Eq (7N)

yields

$$\mathrm{Im}\left\{(1/\lambda z)^4 E_o E_o^* \left[\exp(-\nabla_x^2/2) - \exp(-\nabla_x^2)\right](d_1 \lambda z/2)\right.$$
$$\left. \times \int_{R_2} J_1(\pi|\bar{n}-\bar{v}|d_1/\lambda z)(1/|\bar{n}-\bar{v}|)d\bar{v} \right\} = 0 \quad ; \quad \bar{v},\ \bar{n} \in R_2 \tag{8N}$$

Since $J_1(x)$ and all the other terms on the left side of Eq (9M) are real, the left side is zero and the sufficient condition is satisfied. Therefore, for a point source field and the conditions stated at the beginning of this appendix, Eq (64) is true when $\phi_o(\bar{r}_2) = -\phi(\bar{r}_2)$. For this choice of $\phi_o(\bar{r}_2)$ and the same conditions, the minimum average IMSE of the image of a point source field with a complex amplitude E_o is, from Eq (65)

$$\langle \mathrm{IMSE} \rangle = (1/\lambda z)^2 E_o E_o^* \int_{R_3}\int_{R_2}\int_{R_2} h_{FS}^*(\bar{v},\bar{r}_3) h_{FS}(\bar{n},\bar{r}_3)$$
$$\times \left[1 - 2\langle \exp[\chi(\bar{v})]\rangle + \langle \exp[\chi(\bar{v}) + \chi(\bar{n})]\rangle\right]$$
$$\times d\bar{v}\, d\bar{n}\, d\bar{r}_3 + N_o D_{fo} \quad ; \quad \bar{v},\ \bar{n} \in R_2 \tag{9N}$$

Substituting Eqs (3N) and (4N) into Eq (9N) and using Eq (47) to expand the free-space impulse responses yields

$$\langle \mathrm{IMSE} \rangle = (1/\lambda z)^4 E_o E_o^* \left[1 - 2\exp(-\nabla_x^2/2) + \exp(-\nabla_x^2)\right]$$

$$x \int_{R_3}\int_{R_2} \exp\left[-j2\pi(-\bar{r}_3/\lambda z).\bar{v}\right] d\bar{v} \int_{R_2}$$

$$x \exp\left[-j2\pi(\bar{r}_3/\lambda z).\bar{n}\right] d\bar{n}\, d\bar{r}_3 + N_o D_{fo}$$

$$; \quad \bar{v}, \bar{n} \in R_2 \qquad (10N)$$

where the wave number k in the impulse response is replaced by $2\pi/\lambda$. Note that the second integral is a two-dimensional spatial Fourier transform of circular aperture R_2 where $-\bar{r}_3/\lambda z = -\bar{f}$ is a two-dimensional spatial frequency vector. Note that the third integral is a two-dimensional spatial Fourier transform of the same aperture where $\bar{r}_3/\lambda z = \bar{f}$ is a two-dimensional spatial frequency vector. Therefore, with the proper argument changes Eq (7N) can be used twice in Eq (10N) to give Eq (70):

$$\langle \text{IMSE} \rangle = (d_2/2\lambda z)^2 E_o E_o^* \left[1 - 2\exp(-\nabla_x^2/2) + \exp(-\nabla_x^2)\right]$$

$$x \int_{R_3} \left[J_1(\pi d_2 |\bar{r}_3|/\lambda z)\right]^2 (1/|\bar{r}_3|)^2 d\bar{r}_3$$

$$+ N_o D_{fo} \qquad (70)$$

Before the above process is repeated for an incoherent object field, the object field is restricted to be isoplanatic. For this additional restriction, Eq (64) becomes

$$\text{Im}\left\{\int_{R_3}\int_{R_2}\int_{R_1}\int_{R_1} E_I(\bar{u})E_I^*(\bar{m})h_{FS}(\bar{v},\bar{u})h_{FS}^*(\bar{n},\bar{m})h_{FS}^*(\bar{v},\bar{r}_3)\right.$$

$$\times\, h_{FS}(\bar{n},\bar{r}_3)\langle\exp\left[\chi(\bar{n})\right]\exp\left[-j\phi(\bar{n}) - j\phi_o(\bar{n})\right]$$

$$\times\left[1 - \exp\left[\chi(\bar{v})\right]\exp\left[j\phi(\bar{v}) + j\phi_o(\bar{v})\right]\right]\rangle$$

$$\left.\times\, d\bar{u}\, d\bar{m}\, d\bar{v}\, d\bar{r}_3\right\} = 0 \quad ; \quad \bar{u},\, \bar{m} \in R_1 \quad \bar{v},\, \bar{n} \in R_2 \qquad (11N)$$

For an incoherent object field with real and even object intensity distribution function $I(\bar{u})$, the term $E_I(\bar{u})E_I^*(\bar{m})$ in Eq (12M) is written as a spatial average over the object field

$$\langle E_I(\bar{u})E_I^*(\bar{m})\rangle = I(\bar{u})\,\delta(\bar{u}-\bar{m}) \qquad (12N)$$

Substituting Eq (12N) into Eq (11N) and letting $\phi_o(\bar{r}_2) = -\phi(\bar{r}_2)$ gives

$$\text{Im}\left\{\int_{R_3}\int_{R_2}\int_{R_1} I(\bar{r}_1)h_{FS}(\bar{v},\bar{r}_1)h_{FS}^*(\bar{n},\bar{r}_1)h_{FS}^*(\bar{v},\bar{r}_3)h_{FS}(\bar{n},\bar{r}_3)\right.$$

$$\left.\times\left[\langle\exp\left[\chi(\bar{n})\right]\rangle - \langle\exp\left[\chi(\bar{n}) + \chi(\bar{v})\right]\rangle\right]d\bar{r}_1\, d\bar{v}\, d\bar{r}_3\right\} = 0$$

$$; \quad \bar{v},\, \bar{n} \in R_2 \qquad (13N)$$

Substituting Eqs (3N) and (4N) into Eq (13N) and using Eq (47) to expand the free-space impulse responses yields

$$\text{Im}\left\{(1/\lambda z)^4\left[\exp(-\nabla_x^2/2) - \exp(-\nabla_x^2)\right]\int_{R_1}\int_{R_3}\right.$$

$$\text{x } \exp\left[-j2\pi(\bar{n}-\bar{v}).\bar{r}_3/\lambda z\right]d\bar{r}_3\int_{R_1} I(\bar{r}_1)\exp\left[-j2\pi(\bar{v}-\bar{n}).\bar{r}_1/\lambda z\right]$$

$$\left.\text{x } d\bar{r}_1\ d\bar{v}\right\} = 0 \qquad ;\ \bar{v},\ \bar{n} \in R_2 \qquad (14N)$$

where the order of integration is switched and the wave number k in the impulse response is replaced by $2\pi/\lambda$. Note that the second integral is a two-dimensional spatial Fourier transform of circular aperture R_2 where $(\bar{v}-\bar{n})/\lambda z = \bar{f}$ is a two-dimensional spatial frequency vector. Therefore, with the proper argument change Eq (8M) is used in Eq (14N) to give

$$\text{Im}\left\{(1/\lambda z)^4\left[\exp(-\nabla_x^2/2) - \exp(-\nabla_x^2)\right](d_2\lambda z/2)\right.$$

$$\text{x}\int_{R_2} J_1(\pi|\bar{n}-\bar{v}|d_2/\lambda z)(1/|\bar{n}-\bar{v}|)\int_{R_1} I(\bar{r}_1)$$

$$\left.\text{x } \exp\left[-j2\pi(\bar{v}-\bar{n}).\bar{r}_1/\lambda z\right]d\bar{r}_1\ d\bar{v}\right\} = 0 \quad ;\ \bar{v},\ \bar{n} \in R_2 \qquad (15N)$$

Note that the inner integral of Eq (15N) is a two-dimensional spatial Fourier transform of the object intensity distribution function within circular aperture R_1. Since the function is real and even, its transform is also real. Since $J_1(x)$ and all other terms on the left side of Eq (15N) are

real, the left side is zero and the sufficient condition is satisfied. Therefore, for an isoplanatic, incoherent object field with a real and even object intensity distribution function, and the conditions stated at the beginning of this appendix, Eq (64) is true when $\phi_o(\bar{r}_2) = -\phi(\bar{r}_2)$. For this choice of $\phi_o(\bar{r}_2)$ and the same conditions, the minimum average IMSE of the image of an isoplanatic, incoherent object field with a real and even object intensity distribution function $I(\bar{r}_1)$ is, from Eq (65)

$$\begin{aligned}<\text{IMSE}> = \int_{R_3}\int_{R_2}\int_{R_2}\int_{R_1} & I(\bar{r}_1)h_{FS}(\bar{v},\bar{r}_1)h_{FS}^*(\bar{n},\bar{r}_1)h_{FS}^*(\bar{v},\bar{r}_3) \\ & \times h_{FS}(\bar{n},\bar{r}_3)\left[1 - 2<\exp\left[\chi(\bar{v})\right]> + <\exp\left[\chi(\bar{v})\right]\right. \\ & \left.\times \exp\left[\chi(\bar{n})\right]>\right] d\bar{r}_1\, d\bar{v}\, d\bar{n}\, d\bar{r}_3 + N_o D_{fo} \\ & ;\quad \bar{v},\ \bar{n} \in R_2 \qquad (16N)\end{aligned}$$

Substituting Eqs (3N) and (4N) into Eq (16N) and using Eq (47) to expand the free-space impulse responses yields

$$\begin{aligned}<\text{IMSE}> = {} & (1/\lambda z)^4\left[1 - 2\exp(-\nabla_x^2/2) + \exp(-\nabla_x^2)\right] \\ & \times \int_{R_3}\int_{R_1} I(\bar{r}_1)\int_{R_2}\exp\left[-j2\pi(\bar{r}_1-\bar{r}_3).\bar{v}/\lambda z\right]d\bar{v} \\ & \times \int_{R_2}\exp\left[-j2\pi(\bar{r}_3-\bar{r}_1).\bar{n}/\lambda z\right]d\bar{n}\, d\bar{r}_1\, d\bar{r}_3 + N_o D_{fo} \\ & ;\quad v,\ n \in R_2 \qquad (17N)\end{aligned}$$

where the order of integration is switched and the wave number k in the impulse response is replaced by $2\pi/\lambda$. Note that the third integral is a two-dimensional spatial Fourier transform of circular aperture R_2 where $(\bar{r}_1-\bar{r}_3)/\lambda z = -\bar{f}$ is a two-dimensional spatial frequency vector. Note that the fourth integral is a two-dimensional spatial Fourier transform of the same aperture where $(\bar{r}_3-\bar{r}_1)/\lambda z = \bar{f}$ is a two-dimensional spatial frequency vector. Therefore, with the proper argument changes Eq (7N) is used twice in Eq (17N) to give Eq (71):

$$\langle \text{IMSE} \rangle = (d_2/2\lambda z)^2 \left[1 - 2 \exp(-\nabla_x^2/2) + \exp(-\nabla_x^2) \right]$$

$$\times \int_{R_3}\int_{R_1} I(\bar{r}_1)\left[J_1(\pi d_2 |\bar{r}_3-\bar{r}_1|/\lambda z)\right]^2 (1/|\bar{r}_3-\bar{r}_1|)^2$$

$$\times \, d\bar{r}_1 \, d\bar{r}_3 + N_o D_{fo} \qquad (71)$$

VITA

Kevin William Kirlin was born on 21 February 1952 in Biloxi, Mississippi. He graduated from high school in Herndon, Virginia in 1970 and attended the University of Florida from which he received the degree of Bachelor of Electrical Engineering with Honors in March 1975. At that time he was designated a distinguished military graduate and received a commission in the USAF through the ROTC program. He was employed as an engineering aide with the USA Computer Systems Command, Ft. Belvoir, Virginia until called to active duty in July 1975. He served as a Contract Programs Officer and Base Electrical Engineer in the 401st Civil Engineering Squadron, Torrejon AB, Spain until entering the School of Engineering, Air Force Institute of Technology, in June 1978.

Permanent address: 14912 Carlbern Dr.
Centreville, Virginia 22020

UNCLASSIFIED

SECURITY CLASSIFICATION OF THIS PAGE *(When Data Entered)*

REPORT DOCUMENTATION PAGE		READ INSTRUCTIONS BEFORE COMPLETING FORM
1. REPORT NUMBER AFIT/GEO/EE/79-3	2. GOVT ACCESSION NO.	3. RECIPIENT'S CATALOG NUMBER
4. TITLE *(and Subtitle)* SPATIAL DOMAIN AND SPATIAL FREQUENCY DOMAIN IMAGING		5. TYPE OF REPORT & PERIOD COVERED MS Thesis 6. PERFORMING ORG. REPORT NUMBER
7. AUTHOR(s) Kevin W. Kirlin Captain, USAF		8. CONTRACT OR GRANT NUMBER(s)
9. PERFORMING ORGANIZATION NAME AND ADDRESS Air Force Institute of Technology(AFIT-EN) Wright-Patterson AFB, Ohio 45433		10. PROGRAM ELEMENT, PROJECT, TASK AREA & WORK UNIT NUMBERS
11. CONTROLLING OFFICE NAME AND ADDRESS		12. REPORT DATE December, 1979 13. NUMBER OF PAGES 145
14. MONITORING AGENCY NAME & ADDRESS*(if different from Controlling Office)*		15. SECURITY CLASS. *(of this report)* Unclassified 15a. DECLASSIFICATION/DOWNGRADING SCHEDULE

16. DISTRIBUTION STATEMENT *(of this Report)*

Approved for public release; distribution unlimited

17. DISTRIBUTION STATEMENT *(of the abstract entered in Block 20, if different from Report)*

18. SUPPLEMENTARY NOTES

Approved for public release; IAW AFR 190-17

JOSEPH P. HIPPS, Major, USAF
Director of Public Affairs

19. KEY WORDS *(Continue on reverse side if necessary and identify by block number)*

Spatial Domain	Coherent Transfer Function
Spatial Eigenvalues	Modulation Transfer Function
Degrees of Freedom	Turbulent Atmosphere
Normal Mode Approach	Channel-Matched Filter Receiver
Spatial Frequency Domain	Adaptive Imaging

20. ABSTRACT *(Continue on reverse side if necessary and identify by block number)*

For the frequency domain, a summary of free-space and turbulent transfer functions is presented. For the spatial domain, the Normal Mode Approach to imaging is described followed by a summary of spatial eigenvalue distributions and degrees of freedom expressions. The effect of additive background noise on the useable degrees of freedom of an image field is analyzed. The background noise is shown to have no effect for coherent object fields while

DD FORM 1 JAN 73 1473 EDITION OF 1 NOV 65 IS OBSOLETE

UNCLASSIFIED

SECURITY CLASSIFICATION OF THIS PAGE *(When Data Entered)*

for incoherent object fields the useable degrees of freedom are shown to vary with the signal-to-noise ratio of the imaging system. The spatial domain and frequency domain are shown to be related when certain conditions are satisfied, one of which is space-invariance.

The operation of two ideal, adaptive imaging receivers (the Channel-Matched Filter and Multiplicative-Phase Receiver) is described and their imaging performance is compared using turbulent coherent transfer functions and minimum average integrated mean square error expressions. Compared to the Channel-Matched Filter Receiver, the Multiplicative-Phase Receiver is shown to generate, in general, image fields with larger minimum average, integrated mean square errors.